# THE SOLUTIONS OF A NONLINEAR DIFFERENCE EQUATION FOUND IN NUMERICAL ANALYSIS

Thesis by

Bruce Donald Westermo

In Partial Fulfillment of the Requirements

for the Degree of

Doctor of Philosophy

California Institute of Technology

Pasadena, California

1978

(Submitted on April 5, 1978)

Be bent, and you will remain straight

Be vacant, and you will remain full.

Be worn, and you will remain new.

Lao Tzu

# ACKNOWLEDGMENTS

I wish to extend my deepest gratitude to the following:

to my advisor, Dr. T. K. Caughey, for his assistance, understanding, and patience in guiding me through an invaluable experience;

to the California Institute of Technology and the Applied Mechanics Department for my financial support over the past four years;

to the faculty and students of the Applied Mechanics Department and all other members of the Caltech family for their help and sharing;

to Susan Berkley for expending so much care and energy in the typing of the manuscript; and finally,

to my parents whose unending support and encouragement have brought me this far.

# ABSTRACT

The solutions of a nonlinear difference equation resulting from the trapezoidal quadrature approximation of a piecewise linear differential equation are examined. A phase plane mapping technique is used to find the periodic and unbounded solutions of the difference equation and to determine the stability of these solutions. From the phase plane mappings of the unbounded solutions it is shown that the energy of the bounded solutions can grow and decay by large amounts. The maximum rate of Hamiltonian increase of the unbounded solutions is calculated from the mapping transformations. It is shown that the stability of a solution can only be guaranteed for discrete ranges of the time step with fixed initial conditions. The solutions of the non-autonomous difference equations for a sinusoidal forcing term and the damped difference equations are also examined.

# TABLE OF CONTENTS


| Part | Title | Page |
|---|---|---|
| Acknowledgments | | iii |
| Abstract | | iv |
| Chapter I | Introduction | 1 |
| 1.1 | Finite Difference Equations | 1 |
| 1.2 | The Statement of the Problem | 3 |
| Chapter II | The Solutions for $s = 0$ | 10 |
| 2.1 | The Phase Plane Transformations | 10 |
| 2.2 | The Simple Periodic Solutions | 21 |
| 2.3 | The Complex Periodic Solutions | 28 |
| 2.4 | The Unbounded Solutions | 29 |
| Chapter III | The Solutions for $s>0$ | 36 |
| 3.1 | The Phase Plane Transformations | 36 |
| 3.2 | The Simple Periodic Solutions | 49 |
| 3.3 | Other Periodic Solutions | 58 |
| 3.4 | Energy Growth | 61 |
| 3.5 | The Phase Plane for $\beta<\mu$ | 66 |
| 3.6 | Solutions of the Damped Equations | 66 |
| 3.6.1 | The Damped Finite Difference Equations | 66 |
| 3.6.2 | The Simple Periodic Solutions | 68 |
| 3.6.3 | The Bound on the Solutions | 70 |
| Chapter IV | The Non-Autonomous Equations | 72 |
| 4.1 | The Transformations of the Difference Equations | 72 |
| 4.2 | Analysis of Solutions for $\mu = 0$ | 75 |

| Part | Title | Page |
|---|---|---|
| 4.3 | Analysis of Solutions for $\mu>0$ | 83 |
| Chapter V | The Solutions of the Trapezoidal and Energy Conserving Difference Equations as Approximations to the Differential Equation Solutions | 95 |
| 5.1 | The Dependence of the Solutions on the Time Step | 95 |
| 5.2 | Comparisons of the Energy Conserving and Trapezoidal Algorithms | 100 |
| Chapter VI | Summary and Conclusions | 106 |
| References | | 110 |

# I Introduction

## 1.1 Finite Difference Equations

Finite difference equations stem from a broad range of problems in science. For example, because they are equations with the independent variable defined for only discrete values, difference equations serve as models for such discrete dynamic systems as digital control circuits [4]. Difference equations arise in the process of solving differential equations with a digital computer since the continuous equation must be discretized to convert it into a digitally solvable system. Various techniques of mathematical analysis also involve difference equations. For periodic differential equations, it is often useful to restate the problem in terms of the variables at the beginning and end of a period. The relation between these two states is a difference equation. Assuming that the solutions of certain differential equations are expressible in a series yields recursion relations for the coefficients of the series. These recursion relations are nothing but difference equations.

Over the past two decades digital computers have become extremely efficient and accurate numerical tools for scientific research. Due to their inherent digital capabilities, they are naturally suited for solving difference equations, as opposed to the analog computers' ability to solve differential equations. Although computers are capable of handling most of the current research demands, the state of the art in an analytical understanding of difference equations is far behind the capacity of our numerical tools.

A mathematical understanding of linear difference equations and

their solutions is fairly complete. This is not true for nonlinear difference equations where theory is generally as lacking as for non linear differential equations. The basic concepts of uniqueness, existence, and stability for differential equations can be carried over to difference equations. However, certain useful properties of differential equations can not be applied to difference equations in such a direct manner. For example, the phase plane trajectories of solutions to conservative differential equations are nonintersecting, closed curves. The phase plane mappings of difference solutions are discrete points, and thus the qualititive behavior of the solutions can not be directly inferred from the phase plane trajectories.

As mentioned above, the numerical analysis of dynamic systems with digital computers requires replacing the systems' differential equations with a set of difference equations. The solutions of the difference equations should approximate the differential equation solutions with an acceptable accuracy, but for nonlinear problems it is difficult to analytically determine this accuracy of approximation. The motivation for the particular set of difference equations examined in this dissertation stemmed from the question of the accuracy of the difference equation solutions derived from the trapezoidal rule approximation when applied to a nonlinear dynamic equation [8]. The trapezoidal rule is the interpolatory quadrature formula,

$$\int_{x_0}^{x_1} f(x)dx = \frac{h}{2}(f(x_0) + f(x_1)) - \frac{h^3}{12}\frac{d^2f}{dx^2}(\xi)$$

$$h = x_1 - x_0 \ , \ x_0 < \xi < x_1 \ .$$

For linear problems, the trapezoidal differencing scheme yields difference equations which approximate the differential equation solutions to within an accuracy of $O(\Delta t^2)$, where $\Delta t$ is the step size of the discretized time variable, t. The linear difference solutions also conserve the total energy of the system for all $\Delta t$. However, numerical solutions for some nonlinear equations have shown that the difference solutions for nonlinear problems do not have these attributes [8,9].

## 1.2 The Statement of the Problem

We will consider the conservative, dynamic equation,

$$\frac{d^2x}{dt^2} + f(x) = 0 \quad , \tag{1.1a}$$

with initial conditions

$$x(0) = x_0 \ , \ \frac{dx(0)}{dt} = \dot{x}_0 \quad , \tag{1.1b}$$

and the above equations' trapezoidal rule approximation,[1]

$$\begin{aligned} x_{n+1} - x_n &= \alpha(\dot{x}_{n+1} + \dot{x}_n) \\ \dot{x}_{n+1} - \dot{x}_n &= -\alpha\{f(x_{n+1}) + f(x_n)\} \\ \alpha &= \Delta t/2 \quad . \end{aligned} \tag{1.2}$$

The function f(x) is taken to be

---

[1] For the differential equation solutions, $x(t)$, $\dot{x}(t) \equiv \frac{dx}{dt}$ will be used, but for the difference equation solutions $\dot{x}_n$ is a separate variable.

$$f(x) = \begin{cases} ax & ; \quad |x| \le 1 \\ sx + (a - s)\,\mathrm{sgn}(x) & ; \quad |x| \ge 1 \end{cases} , \tag{1.3}$$

as shown in Fig. 1.1.

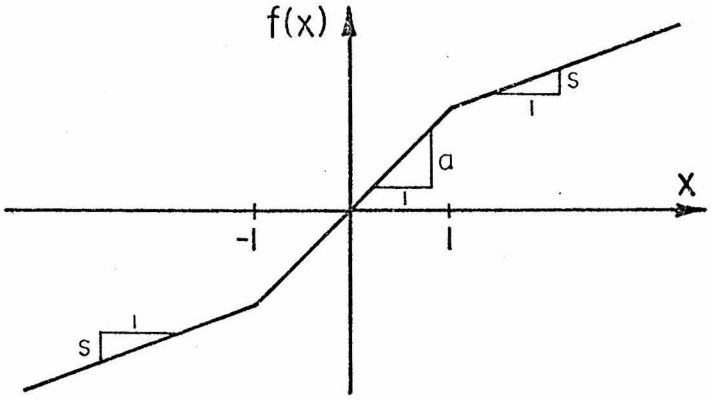


Figure 1.1 - The Function f(x)

f(x) is chosen to be a piecewise linear function of x because such functions have been used in the past as models for bilinear materials and as simplified models for more complex nonlinear dynamic systems. The piecewise linearity of f(x) simplifies the analysis while retaining some basic features of non linearities. The results presented can be extended to solutions for functions composed of multiple linear regions and to large amplitude solutions for functions with linear asymptotes.

Although Eqs. (1.2) are generally implicit, the choice of f(x) allows them to be transformed into a set of explicit difference equations,

$$\begin{aligned} x_{n+1} &= h(x_n + 2\alpha\dot{x}_n - \alpha^2 f(x_n)) \\ \dot{x}_{n+1} &= \frac{x_{n+1} - x_n}{\alpha} - \dot{x}_n \end{aligned} \tag{1.4}$$

$$h(x) = \begin{cases} \dfrac{x}{1+\alpha^2 a} & ; \quad |x| \le 1+\alpha^2 a \\ \dfrac{x}{1+\alpha^2 s} + \alpha^2 \left(\dfrac{s-a}{1+\alpha^2 s}\right) \mathrm{sgn}(x) & ; \quad |x| \ge 1+\alpha^2 a \quad . \end{cases} \tag{1.5}$$

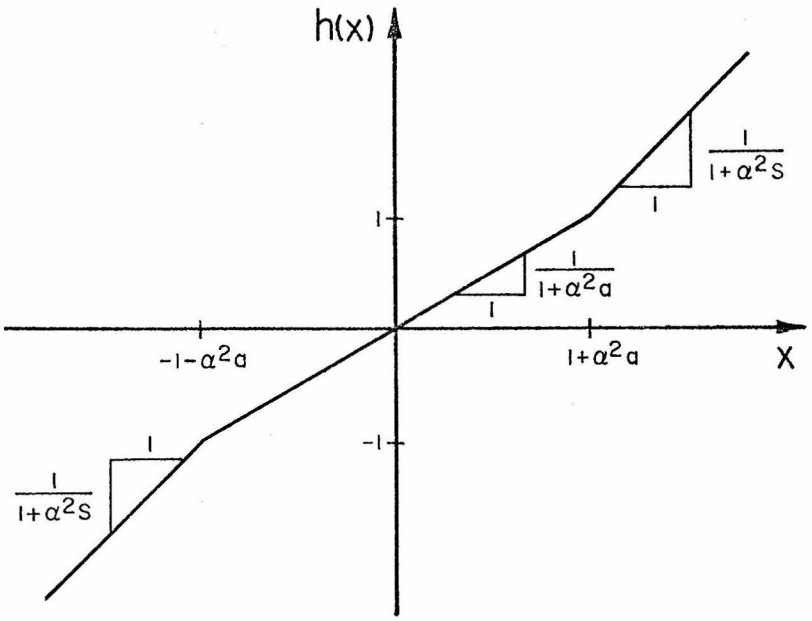


Figure 1.2 - The Function h(x)

Explicit difference equations, in general, have the property that the existence and uniqueness of the solutions is directly obtainable from the equations. Both the functions h(x) in Eq. (1.5) and f(x) in Eq. (1.3) are real and one to one functions of $x \in (-\infty, \infty)$. That is, for every x there is associated one and only one value of f(x) and h(x). Therefore, the solutions to Eqs. (1.2) or (1.4) exist and are unique. These difference equations also have unique solutions for the inverse or backwards problem, i.e. given the state at n, $\underset{\sim}{x}_n$, find the state for

$n-1$, $\underset{\sim}{x}_{n-1}$. This is due to the fact that the inverses of $f(x)$ and $h(x)$ are also one to one functions.

A powerful method for determining the stability of differential equation solutions, Liapunov's direct method, can be extended to handle difference equations [5]. For the explicit, difference equation,

$$\underset{\sim}{x}_{n+1} = F(\underset{\sim}{x}_n, n) \quad \forall n \geq n_0 \ , \tag{1.6}$$

the Liapunov function, $V(n, \underset{\sim}{x}_n)$, is defined such that $V(n, \underset{\sim}{x}_n)$ is a real valued function for all $n \geq n_0$ and all $\underset{\sim}{x}_n$ in G, a domain of the real vector space. If $V(n, \underset{\sim}{x}_n)$ is continuous, bounded from below, and if

$$\dot{V}(n, \underset{\sim}{x}_n) \equiv V(n+1, \underset{\sim}{x}_{n+1}) - V(n, \underset{\sim}{x}_n) \leq 0 \tag{1.7}$$

for all $n \geq n_0$ and for all $\underset{\sim}{x}_n$ in G, then $V(n, \underset{\sim}{x}_n)$ is a Liapunov function of Eq. (1.6) on G. The available stability theory for difference equations, [1,10,11,12], relies on the existence of such Liapunov functions to make any statements about the boundedness and the limit cycles of the solutions. Unfortunately there does not seem to exist any simple Liapunov functions of Eqs. (1.2). From the behavior of the numerical solutions, it appears that if Liapunov functions do exist, they must either be defined for a large number of steps or have a complicated functional dependence on $\underset{\sim}{x}_n$.

All of the solutions to Eqs. (1.2) are oscillatory. That is, in the phase plane, all of the solutions succesively map around the origin. This can be seen be setting $\alpha = 1$ (the results can be shown to hold for all $\alpha > 0$) and defining the function $z_n$ as

$$z_n = x_n + 2\dot{x}_n - f(x_n) \quad . \tag{1.8}$$

Equations (1.2) can then be written as the following explicit difference equation,

$$z_{n+1} - 2z_n + z_{n-1} = -4F(z_n) \tag{1.9}$$

where

$$F(z) = \begin{cases} \dfrac{a}{1+a} z & ; \quad |z| \le 1+a \\ \dfrac{s}{1+s} z + \left(\dfrac{a-s}{1+s}\right) \mathrm{sgn}(z) & ; \quad |z| \ge 1+a \quad . \end{cases} \tag{1.10}$$

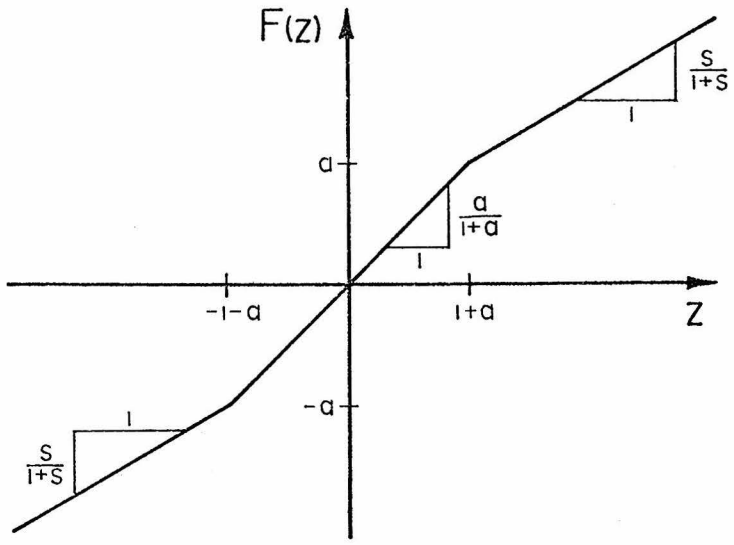


Figure 1.3 - The Function F(z)

The term on the left hand side of Eq. (1.9) is the difference operator (with $\Delta t = 1$) for $\frac{d^2 z}{dt^2}$, the curvature of $z(t)$. Thus Eq. (1.9) shows the curvature of $z$ is always of the opposite sign of $z$ and so the

solutions will be oscillatory.

The methods of solving difference equations vary as much as the equations themselves [2,6,7,13,14]. The oscillatory nature of the solutions to Eqs. (1.2) is an indication that there exist periodic solutions. Therefore a method is chosen that can solve the equations for existing periodic solutions and yet retain enough flexibility to gain insight into the behavior of the non-periodic solutions. A transformation oriented technique will be used where the phase plane mappings of domains are examined for invariance, and consequently, for periodic solutions. The method employed is a straight forward analysis. Since $f(x)$ is a piecewise linear function the phase plane can be divided into different regions, and the governing transformation in each region is linear.

Chapter II is concerned with the solutions of the difference equations where $s = 0$, i.e. the function $f(x)$ is a constant for $|x_n| > 1$. The phase plane is divided into the regions where a particular linear transformation applies and the mappings of these regions is examined. The simple periodic solutions and a set of more complicated periodic solutions are found along with an associated set of unbounded solutions. A bound on the Hamiltonian growth is also calculated.

In Chapter III the solutions for $s > 0$ are examined in a manner similar to Chapter II, with the exception that the associated transformations are trigonometric and not algebraic. The finite set of simple periodic solutions and their stability domains are found from the transformation mappings. Again, a bound on the Hamiltonian growth is calculated. Finally, the damped difference equations are examined. For these

equations both the simple periodic solutions and a bound on the solution growth is found.

Chapter IV deals with examining the non-autonomous difference equations with a sinousoidal forcing function. The change in the solutions' behavior due to the inhomogeneity is discussed, and the dependence of the solutions' period on the phase is found.

Chapter V discusses the aspects of the difference equations which approximate the differential Eq. (1.1a). The period error for the simple periodic solutions is calculated and some solutions for an energy conserving algorithm and the trapezoidal rule algorithm are compared to the exact solutions of the differential equation.

## II The Solutions for $s = 0$

### 2.1 The Phase Plane Transformations

The characteristics of the solutions for $s = 0$ in Eq. (1.3) are slightly different from those for $s>0$. The equations for $s = 0$ will be considered first, as they involve simpler transformations in the phase plane. The equations are

$$x_{n+1} - x_n = \alpha(\dot{x}_{n+1} + \dot{x}_n) \tag{2.1a}$$

$$\dot{x}_{n+1} - \dot{x}_n = -\alpha\left\{f(a, x_{n+1}) + f(a, x_n)\right\} \tag{2.1b}$$

where

$$f(a,x) = \begin{cases} a\ \mathrm{sgn}(x) & ;\ |x| \geq 1 \\ ax & ;\ |x| \leq 1 \end{cases}, \tag{2.2}$$

$$\alpha = \frac{\Delta t}{2} \quad .$$

To simplify the dependence of Eqs. (2.1a) and (2.1b) on the parameter $\alpha$, let

$$\underset{\sim}{y}_n = \begin{Bmatrix} y_n \\ \dot{y}_n \end{Bmatrix} = \begin{Bmatrix} x_n \\ \alpha\dot{x}_n \end{Bmatrix} \tag{2.3}$$

and

$$\beta = \alpha^2 a \quad . \tag{2.4}$$

Equations (2.1a), (2.1b), and (2.2) then become

$$y_{n+1} - y_n = \dot{y}_{n+1} + \dot{y}_n \tag{2.5a}$$

$$\dot{y}_{n+1} - \dot{y}_n = -f(\beta, y_{n+1}) - f(\beta, y_n) \ . \tag{2.5b}$$

Since $f(\beta, y)$ is a piecewise linear function, Eqs. (2.5a,b) can be written as a set of linear equations, each applying to its respective region of the phase plane. These regions are specified by the combinations of the three domains of $y_n$ for $f(\beta, y_n)$ to be linear. The difference equations are implicit, so the domain of $y_{n+1}$ must also be specified. This implies that the phase plane contains nine separate regions of linear transformations. These transformations being,

$$\left.\begin{aligned} &\text{I:} \quad y_n \geq 1 \ , \ y_{n+1} > 1 \\ &\dot{y}_n \geq \frac{1}{2}(1 + 2\beta - y_n) \\ &\underset{\sim}{y}_{n+1} = \underset{\sim}{\underset{\sim}{A}}\underset{\sim}{y}_n - 2\beta \, \underset{\sim}{1} \end{aligned}\right\} \tag{2.6a}$$

$$\left.\begin{aligned} &\text{II:} \quad y_n \geq 1 \ , \ |y_{n+1}| \leq 1 \\ &\frac{1}{2}(-1 - y_n) \leq \dot{y}_n \leq \frac{1}{2}(1 + 2\beta - y_n) \\ &\underset{\sim}{y}_{n+1} = \underset{\sim}{\underset{\sim}{B}}\underset{\sim}{y}_n - \left(\frac{\beta}{1+\beta}\right)\underset{\sim}{1} \end{aligned}\right\} \tag{2.6b}$$

III: $y_n \geq 1 \ , \ y_{n+1} \leq -1$

$\dot{y}_n \leq \frac{1}{2}(-1 - y_n)$

$\underset{\sim}{y}_{n+1} = \underset{\sim}{\underset{\sim}{A}}\underset{\sim}{y}_n$ (2.6c)

IV: $|y_n| \leq 1 \ , \ y_{n+1} \leq -1$

$\dot{y}_n \leq -1$

$\underset{\sim}{y}_{n+1} = \underset{\sim}{\underset{\sim}{C}}\underset{\sim}{y}_n + \beta \underset{\sim}{1}$ (2.6d)

V: $y_n \leq -1 \ , \ y_{n+1} < -1$

$\dot{y}_n \leq -\frac{1}{2}(1 + 2\beta + y_n)$

$\underset{\sim}{y}_{n+1} = \underset{\sim}{\underset{\sim}{A}}\underset{\sim}{y}_n + 2\beta \underset{\sim}{1}$ (2.6e)

VI: $y_n \leq -1 \ , \ |y_{n+1}| \leq 1$

$-\frac{1}{2}(1 + 2\beta + y_n) \leq \frac{1}{2} \leq \dot{y}_n \leq \frac{1}{2}(1 - y_n)$

$\underset{\sim}{y}_{n+1} = \underset{\sim}{\underset{\sim}{B}}\underset{\sim}{y}_n + \left(\frac{\beta}{1+\beta}\right)\underset{\sim}{1}$ (2.6f)

VII: $y_n \leq -1 \ , \ y_{n+1} \geq 1$

$\dot{y}_n \geq \frac{1}{2}(1 + y_n)$

$\underset{\sim}{y}_{n+1} = \underset{\sim}{\underset{\sim}{A}}\underset{\sim}{y}_n$ (2.6g)

$$\text{VIII:}\quad \left.\begin{aligned} &|y_n| \le 1\ ,\ y_{n+1} > 1 \\ &\dot{y}_n > 1 \\ &\underset{\sim}{y}_{n+1} = \underset{\sim}{\underset{\sim}{C}}\underset{\sim}{y}_n - \beta \underset{\sim}{1} \end{aligned}\right\} \quad (2.6h)$$

$$\text{IX:}\quad \left.\begin{aligned} &|y_n| \le 1\ ,\ |y_{n+1}| \le 1 \\ &|\dot{y}_n| \le 1 \\ &\underset{\sim}{y}_{n+1} = \underset{\sim}{\underset{\sim}{D}}\underset{\sim}{y}_n \end{aligned}\right\} \quad (2.6i)$$

with

$$\underset{\sim}{A} = \begin{bmatrix} 1 & 2 \\ 0 & 1 \end{bmatrix}\ ,\quad \underset{\sim}{B} = \frac{1}{1+\beta}\begin{bmatrix} 1 & 2 \\ -\beta & 1-\beta \end{bmatrix}\ ,$$

$$\underset{\sim}{C} = \begin{bmatrix} 1-\beta & 2 \\ -\beta & 1 \end{bmatrix}\ ,\quad \underset{\sim}{D} = \frac{1}{1+\beta}\begin{bmatrix} 1-\beta & 2 \\ -2\beta & 1-\beta \end{bmatrix}, \qquad (2.6j)$$

$$\underset{\sim}{1} = \begin{Bmatrix} 1 \\ 1 \end{Bmatrix}.$$

Figure 2.1 shows the $\underset{\sim}{y}$ phase plane divided into these nine regions. Each region was specified by defining the domain of $\underset{\sim}{y}_n$ and $\underset{\sim}{y}_{n+1}$, and it can be seen from the transformations that in one mapping step;

1) Region I maps onto regions I, II, and III,

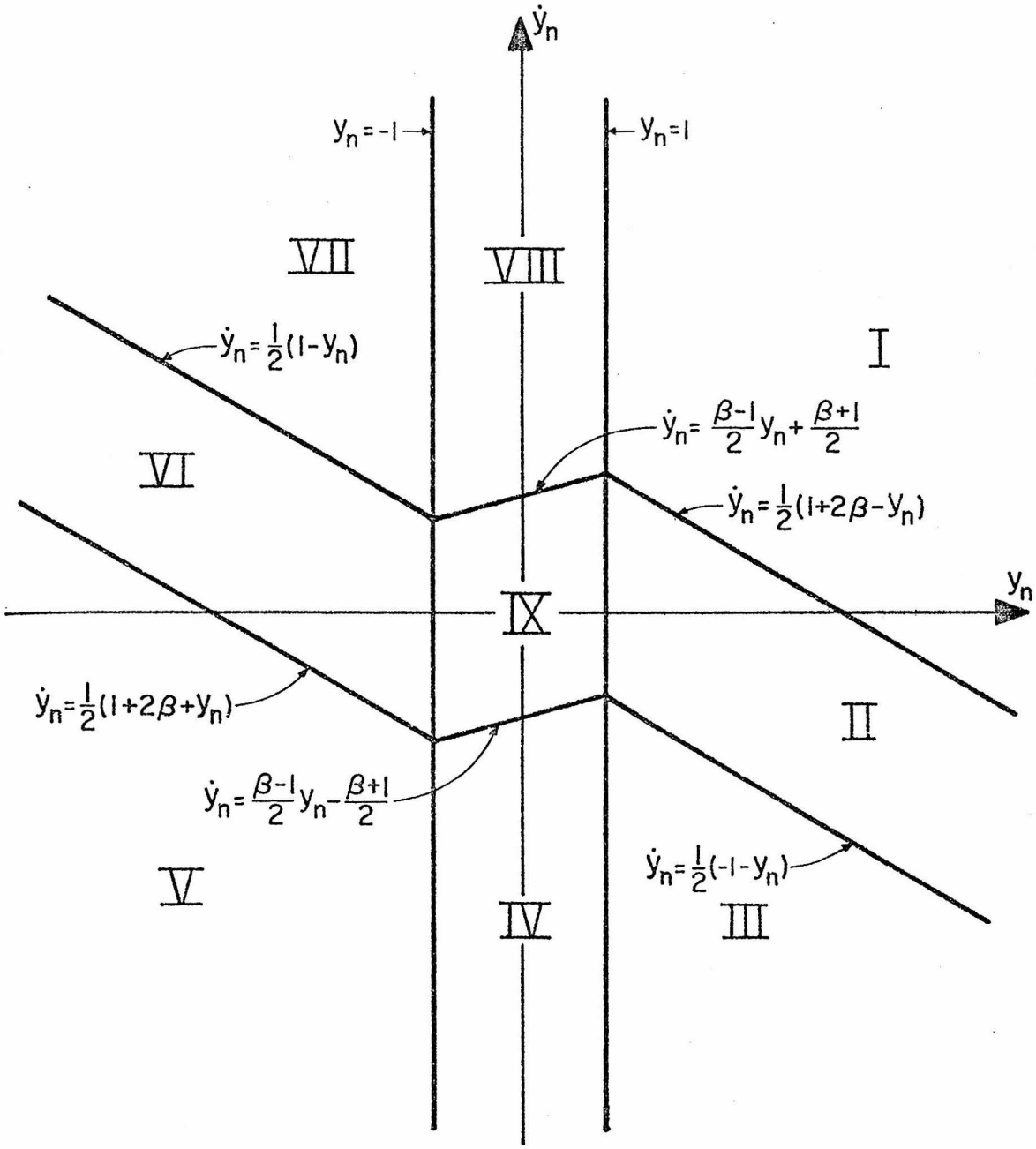


Figure 2.1 - Phase Plane Transformation Regions for $s = 0$

2) Region II maps onto regions IV and IX,

3) Region III maps into region V,

4) Region IV maps into region V,

5) Region V maps onto regions V, VI, and VII,

6) Region VI maps onto regions VIII and IX,

7) Region VII maps into region I,

8) Region VIII maps into region I, and

9) Region IX maps onto regions IV, VIII, and IX.

The function $f(\beta, y)$ is symmetric about $y = 0$, and thus the transformations in each half of the phase plane ($y_n > 0$ or $y_n < 0$) are identical to their counterparts in the other half of the phase plane with the transformation

$$\underset{\sim}{y}_n(\text{in } y_n > 0) = -\underset{\sim}{y}_n(\text{in } y_n < 0) \quad . \tag{2.7}$$

In other words, a set of solutions $\{\underset{\sim}{y}_i\}$ with initial value $\underset{\sim}{y}_0$ will be identical to the solutions $\{\underset{\sim}{y}_i'\}$ with initial value $-\underset{\sim}{y}_0$ for the transformation $\underset{\sim}{y}_i = -\underset{\sim}{y}_i'$. Therefore, it is sufficient to investigate the solution behavior in only half of the phase plane (one half cycle of oscillation) via Eq. (2.7).

Based on the mappings of one transformation region into another, solutions that map into $y_n > 1$ will map into region I k times in a half cycle. The value of k depends on the initial value, $\underset{\sim}{y}_0$. The solutions will then either map into region II and then into region IV, or they will map into region III. The next step will map all of these

solutions into the next half cycle.

Definition 2.1

Those solutions which map into $|y_n|>1$ in one half cycle and do not map into $|y_n|<1$ will be called outer branch solutions (the transformations depend only on the outer linear branches of f). Those solutions which map into $|y_n|>1$ and also map into $|y_n|<1$ in one half cycle will be denoted as the inner branch solutions.

The Hamiltonian of the difference Eqs. (2.5) (which is also the energy of the dynamic system since it is conservative) is

$$H(y,\dot{y}) = \begin{cases} \frac{1}{2}\dot{y}^2+\beta|y|-\frac{\beta}{2} & ; \quad |y|\geq 1 \\ \frac{1}{2}\dot{y}^2+\frac{1}{2}\beta y^2 & ; \quad |y|\leq 1 \ . \end{cases} \tag{2.8}$$

Although the solutions to the differential equation given by Eq. (1.1a) do conserve the Hamiltonian, the solutions of the difference equations in general do not. Calculating the change in the Hamiltonian within each of the nine different transformation regions shows that the energy is conserved only with mappings through regions I, V, and part of region IX. Both regions I and V are the multiple mapping regions in each half plane, and so a solution will conserve its Hamiltonian as it maps within the half planes, $y_n<1$ and $y_n>1$. The Hamiltonian will change when the solution maps from one of these half planes into the other.

The Hamiltonian jump for an outer branch solution, in mapping across the linear region, is calculated from Eqs. (2.6c) and (2.8) and is

$$\Delta H\Big|_{\underset{\sim}{y_0}}^{\underset{\sim}{y_1}} = -2\beta(y_0 + \dot{y}_0) \quad , \tag{2.9}$$

where $\underset{\sim}{y_0}$ lies in region III. Similarly, for the inner branch solutions, the Hamiltonian jump is found from Eqs. (2.6b), (2.6d) and (2.8) to be

$$\Delta H\Big|_{\underset{\sim}{y_0}}^{\underset{\sim}{y_2}} = \left(\frac{\beta}{\beta+1}\right)(2\dot{y}_0 + y_0 - \beta + 1)(y_0 + 1) \quad . \tag{2.10}$$

$\underset{\sim}{y_0}$ lies in region II.

In order to explore the periodic and unbounded solutions to Eqs. (2.5), it is necessary to determine how a solution initially in region I maps through the half plane into region I for the next half cycle. To accomplish this, the complete set of half cycle transformations are formulated by following all of the possible mapping transformations in one half cycle. First, the subregion of region I which contains the forward mapping of regions VII and VIII is calculated. This region, denoted $I_a$, contains one point of all of the solutions of Eqs. (2.5) which map into the outer branches of $f(\beta, y)$ (i.e. $|y_n| > 1$) at least once per half cycle. Figure 2.2 shows region $I_a$ for the half plane $y_n > 0$. The subregions of region $I_a$ that determine the number of mappings a solution makes in region I are found by backwards mapping region $I_a$ through a half cycle back onto itself. To do this, the forward transformation for a solution which initiates and maps back into $I_a$ with k steps, and does so without mapping into $|y_n| < 1$, is calculated from

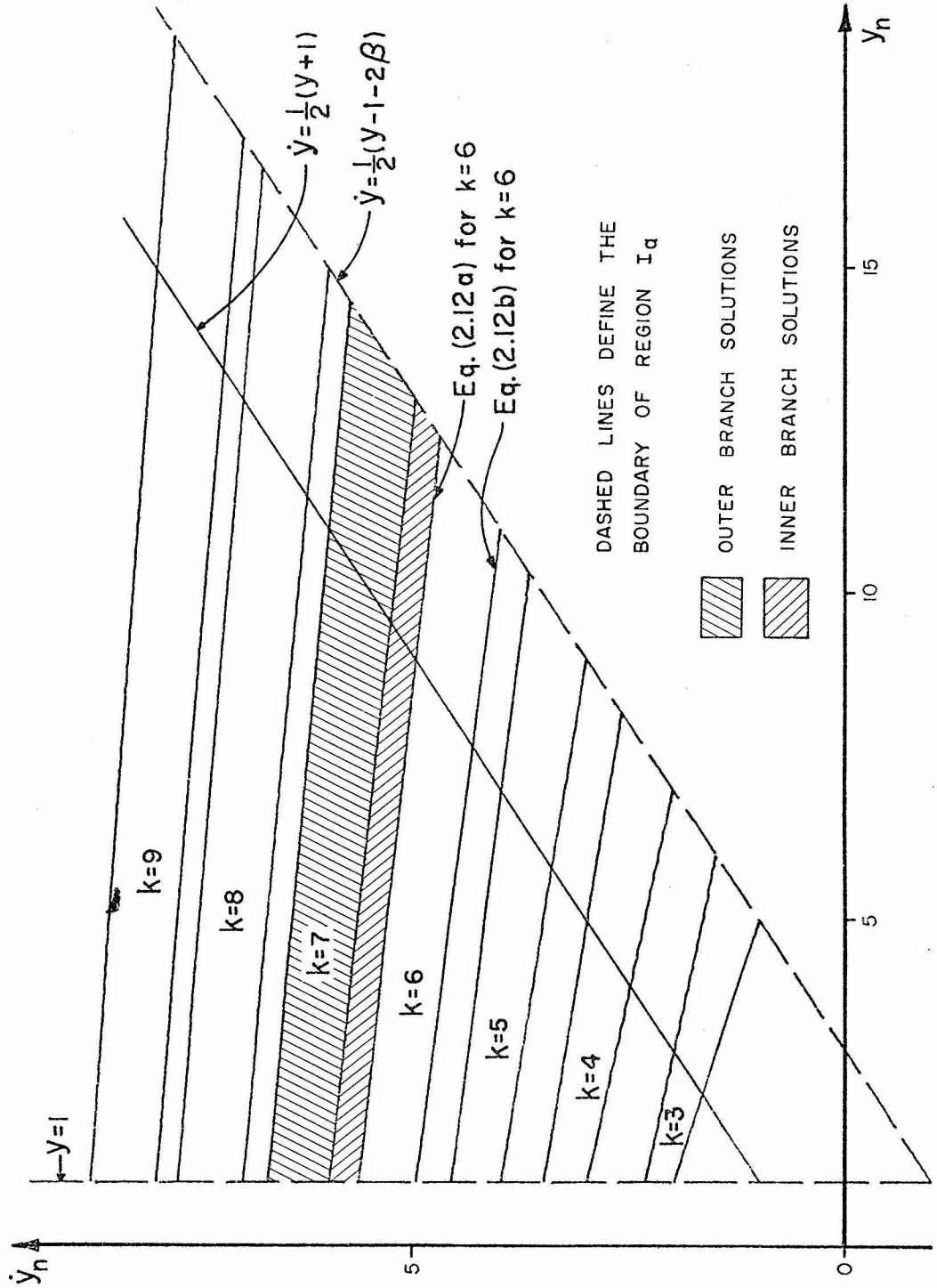


Figure 2.2 - The k-step Mapping Regions of Region $I_a$ for $\beta = 1$

Eqs. (2.6a), (2.6c), and (2.7). This forward transformation for the k-step outer branch solutions is

$$\underset{\sim}{y}_k = -\begin{bmatrix} 1 & 2k \\ 0 & 1 \end{bmatrix} \underset{\sim}{y}_0 + 2\beta \sum_{j=1}^{k-1} \begin{bmatrix} 1 & 2 \\ 0 & 1 \end{bmatrix}^j \begin{Bmatrix} 1 \\ 1 \end{Bmatrix}$$

$$= -\begin{bmatrix} 1 & 2k \\ 0 & 1 \end{bmatrix} \underset{\sim}{y}_0 + 2\beta \begin{Bmatrix} k^2 - 1 \\ k - 1 \end{Bmatrix} . \qquad (2.11)$$

Using Eq. (2.11) and back mapping the boundaries of region $I_a$ given by $y_k = 1$ and $\dot{y}_k = \frac{1}{2}(y_k + 1)$ yields, respectively,

$$\dot{y}^{upper} = \frac{-1}{2k} y + \frac{2\beta k^2 - 2\beta - 1}{2k} \qquad (2.12a)$$

$$\dot{y}^{lower} = \frac{-1}{2(k-1)} y + \frac{2\beta k^2 - 4\beta k + 2\beta + 1}{2(k-1)} . \qquad (2.12b)$$

Thus, points in region $I_a$ between the lines described by Eqs. (2.12a) and (2.12b) will map k times through the half plane back into region $I_a$. The only other solutions possible are the k-step inner branch solutions, and these solutions lie in between the lines described by Eq. (2.12a) for k - 1 steps and Eq. (2.12b) for k steps. Figure 2.2 shows the division of region $I_a$ into these transformation subregions. In a similar manner, the transformation for the class of solutions mapping into $|y_n| < 1$, the inner branch solutions, is found from Eqs. (2.6a), (2.6b), (2.6d), and (2.7), and is

$$\underset{\sim}{y}_k = \frac{1}{1+\beta}\begin{bmatrix} 1-3\beta & 2(1-3\beta)k+8\beta \\ -2\beta & -4\beta k+5\beta+1 \end{bmatrix}\underset{\sim}{y}_0$$

$$+\frac{\beta}{1+\beta}\begin{Bmatrix} 2(3\beta-1)k^2+8(1-\beta)k+10\beta-18 \\ -4\beta k^2+2(5\beta+1)k+4\beta-6 \end{Bmatrix} \qquad (2.13)$$

Since these points map into the linear region, the solutions will map via Eq. (2.13) into the region of $I_a$ bounded by $\dot{y} = \frac{1}{2}(y+1)$ and $\dot{y} = \frac{1}{2}(y-1-2\beta)$, shown in Fig. 2.2. Thus, from this abbreviated phase plane, the behavior of a solution in one half cycle of mappings is given by which subregion of $I_a$ $\underset{\sim}{y}_0$ lies in and the forward mapping of that region, as given by Eqs. (2.11) or (2.13).

The minimum number of steps a solution takes to map through a half cycle, $|y_n|>1$, can not be less than the number of steps per half cycle made by a solution staying in the linear region, $|y_n|<1$. This is due to the fact that the linearized $f(\beta,y)$ for any point $|y_n|>1$ has a slope less than $\beta$. The transformation for solutions in the linear region IX is

$$\underset{\sim}{y}_{n+1} = \begin{bmatrix} \cos\theta & \frac{\sin\theta}{\sqrt{\beta}} \\ -\sqrt{\beta}\sin\theta & \cos\theta \end{bmatrix}\underset{\sim}{y}_n \ , \qquad (2.14)$$

$$\theta = \cos^{-1}\left(\frac{1-\beta}{1+\beta}\right) \ ,$$

and thus $k_{linear}$, which is the number of steps per half cycle of these linear solutions, is

$$k_{linear} = \pi/\cos^{-1}\left(\frac{1-\beta}{1+\beta}\right) . \tag{2.15}$$

The restrictions on $k_{min}$, the minimum number of mappings a solution makes in a half plane, are

$$k_{min} \geq \pi/\cos^{-1}\left(\frac{1-\beta}{1+\beta}\right) \quad , \text{ and} \tag{2.16}$$

$$k_{min} \geq 2 \ .$$

From the dependence of Eqs. (2.12a) and (2.12b) on k, two characteristics of these lines which define the k-step region can be seen: Their $y = 0$ intercepts grow with $O(\beta k)$ and their slope approaches zero with $O(1/k)$. Thus, for large k, the period of a solution in one half cycle, $n_{hc}$, is

$$n_{hc} = \frac{\dot{y}}{\beta} + O\left(\frac{1}{k}\right) \tag{2.17}$$

and thus, the half cycle period of the solutions grows linearly with $\dot{y}$.

## 2.2 The Simple Periodic Solutions

To prove the existence of periodic solutions to Eqs. (2.5), it will be necessary to make use of Brouwer's Fixed Point Theorem.

Theorem 2.1 (Brouwer)

If $\phi$ is a continuous mapping of the closed unit sphere $S = \left\{ x \epsilon E^n \,\middle|\, |x| \leqq 1 \right\}$ of Euclidian n-space into itself, then there exists a point y in S such that $\phi(y) = y$.

A detailed discussion and a proof of this theorem is given in [3]. Clearly, the fixed points for the phase plane mappings are the periodic solutions. It is only necessary to find the phase plane regions that can map back onto themselves to prove the existence of a periodic solution in that region. As a convention, the behavior of a particular solution, in terms of the number of times it maps into the half plane $|y_n| \geq 1$, will be denoted by parentheses with a comma separating the number of times it maps into each half plane. For example, $(k, \ell, m)$ denotes a solution taking k steps in one half cycle, $\ell$ steps in the next, and m in the last half cycle.

The simple periodic solutions of Eqs. (2.5) are defined as the solutions which are periodic in one cycle of the phase plane. The totality of possible mapping patterns for these solutions is denoted by $(\ell, k)$ with $\ell$ and k greater than or equal to the minimum number of steps per half cycle. To find the simple periodic solutions, it is necessary to map region $I_a$ onto itself to determine what type of mapping patterns are possible. The periodic solutions can then be found by solving the transformation equations involved in the mappings for a periodic solution.

The mapping of the k-step region onto itself in one half cycle is shown in Fig. 2.3. From the points defining this mapping (given in Fig. 2.3), the following two statements of the half cycle mapping behavior can be proven (for all $\beta > 0$):

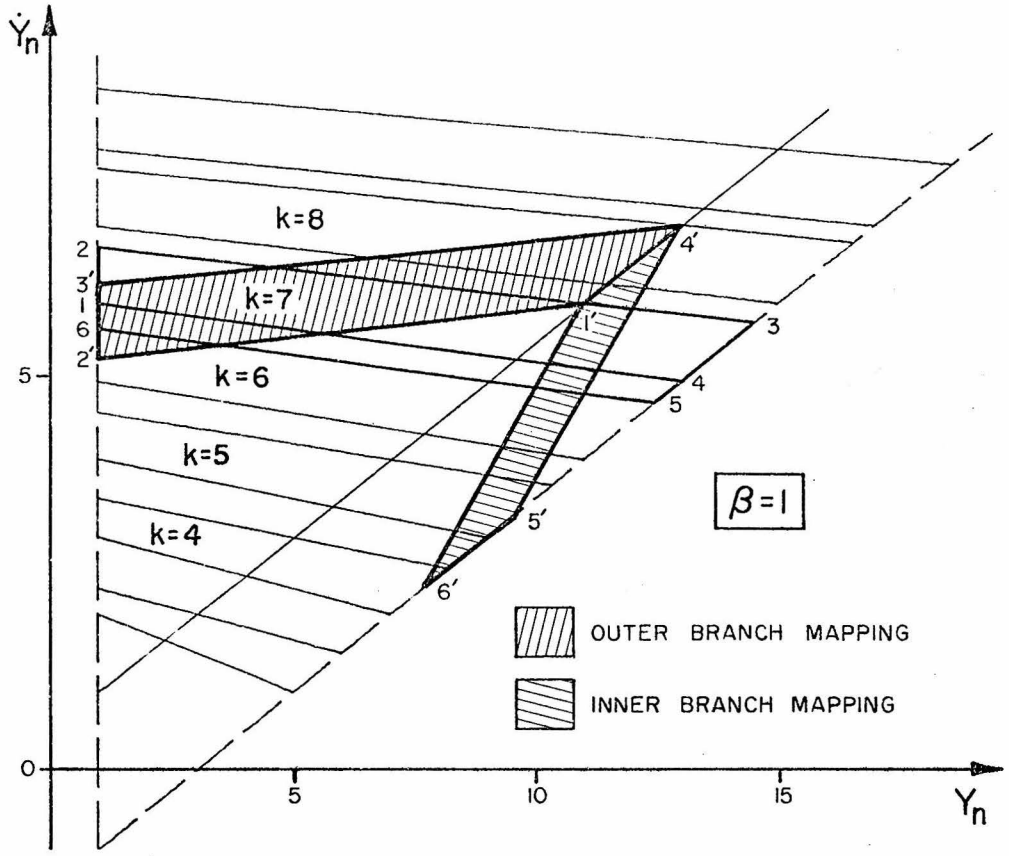


1 : $\{1, \beta(k-1)\}$

2 : $\{1, (\beta k^2 - \beta - 1)/k\}$

3 : $\{(-1 + 2\beta k^2 - 2\beta + k + 2k\beta)/(k+1),\ (\beta k^2 - 2\beta - 1)/(k+1)\}$

4 : $\{1 - 2\beta + 2\beta k,\ \beta(k-2)\}$

5 : $\{(-2 + 2\beta k^2 - 2\beta k + k - 2\beta)/k,\ (-1 + \beta k^2 - 2\beta k - \beta)/k\}$

6 : $\{1, (\beta k^2 - 2\beta k - 1)/(k-1)\}$

1′: $\{4\beta k - 4\beta - 1,\ \beta(k-1)\}$

2′: $\{1, \beta k - 2\beta + (\beta+1)/k\}$

3′: $\{1, (\beta k^2 + 1)/(k+1)\}$

4′: $\{2\beta k - 1,\ \beta k\}$

5′: $\{(2\beta k^2 - 6\beta k + k + 2\beta + 2)/k,\ (\beta k^2 - 4k\beta + \beta + 1)/k\}$

6′: $\{(2\beta k^2 - 10\beta k + k + 1 + 10\beta)/(k-1),\ (\beta k^2 - 6\beta k + 6\beta + 1)/(k-1)\}$

Figure 2.3 - The Half Cycle Mapping of a k-step Region and the Points Defining this Region and its Mapping.

1) The k-step outer branch solution region maps into the (k - 1), k, and (k+1)-step outer branch and the k and (k - 1)-step inner branch regions of the next half cycle.

2) The k-step inner branch region maps into the (k+1), k, (k - 1), (k - 2), and (k - 3)-step outer branch regions and into the (k+1), k, (k - 1), and (k - 2)-step inner branch mapping regions.

These two mapping rules therefore limit the possible combinations of simple periodic outer branch solutions to the mapping patterns (k,k - 1), (k,k), or (k,k+1), and the following theorem can now be stated.

Theorem 2.2

The (k,k) periodic solution exists for all $k \geq k_{min}$ and is given by

$$\underset{\sim}{y}^p = \begin{Bmatrix} y^p \\ \\ \beta(k-1) \end{Bmatrix} , \quad 1 \leq y^p \leq 2\beta k - 1 , \tag{2.18}$$

for all $\beta > 0$.

proof:

From the points defining the k-step region (1, 2, 3, and 4 in Fig. 2.3) and their mappings (1′, 2′, 3′, and 4′), it can be shown that there exists a region which is the set of solutions following a (k,k) mapping.

If part of this region maps onto itself, then there exists a periodic solution by the fixed point theorem. To find the fixed point, the transformations given by Eq. (2.11) yield the following (k,k) transformation

$$\underset{\sim}{y}_{2k} = \begin{bmatrix} 1 & 4k \\ 0 & 1 \end{bmatrix} \underset{\sim}{y}_0 + 4\beta \begin{Bmatrix} -k^2+k \\ 0 \end{Bmatrix} . \tag{2.19}$$

The periodic solution of Eq. (2.19) is $\dot{y}^p = \beta(k-1)$ with the equation for $y^p$ satisfied identically as long as $y^p$ lies in the (k,k) mapping region. From the intercepts of $\dot{y}^p = \beta(k-1)$ with this region, it is found that $1 \le y^p \le 2\beta k - 1$. Figure 2.4 shows some of these periodic solutions plotted in region $I_a$ of the phase plane.

To examine the stability of these periodic solutions, $\underset{\sim}{y}^p$, let $\underset{\sim}{\varphi}_n$ be a perturbation of $\underset{\sim}{y}^p$ such that $\underset{\sim}{y} = \underset{\sim}{y}^p + \underset{\sim}{\varphi}$ always lies in the same transformation region as $\underset{\sim}{y}^p$. Then $f(\beta, y_n^p + \varphi_n) = f(\beta, y_n^p)$, and the perturbation equations of Eqs. (2.5) are

$$\begin{aligned} \varphi_{n+1} - \varphi_n &= \dot{\varphi}_{n+1} + \dot{\varphi}_n \\ \dot{\varphi}_{n+1} - \dot{\varphi}_n &= 0 \ . \end{aligned} \tag{2.20}$$

The solution of which is

$$\left.\begin{aligned} \varphi_n &= \varphi_0 + 2n\dot{\varphi}_0 \\ \dot{\varphi}_n &= \dot{\varphi}_0 \end{aligned}\right\} \tag{2.21}$$

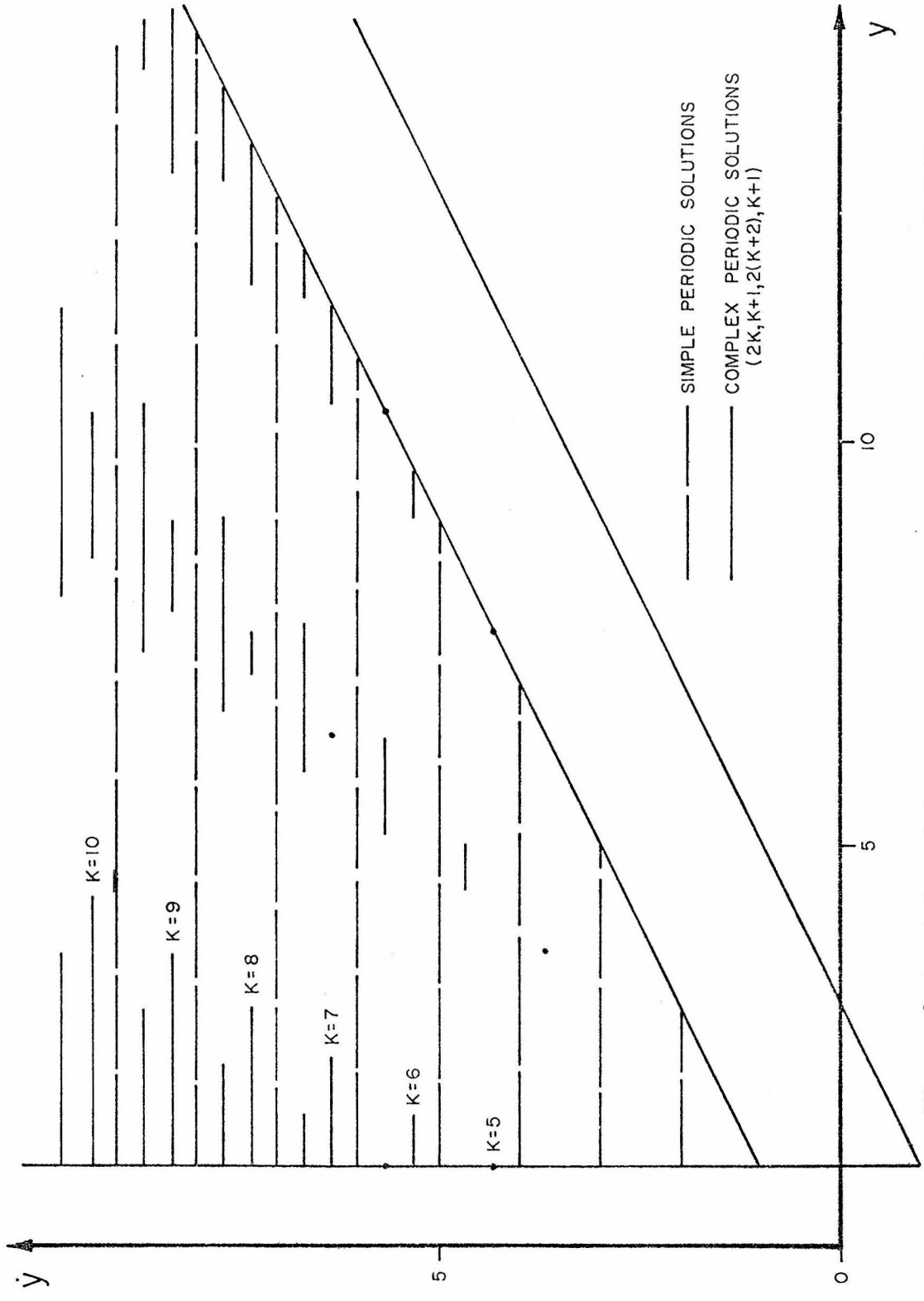


Figure 2.4 - A Set of Complex Periodic Solutions (m = 2 in Eq. (2.25)) and the Simple Periodic Solutions

Thus, for an arbitrary $\underset{\sim}{\varphi}_0$, the perturbations of the periodic solutions are unstable and grow linearly in n. The solutions are stable, however, for $\dot{\varphi}_0 = 0$, and must be as the periodic solutions are lines with $\dot{y}$ = constant.

Although a mapping exists, periodic solutions of the pattern (k,k - 1) and (k,k + 1) do not exist. This is because there are no invariant subregions of the (k,k - 1) or (k,k + 1) mapping regions, and so no fixed point exists.

For the simple periodic inner branch solutions, the following theorem is given.

Theorem 2.3

The periodic solutions which map k times in $|y_n| \geq 1$ and once in $|y_n| < 1$ for a half cycle, and which are periodic in one cycle exist and are

$$\underset{\sim}{y}^{p1} = \beta \begin{Bmatrix} 2k - 1 \\ \\ k - 1 \end{Bmatrix} . \tag{2.22}$$

proof:

Following the reasoning of the previous proof, it can be shown that the k-step linear region (bounded by points 1, 4, 5, and 6 in Fig. 2.3) intersects its mapping (1′, 4′, 5′, and 6′). The transformation equation is Eq. (2.13), which has Eq. (2.22) as a periodic solution.

The stability of these solutions is different from those of the (k,k) outer branch type, and the perturbation equation is

$$\underset{\sim}{\varphi}_{n+1} = \frac{1}{1+\beta}\begin{bmatrix} 1-3\beta & 2(1-3\beta)k+8\beta \\ -2\beta & -4\beta k+5\beta+1 \end{bmatrix}\underset{\sim}{\varphi}_{n} \quad . \tag{2.23}$$

The eigenvalues of this transformation are complex conjugates (hence, stable solutions) for $\beta < 1/k$, and real (unstable solutions) otherwise.

## 2.3 The Complex Periodic Solutions

Since the k-step region maps points into both the $(k-1)$ and $(k+1)$-step regions, it would seem possible that periodic solutions exist which map several times in different regions of $I_a$. The half cycle period of the solutions would grow and decay in the number of steps per half cycle and, consequently, also in the Hamiltonian. Finding these complex periodic solutions involves first synthesizing a possible mapping pattern in terms of the number of steps per half cycle and then checking the resulting transformation for a fixed point.

To exemplify this process, consider a solution which maps into the k-step region m times. Since a simple periodic solution exists for one cycle of mappings, there must exist solutions which will map m times in a k-step region. Now allow the solution to map first into the $(k+1)$-step region and then into the $(k+2)$-step region, where it maps m times. It was demonstrated by the previous analysis that both mappings are separately possible. To make the solution periodic, let it map into the $(k+1)$ and then the k-step regions. If this solution pattern exists it will have a period of $2(m+1)(k+1)$, and a mapping pattern denoted by $(m(k), k+1, m(k+2), k+1)$. Following this pattern

and carrying out the transformations yields, for $m$ an even integer,

$$\underset{\sim}{y}_{2(m+1)(k+1)} = \begin{bmatrix} 1 & 4(k+1)(m+1) \\ 0 & 1 \end{bmatrix} \underset{\sim}{y}_0 - 4\beta \begin{Bmatrix} (m+1)k^2+k-m \\ 0 \end{Bmatrix} \quad (2.24)$$

The periodic solution of Eq. (2.24) is thus

$$\underset{\sim}{y}^{cp} = \begin{Bmatrix} y^{cp} \\ \beta\left(k - \frac{m}{m+1}\right) \end{Bmatrix} \quad (2.25)$$

with the values of $y^{cp}$ such that $\underset{\sim}{y}^{cp}$ is in the region that follows the $(m(k),\ k+1,\ m(k+2),\ k+1)$ mapping. It is necessary to carry out this mapping of the k-step region to find $y^{cp}$, which gets increasingly complicated as $m$ grows. Figure 2.4 shows several of these complex periodic solutions in region $I_a$ of the phase plane.

Since all of these periodic solutions are outer branch solutions, $|y_n| \geq 1$, the stability analysis is the same as for the $(k,k)$ simple periodic solutions (Section 2.2).

## 2.4 The Unbounded Solutions

Numerical calculations of the solutions to Eqs. (2.5) indicated that there is a set of solutions that would, on each half cycle, map up into the next higher step region and continue to grow in this manner unboundedly. To look at a generalization of this kind of growth, consider the previous set of complex periodic solutions. It was noted

that these solutions follow a $(m(k), k+1, m(k+2), k+1)$ mapping. Half of this pattern consists of the $(m(k), k+1)$ mapping, which will be considered the basic building block of a set of the unbounded solutions. The full mapping behavior would be that a solution maps first into the $(k+2)$-step region by $(m(k), k+1)$, then into the $k+4$ step region by $(m(k+2), k+3)$, and continues mapping into a 2-step larger region with each $(m(k), k+1)$ transformation.

To check for the existence of such solutions, the transformation for the pattern $(m(k), k+1)$ is calculated. This is done by carrying out the transformations of each half cycle mapping specified by Eq. (2.11), and the transformation is

$$\underset{\sim}{y}_{mk+k+1} = \begin{bmatrix} 1 & 2(m+1)k+2 \\ 0 & 1 \end{bmatrix} \underset{\sim}{y}_0 - 2\beta \begin{Bmatrix} (m-1)(k^2-2k)+3k^2-3 \\ -1 \end{Bmatrix} . \quad (2.26)$$

If these solutions exist, they will be expressible as functions of both the particular number of steps per half cycle, $k$, and $\beta$; written $\underset{\sim}{y}^u = \underset{\sim}{h}(k, \beta)$. Since these solutions must lie in region $I_a$ and hold for all $k$ greater than some initial step region, $\underset{\sim}{h}$ can grow no faster than $O(k)$. For $\underset{\sim}{y}_0$ and $\underset{\sim}{y}_{mk+k+1}$ in Eq. (2.26) to be members of this set of unbounded solutions two conditions must be satisfied,

$$1) \quad \dot{y}_{mk+k+1} = \dot{y}^u(k+2) \ , \ \dot{y}_0 = \dot{y}^u(k) \ ,$$

and

2) $y_{mk+k+1} - y_0$ = a function of $m$ and $\beta$ only.

The first of these conditions states that if $\dot{y}_0$ is an unbounded solution, $\dot{y}_0 = \dot{y}^u(k,\beta)$, then its mapping into the $(k+2)$-step region must also be an unbounded solution for $k+2$ steps, $\dot{y}_{mk+k+1} = \dot{y}^u(k+2,\beta)$. This is essentially a periodicity condition for growing solutions. The solutions, $\underset{\sim}{\dot{y}}^u$, must lie within region $I_a$, and so as $k$ grows, $y^u$ can grow by at most a constant with each mapping. This is the restriction in condition 2.

The form $\dot{y}^u = ak+b$ satisfies the requirement that $\dot{y}^u = O(k)$. By applying condition 1, it is found that $a = \beta$. The equation for the $y$ component of Eq. (2.26) then becomes

$$y_{mk+k+1} - y_0 = 2[b(m+1)+\beta(m+2)]\,k + 4(\beta+m-1) \quad . \tag{2.27}$$

Applying condition 2 to Eq. (2.27) we find that $b = -\beta\dfrac{m+2}{m+1}$, and thus

$$\dot{y}^u = \beta\left(k - \frac{m+2}{m+1}\right) \quad . \tag{2.28}$$

The solution, $y^u$, can not be directly determined from Eq. (2.25) as is to be expected. This is because the perturbation equation for the unbounded solutions is the same as Eq. (2.20), and $y^u$ is the range of values that follow that mapping pattern. As in the case for the complex periodic solutions, these mappings become complicated for $m>1$. The case of $m = 1$ shows the simplest pattern where the solutions grow by one step per half cycle. From the half cycle mapping of the k-step

region shown in Fig. 2.3, $\underset{\sim}{y}^u$ must lie between the intercepts of $\dot{y}^u = \beta\left(k - \frac{m+2}{m+1}\right)$ and the lines 1 - 4 and $\dot{y} = \frac{1}{2}(y + 1)$. This restriction yields

$$\beta(k - 1) + 1 \leq y^u(m = 1) \leq 2\beta\left(k - \frac{3}{2}\right) - 1 \quad . \tag{2.29}$$

Figure 2.5 shows these unbounded solutions in region $I_a$ of the phase plane for $m = 1, 2$, and 3.

Equation (2.29) also implies that there is a minimum $k$ for such unbounded solutions, such that all solutions, $\underset{\sim}{y}^u$, for $k$ greater than or equal to this minimum behave as predicted. These solutions must follow a different mapping behavior before they map onto the regions which contain the unbounded solutions. Some of these solutions were numerically backmapped. They mapped into the linear region, $|y_n| < 1$, and followed a complicated mapping behavior. Eventually these solutions backmapped into regions that, in this reverse solution, corresponded to the growing solutions of the forward problem. Generally, it seems that the growing solutions come from unboundedly large values and map with the pattern $(k, m(k - 1), k - 2, m(k - 3)\ldots)$ down to a point where they map into the linear region. From there they eventually map away from the origin of the phase plane with $(k, m(k + 1), k + 2, \ldots)$.

It has been shown that the growth in the Hamiltonian for solutions, $\underset{\sim}{y}_n$, is bounded by an exponential growth given by

$$H_n \leq H_0 e^{\alpha n} \quad , \quad \alpha > 0 \tag{2.30}$$

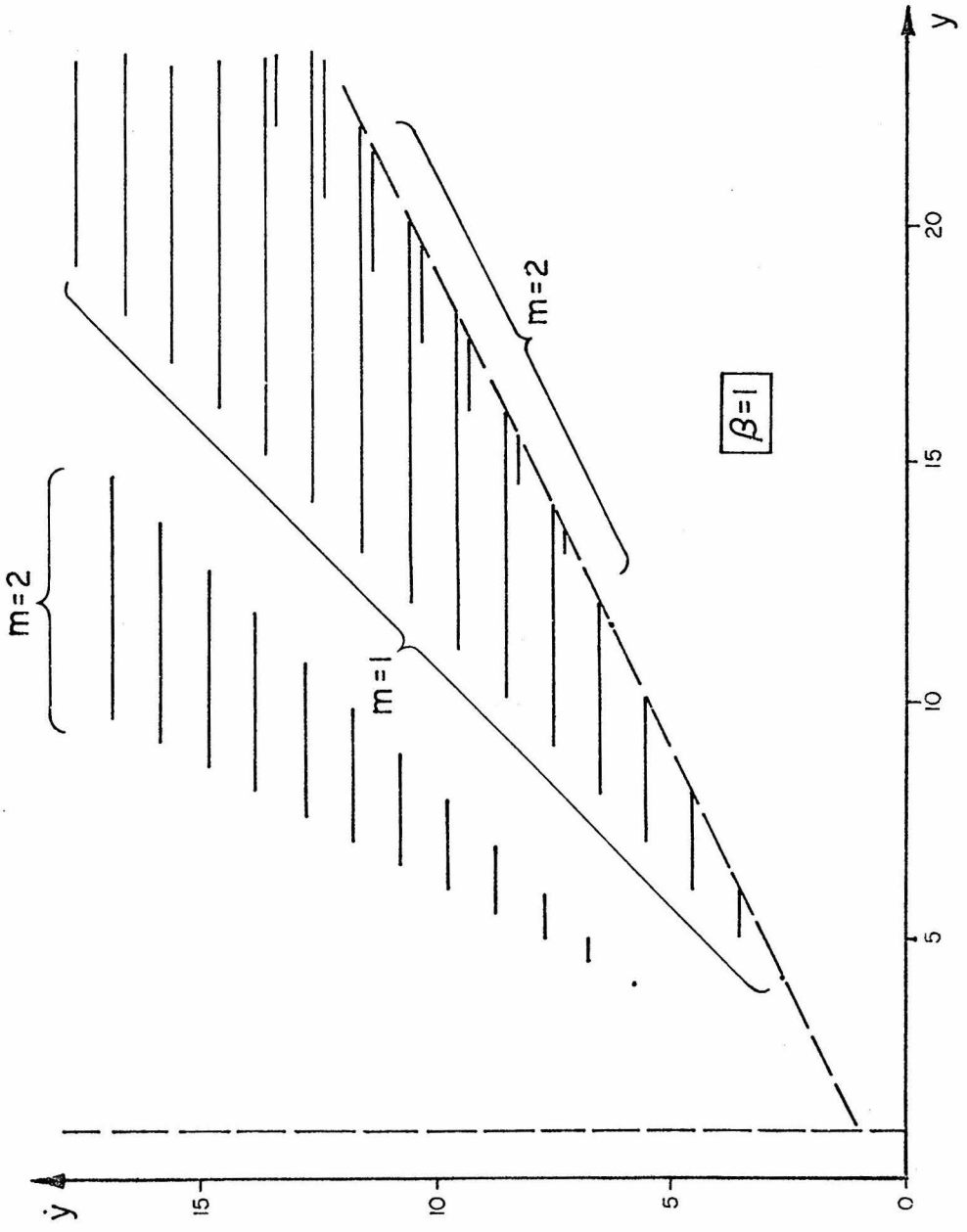


Figure 2.5 - Unbounded Solutions in Region $I_a$ for $m = 1$ and 2 in Eq. (2.28)

with $\alpha$ equal to a constant [8]. For the set of unbounded solutions analyzed, the actual growth in the Hamiltonian can be calculated from its jump in one transformation of the (m(k), k+1) pattern. Applying the transformation for this pattern, given by Eq. (2.26), to Eq. (2.8), and using Eq. (2.28), it is found that

$$\Delta H\Big|_0^{mk+k+1} = 2\beta\left\{\beta k - (\beta + m)\left(\frac{m+2}{m+1}\right) + 2m + 2\beta + 1\right\} . \qquad (2.31)$$

The average increase in the Hamiltonian per step is

$$\Delta H_{ave} = \frac{2\beta}{(m+1)k+1}\left\{\beta k - (\beta+m)\left(\frac{m+2}{m+1}\right) + 2m + 2\beta + 1\right\} . \qquad (2.32)$$

For large k Eq. (2.32) becomes

$$\Delta H_{ave} = \frac{2\beta^2}{(m+1)} + O(1/k) \qquad (2.33)$$

and thus for n large

$$H_n = \frac{2\beta^2}{(m+1)}n + O(1) . \qquad (2.34)$$

With the jump in the Hamiltonian known for each mapping (Eqs. (2.9) and (2.10)), an upper bound on the Hamiltonian growth can be derived using the results of the mapping analysis. Since the Hamiltonian is conserved for all mappings in regions I and V, the maximum possible

Hamiltonian jump per half cycle is given by Eq. (2.9) for $y_0 = 1$,

$$\Delta H_{max} = -2\beta(\dot{y}+1) \quad , \quad (\dot{y}<0) \quad . \tag{2.35}$$

Averaging this maximum jump over the number of steps per half cycle, $n_{hc}$, yields

$$\Delta H \leq \frac{-2\beta}{n_{hc}}(\dot{y}+1) \quad . \tag{2.36}$$

From the transformation analysis of Section 2.1, it was found that the half cycle period is linear in $\dot{y}$. Thus Eqs. (2.36) and (2.17) yield

$$\Delta H \leq 2\beta^2 + O(1/n_{hc}) \quad . \tag{2.37}$$

For n large then,

$$H_n \leq 2\beta^2 n + O(1) \quad , \tag{2.38}$$

and the Hamiltonian for all solutions is thus bounded by an O(n) growth.

## III The Solutions for $s>0$

### 3.1 The Phase Plane Transformations

The analysis presented in the previous chapter can now be extended to the more general set of Eqs. (2.5a) and (2.5b) with $f(\beta,\mu,y)$ given by

$$f(\beta,\mu,y) = \begin{cases} \mu y + (\beta-\mu)\mathrm{sgn}(y) & ; \ |y| \geq 1 \\ \beta y & ; \ |y| \leq 1 \end{cases} \qquad (3.1)$$

$$\mu = \alpha^2 s \ .$$

The solutions of Eqs. (2.5a) and 2.5b) for $\beta > \mu$ will be examined first, and generalizations of these solutions to the solutions for $\beta < \mu$ will be discussed in Section 3.5. Clearly, $\beta = \mu$ reduces Eqs. (3.1), (2.5a), and (2.5b) to a linear problem.

Following the method of Chapter II, the phase plane is divided into the nine regions, Fig. 3.1, each with its linear transformation specified by the solutions location on the branches of $f(\beta,\mu,y)$. The regions and their transformations are

$$\left.\begin{aligned} &\text{I:} \quad y_n \geq 1, \ y_{n+1} > 1 \\ &\dot{y}_n > \frac{1}{2}\left\{(\mu-1)y_n + 1 + 2\beta - \mu\right\} \\ &\underset{\sim}{y}_{n+1} = \underset{\sim}{A}\underset{\sim}{y}_n - \frac{2(\beta-\mu)}{1+\mu}\underset{\sim}{1} \end{aligned}\right\} \qquad (3.2a)$$

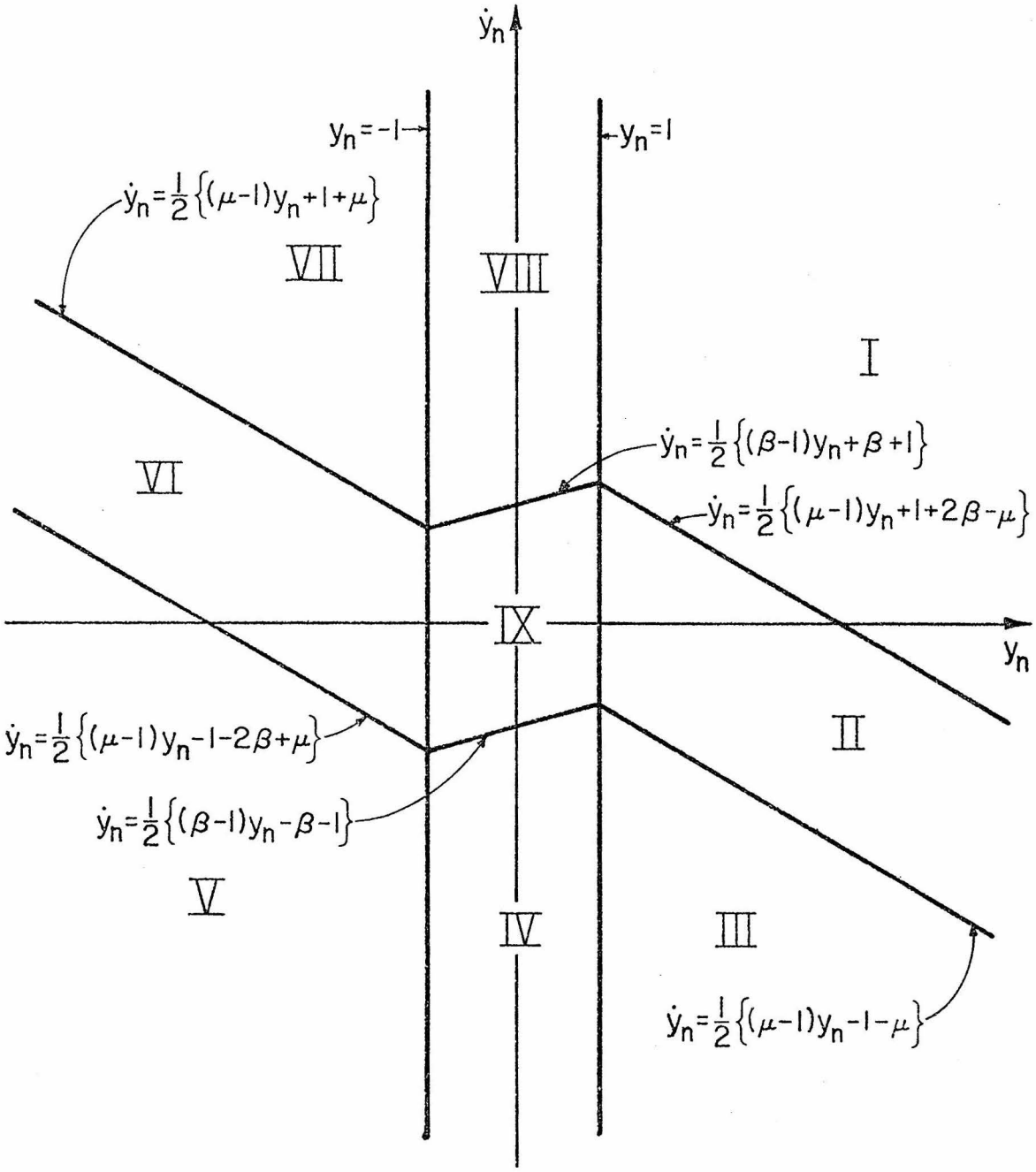


Figure 3.1 - Phase Plane Transformation Regions for $s>0$

II: $y_n \geq 1, \ |y_{n+1}| \leq 1$

$$\frac{1}{2}\left\{(\mu-1)y_n - 1 - \mu\right\} \leq \dot{y}_n \leq \frac{1}{2}\left\{(\mu-1)y_n + 1 + 2\beta - \mu\right\}$$

$$\underset{\sim}{y}_{n+1} = \underset{\sim}{B}(\beta,\mu)\underset{\sim}{y}_n + \frac{(\mu-\beta)}{1+\beta}\underset{\sim}{1} \qquad (3.2b)$$

III: $y_n \geq 1, \ y_{n+1} \leq -1$

$$\dot{y}_n \leq \frac{1}{2}\left\{(\mu-1)y_n - 1 - \mu\right\}$$

$$\underset{\sim}{y}_{n+1} = \underset{\sim\sim}{A}\underset{\sim}{y}_n \qquad (3.2c)$$

IV: $|y_n| \leq 1, \ y_{n+1} < -1$

$$\dot{y}_n \leq \frac{1}{2}\left\{(\beta-1)y_n - 1 - \beta\right\}$$

$$\underset{\sim}{y}_{n+1} = \underset{\sim}{B}(\mu,\beta)\underset{\sim}{y}_n + \frac{\beta-\mu}{1+\mu}\underset{\sim}{1} \qquad (3.2d)$$

V: $y_n \leq -1, \ y_{n+1} < -1$

$$y_n < \frac{1}{2}\left\{(\mu-1)y_n - 1 - 2\beta + \mu\right\}$$

$$\underset{\sim}{y}_{n+1} = \underset{\sim\sim}{A}\underset{\sim}{y}_n + \frac{2(\beta-\mu)}{1+\mu}\underset{\sim}{1} \qquad (3.2e)$$

VI: $y_n \leq -1, \ |y_{n+1}| \leq 1$

$$\frac{1}{2}\left\{(\mu-1)y_n - 1 - 2\beta + \mu\right\} \leq \dot{y}_n \leq \frac{1}{2}\left\{(\mu-1)y_n + 1 + \mu\right\}$$

$$\underset{\sim}{y}_{n+1} = \underset{\sim}{B}(\beta,\mu)\underset{\sim}{y}_n + \frac{(\mu-\beta)}{1+\beta}\underset{\sim}{1} \qquad (3.2f)$$

VII: $y_n \leq -1,\ y_{n+1} \geq 1$

$$\dot{y}_n > \frac{1}{2}\left\{(\mu-1)y_n + 1 + \mu\right\}$$

$$\underset{\sim}{y}_{n+1} = \underset{\sim\sim}{A}\underset{\sim}{y}_n \qquad (3.2g)$$

VIII: $|y_n| \leq 1,\ y_{n+1} > 1$

$$\dot{y}_n > \frac{1}{2}\left\{(\beta-1)y_n + 1 + \beta\right\}$$

$$\underset{\sim}{y}_{n+1} = \underset{\sim}{B}(\mu,\beta)\underset{\sim}{y}_n + \frac{\mu-\beta}{1+\mu}\underset{\sim}{1} \qquad (3.2h)$$

IX: $|y_n| \leq 1,\ |y_{n+1}| < 1$

$$\frac{1}{2}\left\{(\beta-1)y_n - 1 - \beta\right\} \leq y_n \leq \frac{1}{2}\left\{(\beta-1)y_n + 1 + \beta\right\}$$

$$\underset{\sim}{y}_{n+1} = \underset{\sim\sim}{D}\underset{\sim}{y}_n \qquad (3.2i)$$

with

$$A = \begin{bmatrix} \frac{1-\mu}{1+\mu} & \frac{2}{1+\mu} \\ \frac{-2\mu}{1+\mu} & \frac{1-\mu}{1+\mu} \end{bmatrix} = \begin{bmatrix} \cos\theta & \frac{\sin\theta}{\sqrt{\mu}} \\ -\sqrt{\mu}\sin\theta & \cos\theta \end{bmatrix}$$

$$\theta = \cos^{-1}\left(\frac{1-\mu}{1+\mu}\right)$$

$$B(\beta,\mu) = \begin{bmatrix} \frac{1-\mu}{1+\beta} & \frac{2}{1+\beta} \\ \frac{-(\beta+\mu)}{1+\beta} & \frac{1-\beta}{1+\beta} \end{bmatrix} \qquad D = \begin{bmatrix} \frac{1-\beta}{1+\beta} & \frac{2}{1+\beta} \\ \frac{-2\beta}{1+\beta} & \frac{1-\beta}{1+\beta} \end{bmatrix}. \qquad (3.2j)$$

Basically, the solutions in mapping through the half plane for $\mu > 0$ are similar to the solutions for $\mu = 0$. That is, in the phase plane, both solutions will map $k$ times into $|y_n| > 1$, and then will either map into the linear region, $|y_n| < 1$, or onto the outer branch of the next half cycle. The subregion of $I_a$ which contains all of the solutions that

mapped from $|y_{n-1}|<1$ into $|y_n|>1$ is again designated region $I_a$. Region $I_a$ contains only one point of each of the possible solutions of Eqs. (2.5) in a half cycle of the phase plane. Thus it is sufficient to consider only this subset of points and its mappings in a half cycle.

The backwards mapping of region $I_a$ onto itself during one half cycle, given the appropriate transformations specified by Eqs. (3.2), will then yield the subregion of $I_a$ containing the k-step outer branch solutions. To be more explicit, region $I_a$ is the forward mapping of regions VII and VIII into region I, as defined by the lines

$$y_n = 1$$

$$\dot{y}_n = \frac{1}{2}\left\{(1-\mu)y_n + 1 + \mu\right\} = \sqrt{\mu}\,\frac{\cos\theta}{\sin\theta}y_n - \frac{1}{2}(1+2\beta-\mu) \quad . \qquad (3.3)$$

Region Ia is backmapped onto the region $I_a$ for the previous half cycle through k-steps to determine the k-step mapping region.

This backmapping of the boundaries of $I_a$ in Eq. (3.3) defines the k-step outer branch mapping region as lying between the lines

$$y^{upper} = -\sqrt{\mu}\,\frac{\cos k\theta}{\sin k\theta}y + \frac{\sqrt{\mu}}{\sin k\theta}\left\{-1 + \frac{\beta-\mu}{(1+\mu)(1-\cos\theta)}\left(a_{k-1} + \frac{b_{k-1}}{\sqrt{\mu}}\right)\right\} \qquad (3.4a)$$

$$\dot{y}^{lower} = -\sqrt{\mu}\,\frac{\cos(k-1)\theta}{\sin(k-1)\theta}y + \frac{\sqrt{\mu}}{\sin k\theta}\left\{1 + \frac{\beta-\mu}{(1+\mu)(1-\cos\theta)}\left(-a_{k-1} + \frac{b_{k-1}}{\sqrt{\mu}}\right)\right\} \qquad (3.4b)$$

with

$$a_k = \cos\theta + \cos k\theta - \cos(k+1)\theta - 1$$
$$b_k = \sin\theta + \sin k\theta - \sin(k+1)\theta \quad . \tag{3.4c}$$

Fig. 3.2 shows region $I_a$ and its subdivision into the k-step regions. The solutions mapping k times in $y_n \geq 1$ and once in $|y_n| < 1$ in a half cycle will thus lie between $\dot{y}^{lower}(k+1)$ and $\dot{y}^{upper}(k)$. The transformation of a k-step solution is found by mapping the solution k - 1 times in region I and once in region III, and is

$$\left.\begin{aligned} \underset{\sim}{y}_k &= \begin{bmatrix} -\cos k\theta & \dfrac{-\sin k\theta}{\sqrt{\mu}} \\ \sqrt{\mu}\sin k\theta & -\cos k\theta \end{bmatrix} \underset{\sim}{y}_0 + \begin{Bmatrix} f_1 \\ f_2 \end{Bmatrix} \\ f_1 &= \frac{(\beta-\mu)}{(1+\mu)(1-\cos\theta)}\left(a_{k-1} + b_{k-1}/\sqrt{\mu}\right) \\ f_2 &= \frac{(\beta-\mu)}{(1+\mu)(1-\cos\theta)}\left(a_{k-1} - \sqrt{\mu}\, b_{k-1}\right) \end{aligned}\right\} \tag{3.5}$$

with $a_k$ and $b_k$ given by Eq. (3.4c). By definition $\underset{\sim}{y}_k$ is in region $I_a$.

The transformation for those solutions which map k - 1 times in $y_n \geq 1$ and once in $|y_n| < 1$ is calculated in a similar manner, and is

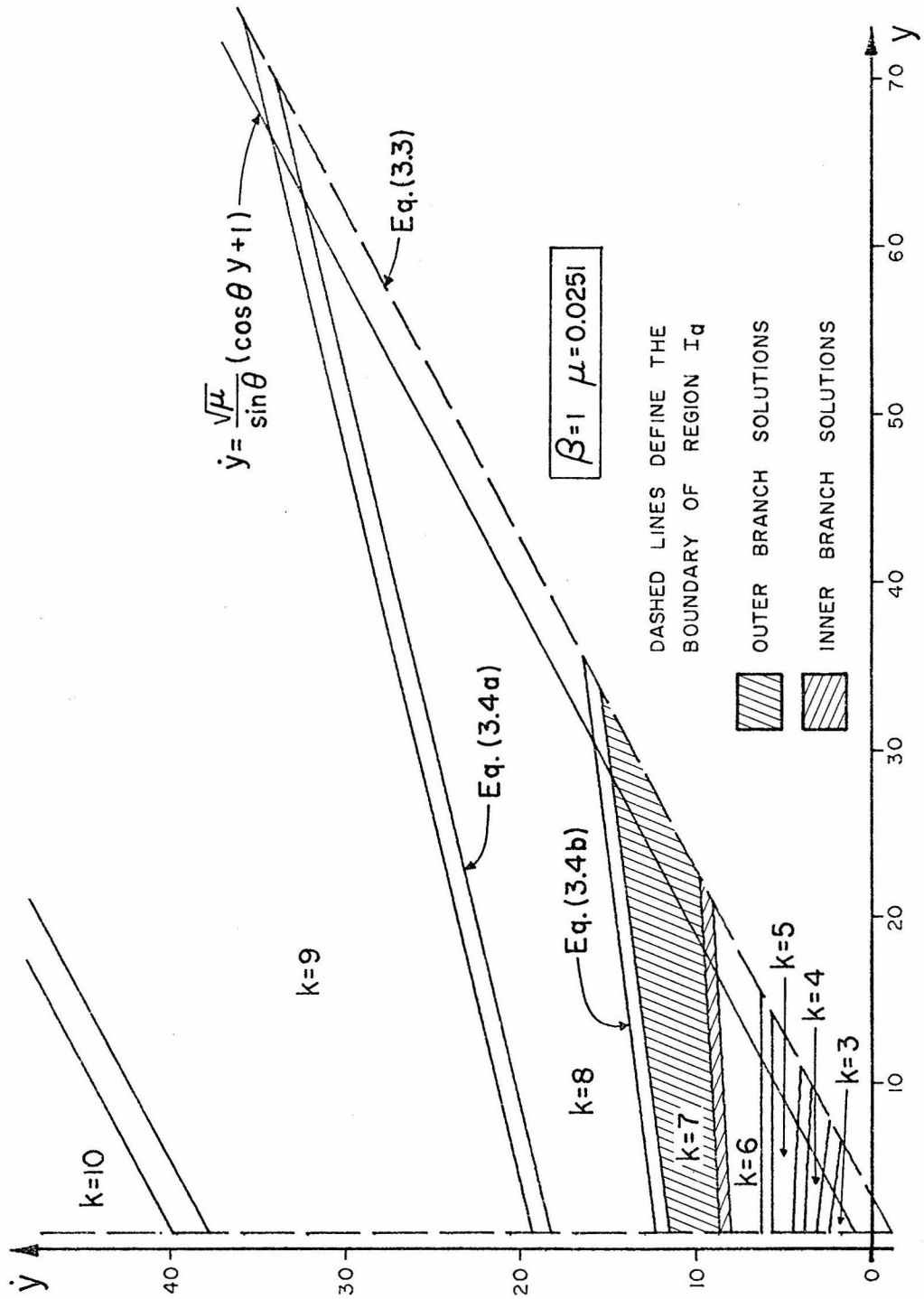


Figure 3.2 - The k-step Mapping Regions of Region $I_a$

$$\underset{\sim}{y}_k = \frac{-1}{(1+\beta)(1+\mu)} \left[ \underset{\sim}{E}\,\underset{\sim}{y}_0 + \begin{Bmatrix} g_1 \\ g_2 \end{Bmatrix} \right]$$

where

$$\left.\begin{aligned}
e_{11} &= \{1 - 3(\beta+\mu) + \beta\mu\}\cos(k-2)\theta - 4\sqrt{\mu}\,(1-\beta)\sin(k-2)\theta \\
e_{12} &= \{1 - 3(\beta+\mu) + \beta\mu\}\frac{\sin(k-2)\theta}{\sqrt{\mu}} + 4(1-\beta)\cos(k-2)\theta \\
e_{21} &= -\{1 - 3(\beta+\mu) + \beta\mu\}\sqrt{\mu}\sin(k-2)\theta - 2(1-\mu)(\beta+\mu)\cos(k-2)\theta \\
e_{22} &= \{1 - 3(\beta+\mu) + \beta\mu\}\cos(k-2)\theta - 2(1-\mu)(\beta+\mu)\frac{\sin(k-2)\theta}{\sqrt{\mu}} \\
g_1 &= \{1 - 3(\beta+\mu) + \beta\mu\}c_1 + 4(1-\beta)c_2 + 2(\beta-\mu)(\beta-1) \\
g_2 &= -2(1-\mu)(\beta+\mu)c_1 + \{1 - 3(\beta+\mu) + \beta\mu\}c_2 + 2\beta^2 - 2\mu^2 \\
c_1 &= \frac{\mu-\beta}{(1+\mu)(1-\cos\theta)}\left\{a_{k-3} + \frac{b_{k-3}}{\sqrt{\mu}}\right\} \\
c_2 &= \frac{\mu-\beta}{(1+\mu)(1-\cos\theta)}\left\{a_{k-3} - \sqrt{\mu}\,b_{k-3}\right\}
\end{aligned}\right\} \quad (3.6)$$

Again, $a_k$ and $b_k$ are given in Eq. (3.4c).

There exists a bound on the maximum number of steps per half cycle, denoted as $k_{max}$, by virtue of the fact that for any $k > k_{max}$ the backmapping of $I_a$ with $k$ steps does not map into $I_a$ but beyond this region and into the previous half cycle of the phase plane. Thus, some part of region $I_a$ which has been backmapped $k$ times must map onto $I_a$. It can be seen from Fig. 3.2 that for this condition to hold

the slope of the lower line defining the boundary of the $k_{max}$ step region must be positive and finite. Equation (3.4b) defines this lower boundary of the $k_{max}$ step region, and thus, $k_{max}$ is defined by

$$k_{max} = \max_{k=1,2,3\ldots} \{k\}$$

such that

$$\infty > -\sqrt{\mu}\cos(m-1)\theta/\sin(m-1)\theta\,,\quad 0<m\leq k\,,$$

and

$$-\sqrt{\mu}\cos k_{max}\theta/\sin k_{max}\theta < 0\quad .$$

These conditions imply

$$k_{max} < \frac{\pi}{\theta} + 1\quad . \tag{3.7}$$

$k_{min}$ is defined as it is for the $\mu = 0$ solutions and is given by Eq. (2.16).

To analyze the general solution behavior in mapping from one half cycle onto the next, each of the solutions in the k-step region is forward mapped into region $I_a$ of the next half cycle. For those k-step solutions which map only in the outer branches, $|y_n| \geq 1$, the k-step transformation is given by Eq. (3.5) and maps the k-step region of $I_a$ into that area of region $I_a$ bounded by

$$\dot{y}^{upper} = \sqrt{\mu}\ \mathrm{ctn}(k+1)\theta\, y + \frac{(1+2\beta-\mu)\sin\theta}{2\sin(k+1)\theta} - \sqrt{\mu}\ \mathrm{ctn}(k+1)\theta f_1 + f_2 \qquad (3.8a)$$

and

$$\dot{y}^{lower} = \sqrt{\mu}\ \mathrm{ctn}\, k\theta\ y + \sqrt{\mu}/\sin k\theta - \sqrt{\mu}\ \mathrm{ctn}\, k\theta\, f_1 + f_2 \qquad (3.8b)$$

with $f_1$ and $f_2$ given in Eq. (3.5). Similarly, for those k-step solutions mapping into $|y_n|<1$, Eq. (3.6) implies that the inner branch solutions map between

$$\dot{y}^{upper} = \frac{\left(e_{21}+\sqrt{\mu}\ \mathrm{ctn}\ \theta\ e_{22}\right)}{\left(e_{11}+\sqrt{\mu}\ \mathrm{ctn}\ \theta\ e_{12}\right)} y + \frac{\eta}{\left(e_{11}+\sqrt{\mu}\ \mathrm{ctn}\ \theta\ e_{12}\right)} \left\{ -\frac{\gamma}{2} - \left(e_{21}+\sqrt{\mu}\ \mathrm{ctn}\ \theta\, e_{22}\right) g_1 \right\} + \eta g_2 \ , \qquad (3.9a)$$

$$\eta = -\frac{1}{(1+\beta)(1+\mu)} \ , \ \gamma = 1+2\beta-\mu$$

and

$$\dot{y}^{lower} = \frac{e_{22}}{e_{12}} y - \frac{\eta}{e_{12}} \{ -1 - e_{22} g_1 \} + \eta g_2 \qquad (3.9b)$$

in the linear mapping subregion of $I_a$. $e_{11}$, $e_{12}$, $e_{21}$, $e_{22}$, $g_1$, and $g_2$ are given in Eq. (3.6). Figures 3.3 show the forward mappings of the k-step region for $\mu = 0.006$ and $k = 6$, 10, and 14.

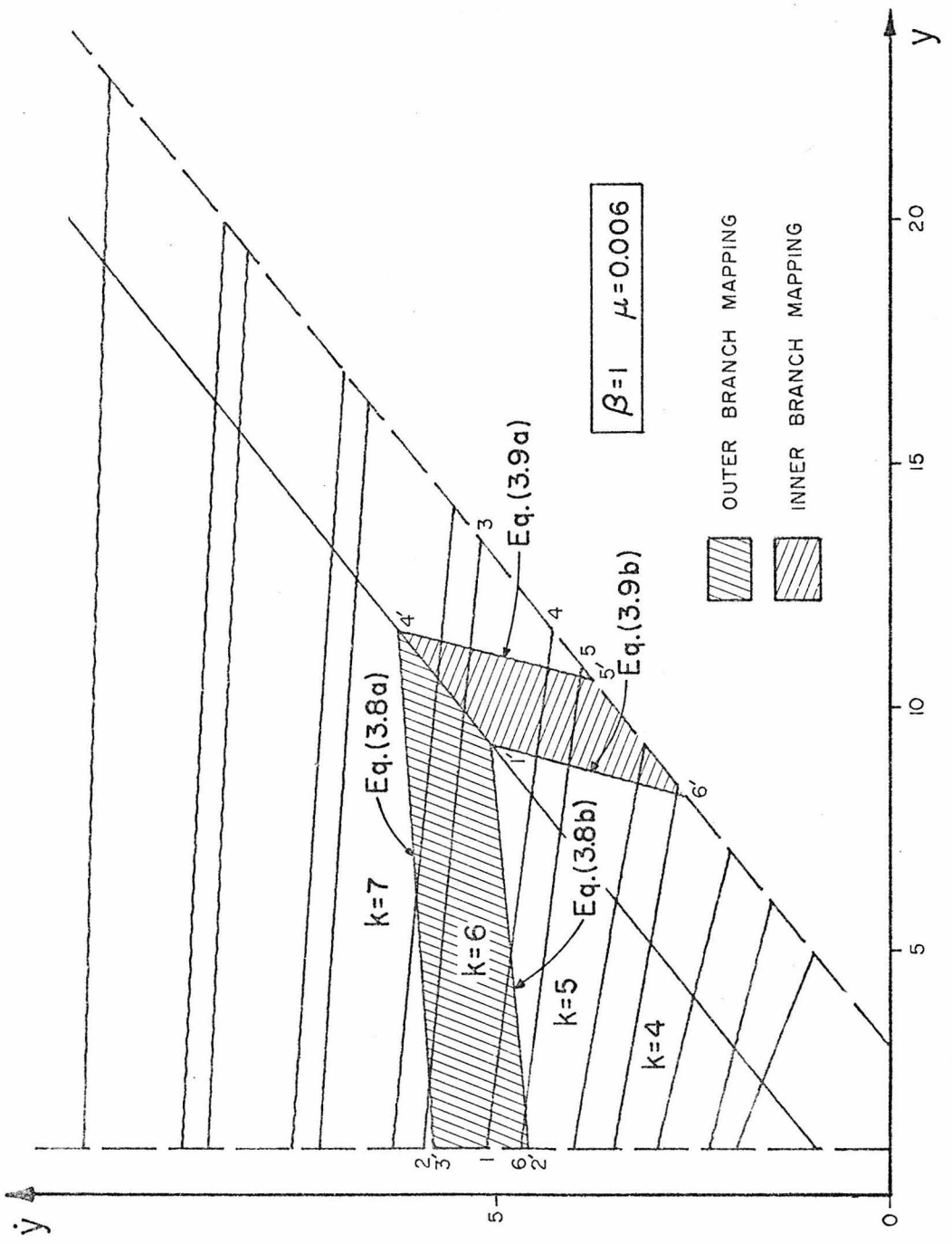


Figure 3.3a - Half Cycle Mapping of a k-step Region (k = 6)

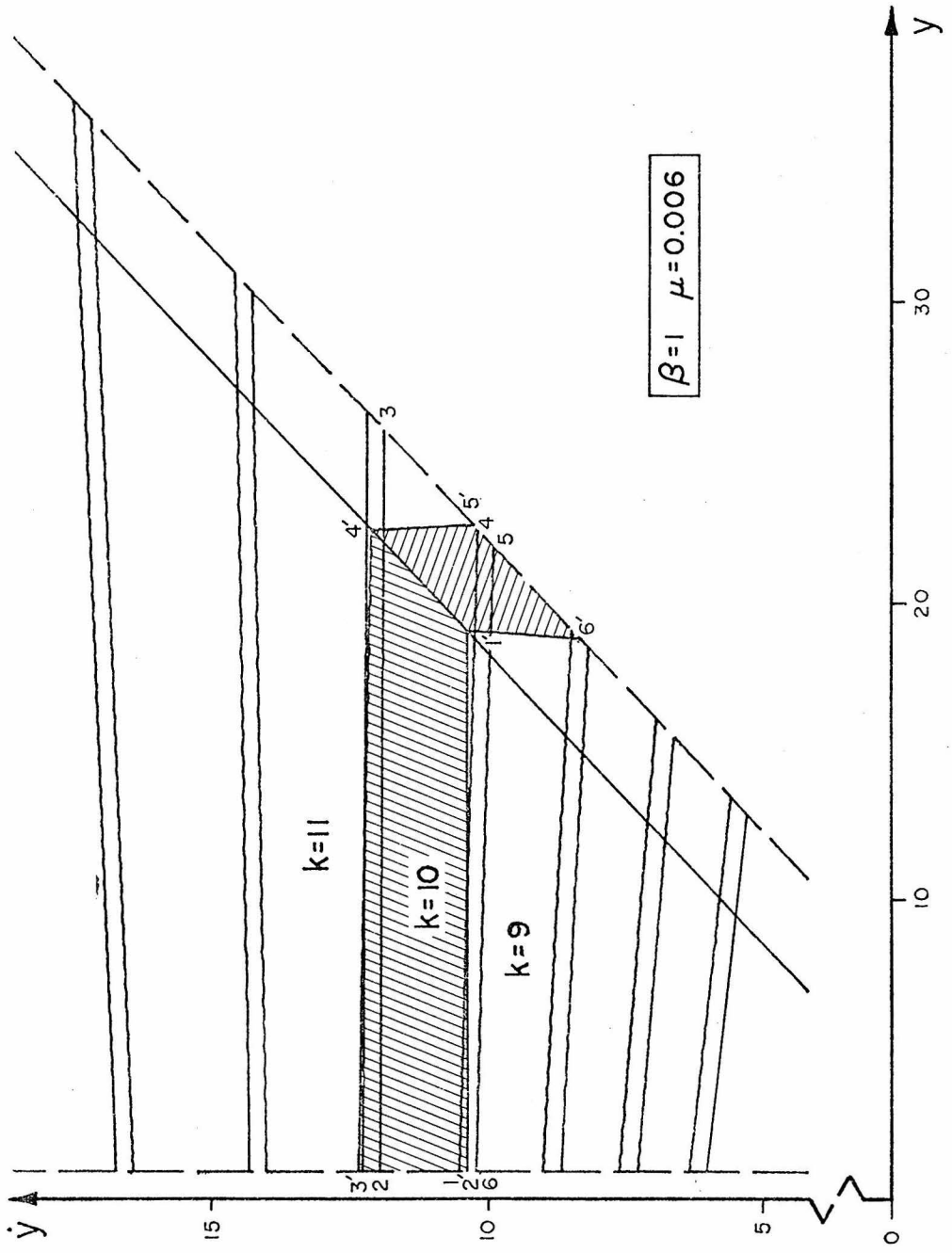


Figure 3.3b - Half Cycle Mapping of a k-step Region (k = 10)

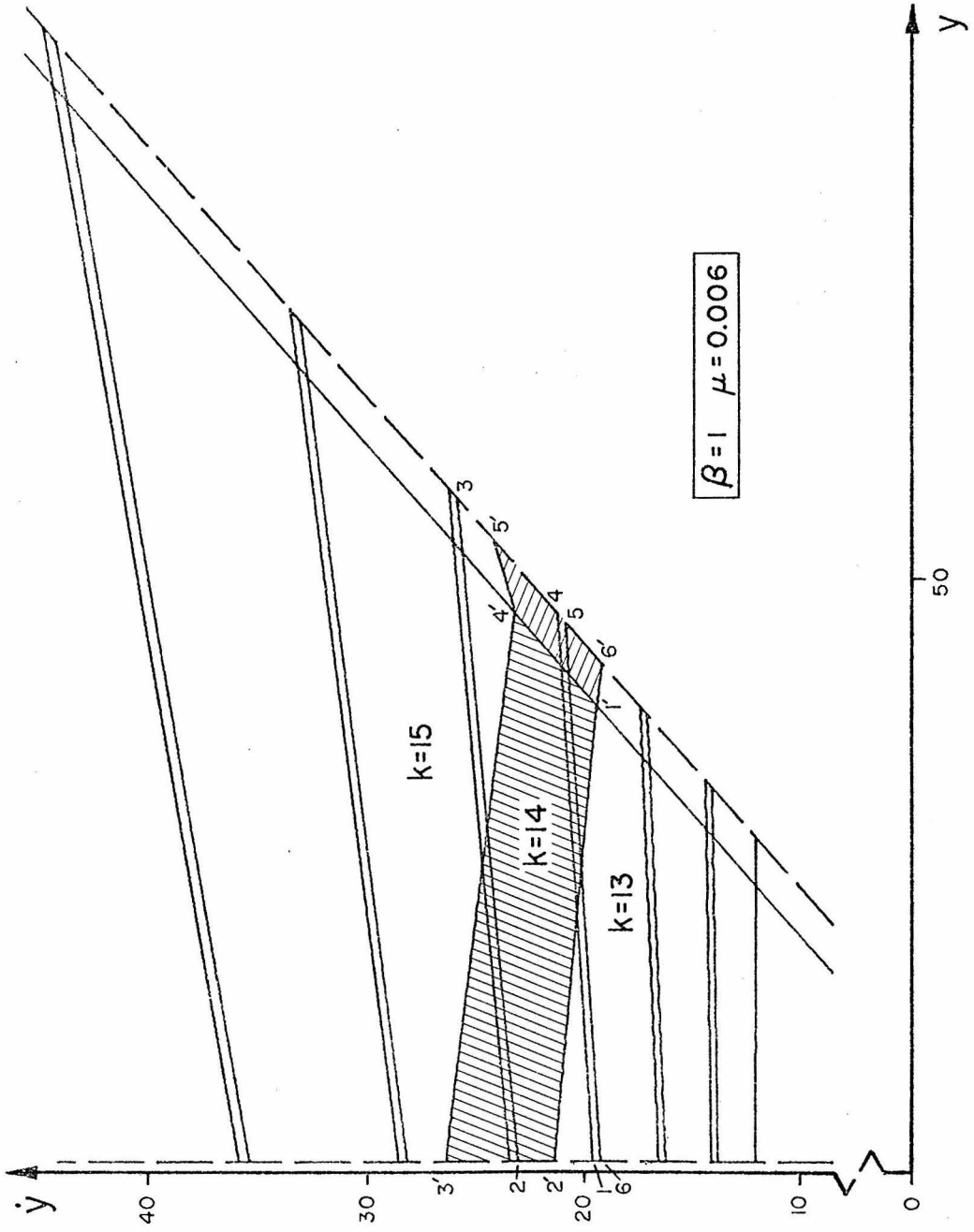


Figure 3.3c - Half Cycle Mapping of a k-step Region (k = 14)

From the equations defining the mapping of a k-step region and from Figs. 3.3, it can be seen that there is a difference in the mapping configuration between values of $k<k_{max}/2$ compared to $k>k_{max}/2$. This shows up in comparing the mapping of the k-step region between Fig. 3.3a and Fig. 3.3c. Point 3 of the k-step region is mapped into the $(k+1)$-step region for $k>k_{max}/2$, while point 4 is mapped into the $(k+1)$-step region for $k<k_{max}/2$. This change in mapping behavior will later explain why some types of solutions were found to exist within only one or the other of these ranges of k.

To determine exactly what areas of $I_a$ the k-step region maps onto, the points which define the mapping of the k-step regions are compared to the points which define the mapping regions in $I_a$. For $\beta>\mu$ and $k_{min}<k\leq k_{max}$ it can be proven that;

1) The outer branch solutions mapping k steps in one half cycle can map only onto the $(k-1)$, k, or $(k+1)$-step regions of the outer branch solutions, or onto the k or $(k+1)$-step regions of the inner branch solutions, and
2) The inner branch solutions mapping k steps in one half cycle can map only onto the $(k-1)$, k, or $(k+1)$-step regions of the outer branch solutions, or onto the $(k-1)$, k, or $(k+1)$-step regions of the inner branch solutions.

## 3.2 The Simple Periodic Solutions

Similar to the $\mu = 0$ case of the previous chapter we now seek

the solutions periodic in one cycle with the pattern (k,k) and state the following theorem.

Theorem 3.1

For $\beta > \mu$ and for all k such that $k_{min} < k \leq k_{max} - 1$ there exist (k,k) periodic outer branch solutions whose solution in region $I_a$ of the phase plane is given by

$$\underset{\sim}{y}^p = \frac{(\beta - \mu)(\cos\theta + \cos(k-1)\theta - \cos k\theta - 1)}{(1+\mu)(1-\cos\theta)(1+\cos k\theta)} \begin{Bmatrix} 1 \\ 1 \end{Bmatrix} . \tag{3.10}$$

proof:

From the discussion in Section 3.1 on the mapping of a k-step region in a half cycle it is known that there exist outer branch solutions which map with a (k,k) pattern. The transformation for a (k,k) mapping is found from Eq. (3.5) and is

$$\underset{\sim}{y}_{2k} = \begin{bmatrix} \cos 2k\theta & \sin 2k\theta/\sqrt{\mu} \\ -\sqrt{\mu}\sin 2k\theta & \cos 2k\theta \end{bmatrix} \underset{\sim}{y}_0 + \begin{Bmatrix} (\cos k\theta - 1)f_1 + \frac{\sin k\theta}{\sqrt{\mu}} f_2 \\ -\sqrt{\mu}\sin k\theta\, f_1 + (\cos k\theta - 1)f_2 \end{Bmatrix} \tag{3.11}$$

with $f_1$ and $f_2$ given in Eq. (3.5). The periodic solution of Eq. (3.11) is given by Eq. (3.10). For $k_{min} < k \leq k_{max} - 1$ these solutions can be

shown to lie within the k-step region of $I_a$. Note that the restriction on k implies $\mu < 1/3$, since $k_{max} = 3$ for $\mu = 1/3$ and $k_{min} = 2$ for all $\beta > 1/3$.

To examine the stability of these periodic solutions to perturbations, let $\underset{\sim}{y} = \underset{\sim}{y}^p + \underset{\sim}{\varphi}$ and assume $\underset{\sim}{\varphi}$ is small enough such that the solutions, $\underset{\sim}{y}$, will follow the same mappings as the periodic solution, $\underset{\sim}{y}^p$. Thus the (k,k) transformation given by Eq. (3.11) will hold, and by subtracting the periodic solution we obtain the perturbation equation

$$\underset{\sim}{\varphi}_{2k} = \begin{bmatrix} \cos 2k\theta & \dfrac{\sin 2k\theta}{\sqrt{\mu}} \\ -\sqrt{\mu}\sin 2k\theta & \cos 2k\theta \end{bmatrix} \underset{\sim}{\varphi}_0 \qquad (3.12)$$

or

$$\underset{\sim}{\varphi}_{n+1} = \underset{\sim}{A}\underset{\sim}{\varphi}_n \quad \text{with} \quad \underset{\sim}{A} = \begin{bmatrix} \cos\theta & \dfrac{\sin\theta}{\sqrt{\mu}} \\ -\sqrt{\mu}\sin\theta & \cos\theta \end{bmatrix} . \qquad (3.13)$$

The determinant of $\underset{\sim}{A}$ is unity and the eigenvalues are complex conjugates with

$$\lambda_{1,2} = \cos\theta \pm i \sin\theta \ ,$$

and so there exists a conserved, quadratic equation for $\underset{\sim}{\varphi}_n$ which is

$$\dot{\varphi}_n^2 + \mu\varphi_n^2 = c \ , \qquad (3.14)$$

with c a constant for all n. Therefore, for $\underset{\sim}{\varphi}_n$ sufficiently small, the perturbations from the periodic solutions are bounded and map onto the ellipse given by Eq. (3.14). To determine the maximum possible bounded perturbation let $c = 0$. Then $\underset{\sim}{\varphi}_n = \underset{\sim}{0}$ (from Eq. (3.14)), and $\underset{\sim}{y}$ will identically follow the periodic solutions mapping. As c is increased, the ellipse will finally grow large enough such that some of its segments will map into the linear branch. This is because the k-step region of $I_a$ is bounded by the regions mapping solutions into $|y_n|<1$. Thus the maximum c in Eq. (3.14) (which defines the maximum stability region) is such that the stability ellipse about any of the $2k$ periodic solution points is just tangent to $|y_n| = 1$. From the position of region $I_a$ in the phase plane and from the transformation of solutions in region I it can be shown that the distance from any simple periodic solution to the line $y_n = 1$ is a minimum for the solution points in region $I_a$ and region III. Furthermore, since $\mu < 1/3$, the ellipse has its major axis in the y direction. In region $I_a$ the stability ellipse is tangent to $y_n = 1$ at $\dot{\varphi}_n = 0$, $\varphi_n = y^p - 1$ which implies $c = \mu(y^p - 1)^2$. It can also be shown that the same conditions hold in region III, as the periodic solution points in III are

$$\underset{\sim}{y}^p_{III} = \begin{Bmatrix} y^p_I \\ \\ -\dot{y}^p_I \end{Bmatrix} . \qquad (3.15)$$

Thus the boundary of the largest stability region of a periodic solution is given by

$$\dot{\varphi}_n^2 + \mu \varphi_n^2 = \mu(y^p - 1)^2 \quad . \tag{3.16}$$

Figure 3.4 shows these stability regions for $\mu = 0.025$, $\beta = 1$.

These perturbations of the periodic solutions are themselves periodic when $\cos^{-1}\{(1-\mu)/(1+\mu)\} = \theta = \frac{2\pi}{m}$, where $m$ is an integer. In this case the perturbation equation, Eq. (3.13), reduces to a periodic equation for $m$ steps, that is

$$\underset{\sim}{\varphi}_{n+m} = A^m \underset{\sim}{\varphi}_n = \underset{\sim}{\varphi}_n \quad .$$

The perturbation must map back into its original stability region for $\underset{\sim}{y}_n$ to be periodic. Thus the period of $\underset{\sim}{y}_n$, denoted as $\rho$, will be the product of the least common multipliers of $2k$ and $m$. The constraint on the size of the perturbation was that $y$ always map in the same region as $\underset{\sim}{y}^p$. This meant that the maximum perturbation is such that $y_n \geq 1$ for each step. With $\underset{\sim}{y}_n$ periodic in $\rho$ steps this implies that the maximum stability region is the polygon formed by mapping the line $y_n = 1$ around $\underset{\sim}{y}^p$ with $\rho$ steps. These stability regions for $\theta = \pi/12$ are shown plotted in Fig. 3.5.

The stability of the periodic solutions to changes in $\mu$ and $\beta$ is also an important aspect of these difference equations for practical applications. This analysis can be accomplished by considering the stability region of a periodic solution, $\underset{\sim}{y}^p$, for the parameters, $\mu$

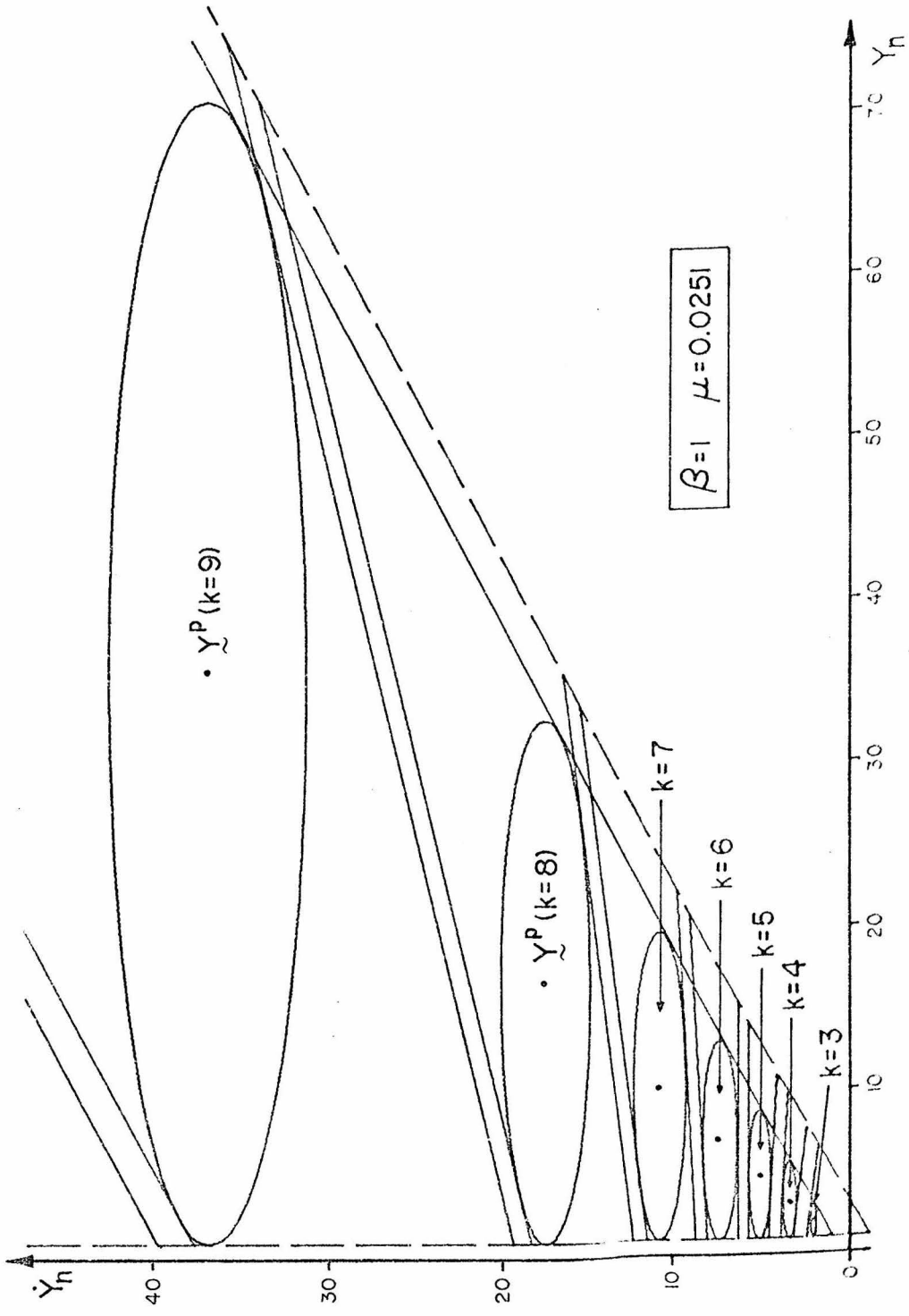


Figure 3.4 - Stability Regions of the Simple Periodic Solutions

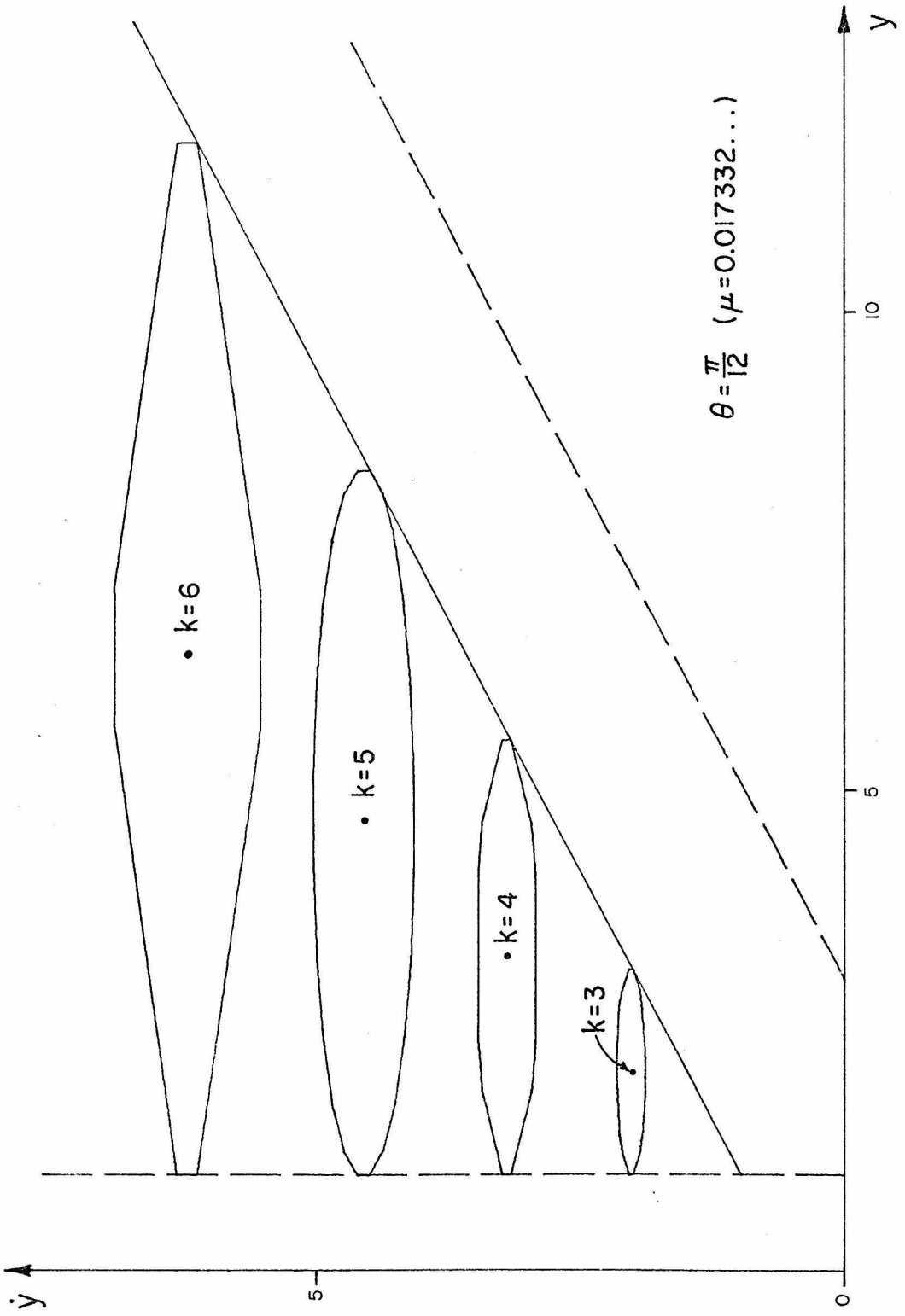


Figure 3.5 - First Few Polygonal Stability Regions of the Simple Periodic Solutions

and $\beta$, and denoting the perturbed parameters as $\mu'$ and $\beta'$. As long as $\beta' > \mu'$ and $\mu' > 1/3$ there will exist a set of simple periodic solutions for the parameters $\mu'$ and $\beta'$. By $\underset{\sim}{y}^{p'}$ we will denote the periodic solution for the primed parameters which lies closest to $\underset{\sim}{y}^{p}$ in the phase plane. Thus the solution to the perturbed system $(\mu', \beta')$ will have a bounded solution if $\underset{\sim}{y}^{p}$ lies within the stability ellipse about $\underset{\sim}{y}^{p'}$ for the parameters $\mu'$ and $\beta'$. Since all of the simple (k,k) periodic solutions lie on the line $\dot{y} = y$, $\underset{\sim}{y}^{p}$ is bounded for perturbations of $\mu$ and $\beta$ if

$$y^{p'} - \sqrt{\frac{\mu'}{1+\mu'}}\,(y^{p'} - 1) \le y^{p} \le y^{p'} + \sqrt{\frac{\mu'}{1+\mu'}}\,(y^{p'} - 1) \qquad (3.17)$$

as shown in Fig. 3.6.

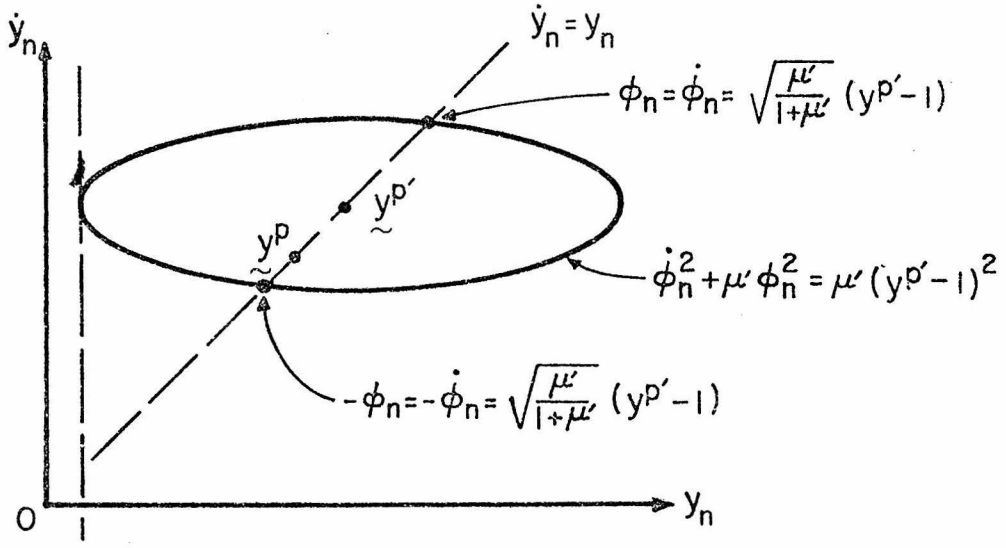


Figure 3.6 - Stability Region of a Periodic Solution, $\underset{\sim}{y}^{p'}$, for the Perturbed Parameters $\mu'$ and $\beta'$

The (k,k) inner branch periodic solutions are found in a similar manner as the outer branch periodic solutions were. This is because it is known from Section 3.1 that the (k,k) inner branch mapping exists. These periodic solutions are calculated from the associated (k,k) transformation, Eq. (3.6), and they are

$$\underset{\sim}{y}^{p1} = \frac{-(1+\beta)(1+\mu)}{\{2(1+\beta)(1+\mu)+e_{11}+e_{22}\}} \begin{pmatrix} [(1+\beta)(1+\mu)+e_{22}]g_1 + e_{12}g_2 \\ [(1+\beta)(1+\mu)+e_{11}]g_1 + e_{21}g_2 \end{pmatrix} \tag{3.18}$$

with $e_{11}$, $e_{12}$, $e_{21}$, $e_{22}$, $g_1$, and $g_2$ given in Eq. (3.6). The algebraic complexity of Eq. (3.18) does not easily lend itself to proving that this solution lies within the mapping region of the (k,k) inner branch solutions. However, all of the periodic solutions that were tested numerically did exist.

For the stability analysis of such periodic solutions, we again let $\underset{\sim}{y} = \underset{\sim}{y}^p + \underset{\sim}{\varphi}$ with $\underset{\sim}{\varphi}$ small enough such that $\underset{\sim}{y}$ follows the mappings of $\underset{\sim}{y}^p$. The perturbation equation then becomes

$$\underset{\sim}{\varphi}_{n+1} = \frac{-1}{(1+\beta)(1+\mu)} \underset{\sim}{E}\underset{\sim}{\varphi}_n \tag{3.19}$$

with the components of $\underset{\sim}{E}$ ($e_{11}$, $e_{12}$, $e_{21}$, and $e_{22}$) given in Eq. (3.6). The determinant of $\frac{-1}{(1+\beta)(1+\mu)}\underset{\sim}{E}$ is unity, and the eigenvalues must be complex conjugates for $\underset{\sim}{\varphi}_n$ to be bounded. Thus for Eq. (3.19) to admit only bounded perturbations,

$$\left|(1 - 3\beta - 3\mu + \beta\mu)\cos(k - 1)\theta + \frac{1}{\sqrt{\mu}}(3\mu\beta + \mu^2 - 3\mu - \beta)\sin(k - 1)\theta\right|$$

$$< (1 + \beta)(1 + \mu) \quad . \qquad (3.20)$$

For those values of $\beta$, $\mu$, and $k$ that satisfy Eq. (3.20), the stability region will be defined by ellipses since Eq. (3.19) will have a conserved quadratic form.

## 3.3 Other Periodic Solutions

Numerical solutions of Eqs. (2.5a) and (2.5b) for various values of $\mu$ and $\beta$ have shown that there exist periodic solutions with a structure more complex than that of the simple periodic solutions. In particular, for the number of steps per half cycle greater than $\pi/2\theta$, periodic solutions following an $(mk, k - 1)$ pattern exist with the range of values of $m$ dependent on $k$ and $\theta$. To prove the existence of these periodic patterns it would be necessary to prove the $(mk, k - 1)$ mapping can map onto itself. This quickly becomes complicated with increasing $m$. From these numerical solutions, however, it was noticed that the periodic solutions for larger $m$ were grouped closer to the $(k,k)$ periodic solutions in the phase plane than those of smaller $m$. In other words, those periodic solutions closest to the stability boundary for the $(k,k)$ solutions map a greater number of times in the k-step region before mapping into the $(k - 1)$-step region and completing its period. These solutions can then be viewed as perturbations of the $(k,k)$ solutions that eventually mapped into the $(k - 1)$-step region instead of the k-step region and completed a

periodic solution.

Since all of these periodic solutions map only into the outer branches, the perturbation equation for solutions $\underset{\sim}{y} = \underset{\sim}{\varphi} + \underset{\sim}{y}^p$, given by Eq. (3.14), still holds. As the number of mappings onto region $I_a$ necessary to complete the period of the solution increases, we must locate each of the mappings onto region $I_a$ and from those determine a maximum possible $c$ in Eq. (3.14). For the numerical solutions examined, a bound similar to the $(k,k)$ periodic solution was valid where $c = \mu(\hat{y}^p - 1)^2$, and where $\hat{y}^p$ was the point of the $(mk, k-1)$ periodic solution that mapped in $I_a$ closest to $y_n = 1$. Figure 3.7 shows a set of these $(mk, k-1)$ periodic solutions and their associated stability regions.

A similar type of periodic solution was also noticed. It followed a $(mk, k+1)$ mapping pattern and the characteristics of these solutions were similar to those mentioned above.

Unlike the behavior of the solutions for $\mu = 0$, the number of steps per half cycle of any solution for $\mu > 0$ is bounded. Because of this the number of simple periodic solutions is also bounded. However, the transformations show there exists an unbounded set of complex periodic solutions that lie beyond the last simple periodic solution. This is most easily seen for the case when $\theta = \pi/\ell$ ($\ell$ = integer). Here $k_{max} = \ell$, and the $k_{max}$ step outer branch transformation reduces to

$$\underset{\sim}{y}_{k_{max}} = \underset{\sim}{y}_0 + \frac{\beta - \mu}{1 + \mu} \begin{Bmatrix} 1/\mu \\ -1 \end{Bmatrix}, \tag{3.21}$$

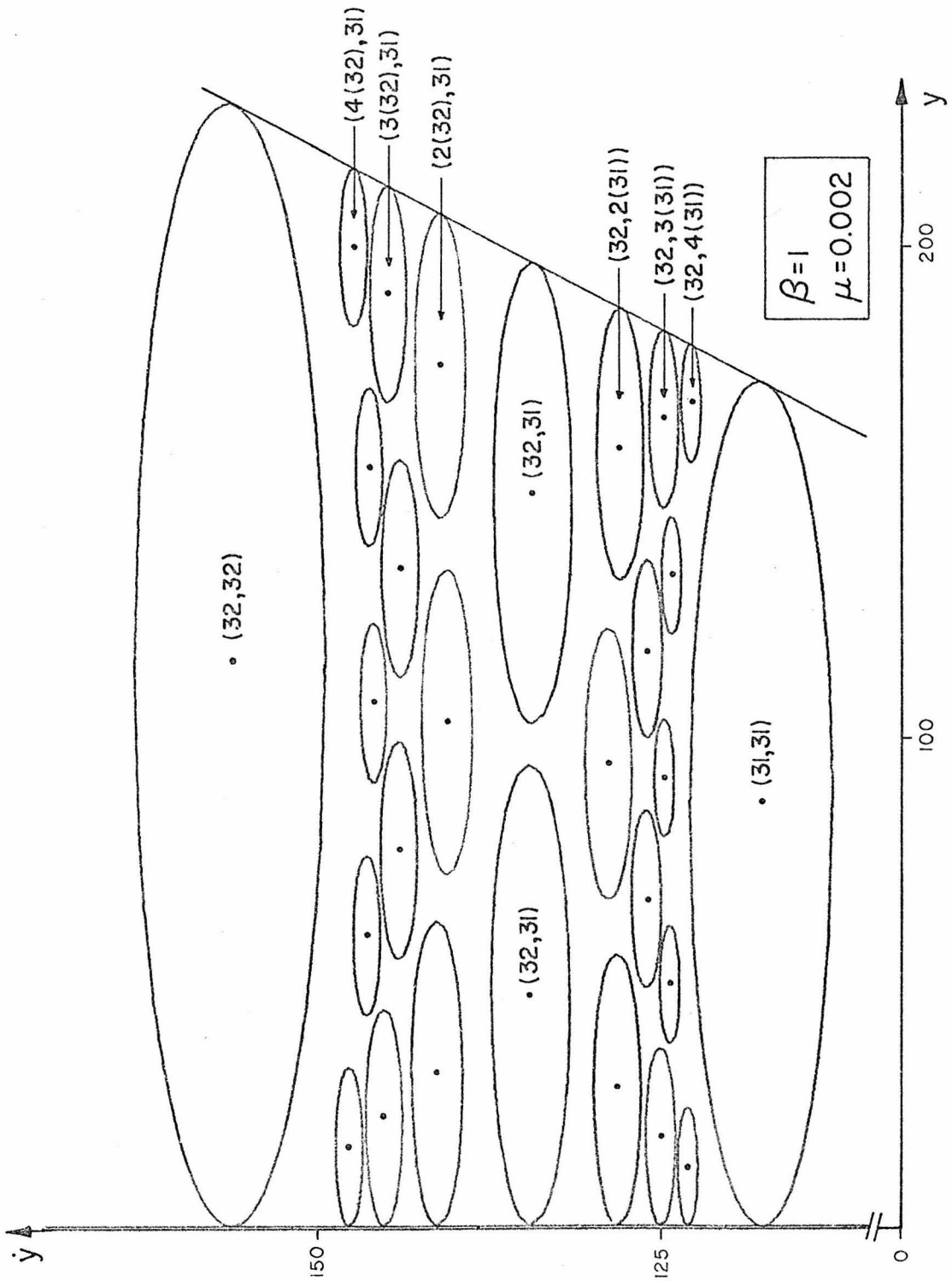


Figure 3.7 - A Group of Complex Periodic Solutions and their Stability Regions

which is simply a translation of the solution in the $k_{max}$ -step region of $I_a$. With a sufficient number of such transformations the solution will map into the $(k_{max} - 1)$-step region and then back into the $k_{max}$ - step region. Using periodic solutions of the form $(mk_{max}, k_{max} - 1)$, with $k_{max}\,\theta = \pi$, yields the periodic solution

$$\underset{\sim}{y}^p = \frac{\beta - \mu}{(1+\mu)(1-\cos\theta)} \begin{Bmatrix} 4\cos\theta(2\cos^2\theta + \cos\theta - 2) \\ m - 4\sqrt{\mu}\sin\theta(\cos^2\theta + \cos\theta - 1) \end{Bmatrix} . \tag{3.22}$$

As can be seen from the above equation, these solutions are fixed in $y$ with only $m$ varying, and they grow without bound in $\dot{y}$ as $m$ increases. Figure 3.8 shows this set's first few periodic solutions and the associated polygonal stability regions for $\theta = \frac{\pi}{5}$ $(\mu = 0.105578..)$.

## 3.4 Energy Growth

For the system of equations with $\mu > 0$, the Hamiltonian of $\underset{\sim}{y}$ is

$$H_n = \begin{cases} \frac{1}{2}\dot{y}_n^2 + \frac{1}{2}\beta y_n^2 & ; \quad |y_n| \le 1 \\ \frac{1}{2}\dot{y}_n^2 + \frac{1}{2}\mu y_n^2 + (\beta - \mu)\,|y_n| + \frac{\mu - \beta}{2} & ; \quad |y_n| \ge 1 \end{cases} . \tag{3.23}$$

It can be shown that, similar to the $\mu = 0$ case, the transformations of regions I and V (shown in Fig. 3.1) conserve $H_n$ for each step. Thus any growth or decay in $H_n$ occurs when a solution is mapped from one half cycle to the next, either through region III or regions II

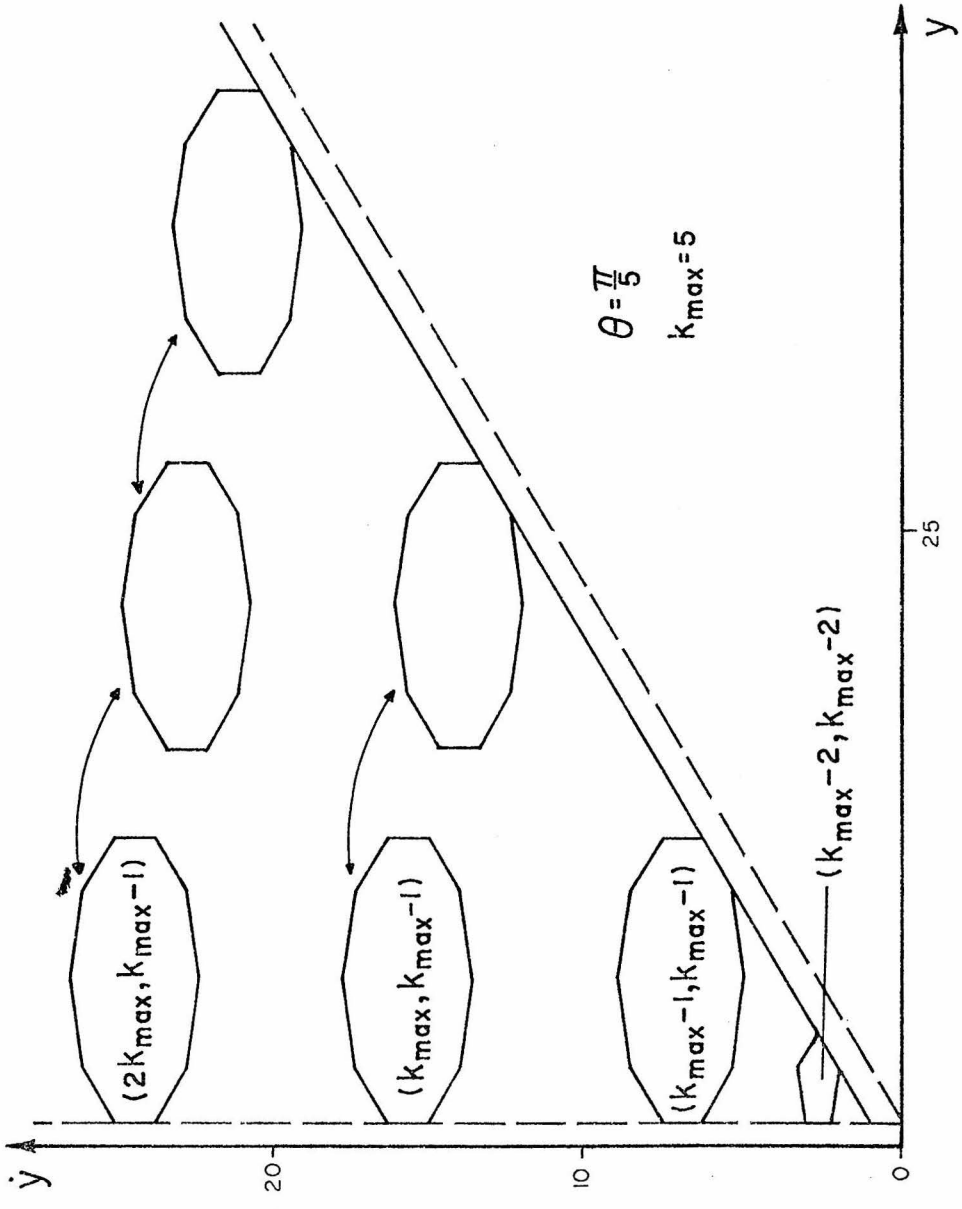


Figure 3.8 - Stability Regions of the First Few $(mk_{max}, k_{max} - 1)$ Periodic Solutions

and IV. The change in the Hamiltonian for those solutions mapping through region III (i.e., the outer branch solutions) is

$$\Delta H = -2\left(\frac{\beta-\mu}{1+\mu}\right)(y_0+\dot{y}_0) \tag{3.24}$$

where $\underset{\sim}{y_0}$ is in region III. The Hamiltonian change for those solutions mapping into regions II and IV is

$$\Delta H = (\beta-\mu)(d+1)(2\dot{y}_0+d(\beta-\mu)-1) \tag{3.25}$$

where $\underset{\sim}{y_0}$ is in region II on the line

$$\dot{y}_0 = \frac{\mu-1}{2}(y_0+d) \quad \text{with} \quad -1-\mu \le d \le 1+2\beta-\mu \ .$$

To obtain an upper bound on the rate of growth of the Hamiltonian, it is noted that both Eqs. (3.24) and (3.25) allow at most a linear growth with $\underset{\sim}{y}$ of the maximum positive Hamiltonian jump for each half cycle. For the outer branch solution this maximum jump occurs at $y_0 = 1$ where

$$\Delta H = -2\left(\frac{\beta-\mu}{1+\mu}\right)(\dot{y}_0+1) \ . \tag{3.26}$$

For $\beta > \mu$ this growth is larger than the growth possible for the inner branch solutions (Eq. 3.25). The maximum Hamiltonian on the next half cycle (for $\dot{y}$ large) will then be

$$\left.\begin{aligned} H' = H + \Delta H &= \frac{1}{2}\dot{y}_0^2 - 2\left(\frac{\beta - \mu}{1+\mu}\right)\dot{y}_0 + O(1) \\ &= \frac{1}{2}\dot{y}_0'^2 + O(1) \quad . \end{aligned}\right\} \tag{3.27}$$

Taking $\dot{y}$ as positive, this gives $\dot{y}'$ ($\dot{y}$ on the next half cycle) as

$$\dot{y}' = \dot{y}\left[1 + 2\left(\frac{\beta - \mu}{1+\mu}\right)\dot{y} + O(1/\dot{y}^2)\right]^{\frac{1}{2}} \tag{3.28}$$

The maximum jump of $\dot{y}$ in one half cycle is thus

$$\dot{y}' - \dot{y} = 2\left(\frac{\beta - \mu}{1+\mu}\right) + O(1/\dot{y}) \quad . \tag{3.29}$$

Since the period is bounded for large $\dot{y}$ (i.e., the number of steps must be equal to $k_{max}$ or $k_{max} - 1$), the maximum average growth in $\dot{y}$ per step is

$$\Delta\dot{y} = \frac{2}{k_{max} - 1}\left(\frac{\beta - \mu}{1+\mu}\right) \quad . \tag{3.30}$$

The growth in $\dot{y}_n$ is then given as

$$\dot{y}_n = \frac{2}{k_{max} - 1}\left(\frac{\beta - \mu}{1+\mu}\right)n + O(1) \quad , \tag{3.31}$$

and the maximum Hamiltonian growth is

$$H_n = \left[ \frac{2(\beta - \mu)}{(k_{max} - 1)(1 + \mu)} \right]^2 n^2 + O(n) \quad . \tag{3.32}$$

The bound on the maximum number of steps per half cycle has increased the possible Hamiltonian growth to $O(n^2)$, rather than $O(n)$ for $\mu = 0$. However both bounds are still much tighter than the exponential bound mentioned in Section 2.4.

In the numerical computations performed, no solutions were found which exhibited a possible behavior pattern for such an unbounded growth. If those solutions do exist their patterns must be fairly complex due to the nonlinear difference equations' asymptoting the linear equations for large $\underset{\sim}{y}$. However, solutions which exhibited large fluctuations in $H_n$ were found numerically. These solutions mapped from regions of a few steps per half cycle up to larger step number regions with a mapping pattern identical to those found for the unbounded solutions for $\mu = 0$ in Section 2.4. The growth ceases when the solution mapped into the neighborhood of the $k_{max}/2$ - step region. Eventually, following the inverse of the growth pattern, the solutions mapped back down into the vicinity of its starting point. It was seen in Section 3.1 that the half cycle mappings of the step regions change their behavior for the number of steps per half cycle greater than or less than $k_{max}/2$. It is this change that most likely bounds these quasi growing solutions, since their mapping patterns must change to grow past the $k_{max}/2$ - step region. Although these solutions are bounded by this limit, $k_{max}$ grows without bound for $\mu$ approaching zero, and thus, so may these solutions.

## 3.5 The Phase Plane for $\beta < \mu$

With the outer branch slope of $f(\beta, \mu, y)$ greater than the slope of the inner branch, the period of the solutions mapping in $|y_n| < 1$ will be greater than those mapping in $|y_n| > 1$ by virtue of Eqs. (2.16) and (3.7). Because of this, the division of region $I_a$ into the k-step mapping regions will be different. The sign change in the term $\beta - \mu$ (see Eqs. (3.4)) changes the sign of the $\dot{y}$ intercept of those lines defining the k-step region. Thus, the only k-step outer branch regions which will map onto region $I_a$ are those where the slope of the boundaries, $-\sqrt{\mu}\cos k/\sin k\theta$, is greater than the slope of the line which defines region $I_a$, $\sqrt{\mu}\cos\theta/\sin\theta$. With this requirement there will be at most two constant step regions for the outer branch solutions. Figure 3.9 shows the division of region $I_a$ into these k-step regions. It can be shown that there will exist at most one simple outer branch periodic solution.

The calculations for a bound on the maximum Hamiltonian growth carry through in the same manner as in Section 3.4. The bound on the Hamiltonian growth for $\mu > \beta$ is given by Eq. (3.32).

## 3.6 Solutions of the Damped Equations

### 3.6.1 The Damped Finite Difference Equations

When the application allows it, a small amount of linear damping is frequently added to the dynamic equations to insure the boundedness of the solutions. Consider then the original differential equation with damping proportional to $\dot{x}$ added to give

$$\ddot{x} + \xi\dot{x} + f(x) = 0 \quad . \tag{3.33}$$

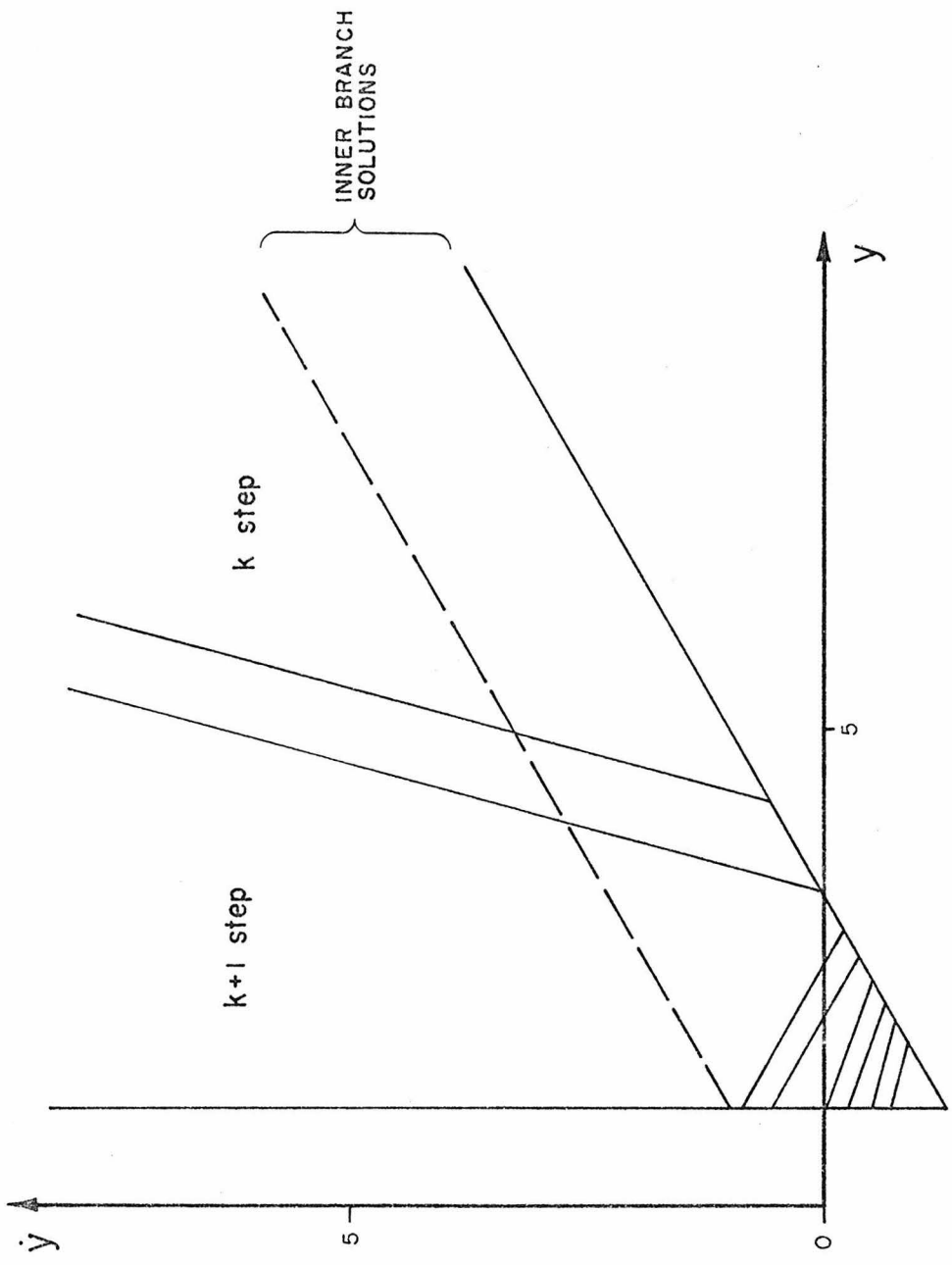


Figure 3.9 - Region $I_a$ of the Phase Plane for $\beta < \mu$

Applying the trapezoidal rule we obtain the following set of difference equations

$$\begin{aligned} y_{n+1} - y_n &= \dot{y}_{n+1} + \dot{y}_n \\ \dot{y}_{n+1} - \gamma \dot{y}_n &= -f(\beta, \mu, y_{n+1}) - f(\beta, \mu, y_n) \end{aligned} \tag{3.34}$$

with

$$\underset{\sim}{y}_n = \begin{Bmatrix} x_n \\ \alpha \dot{x}_n \end{Bmatrix}, \quad \gamma = \frac{1-\xi}{1+\xi}, \quad 0 < \xi \leq 1, \quad 0 \leq \gamma < 1$$

$$\beta = \frac{\alpha^2}{1+\xi} a, \quad \mu = \frac{\alpha^2}{1+\xi} s,$$

and $f(\beta, \mu, y_n)$ is given in Eq. (3.1). The transformations and their respective mapping regions are found by following the same analysis demonstrated in Sections 2.1 and 3.1. The effect of the damping on the solution mappings in the phase plane is to weight the mapping of the k-step solutions more towards the k-1, k-2, ... etc.-step mapping regions. For sufficiently small damping, $\xi$, it can be shown that the (k,k) outer branch mapping patterns exist, and thus so do the (k,k) outer branch simple periodic solutions.

### 3.6.2 The Simple Periodic Solutions

The transformations for the mapping of the outer branch solutions, $|y_n| \geq 1$, are similar to those given by Eqs. (3.2a), (3.2c), (3.2e), and (3.2g). The exception is that $\underset{\sim}{A}$ is now replaced by

$$\underset{\sim}{A} = \frac{1}{1+\mu}\begin{bmatrix} 1-\mu & \gamma \\ -2\mu & \gamma-\mu \end{bmatrix}, \tag{3.35}$$

which is calculated from Eq. (3.34). The eigenvalues of $\underset{\sim}{A}$ are

$$\lambda_{1,2} = \frac{1+\gamma-2\mu \pm \sqrt{(\gamma-1)^2 - 8\mu(1+\gamma)}}{2(1+\mu)}, \tag{3.36}$$

and

$$||\lambda_{1,2}|| < 1 \quad \text{for} \quad \gamma < 1 . \tag{3.37}$$

Since the eigenvalues are distinct and non-zero, there exists a linear transformation, $\underset{\sim}{T}$, that diagonalizes $\underset{\sim}{A}$ such that

$$\underset{\sim}{A} = \underset{\sim}{T}^{-1}\underset{\sim}{\Lambda}\underset{\sim}{T}, \quad \underset{\sim}{\Lambda} = \begin{bmatrix} \lambda_1 & 0 \\ 0 & \lambda_2 \end{bmatrix}. \tag{3.38}$$

With this the transformation for a k-step half cycle mapping can be written as

$$\underset{\sim}{y}_k = \underset{\sim}{T}^{-1}\underset{\sim}{\Lambda}^k \underset{\sim}{T}\underset{\sim}{y}_0 - \frac{2(\beta-\mu)}{1+\mu}\underset{\sim}{T}^{-1}\sum_{j=1}^{k-1}\underset{\sim}{\Lambda}^j \underset{\sim}{T}\begin{Bmatrix} 1 \\ 1 \end{Bmatrix}. \tag{3.39}$$

The (k,k) simple periodic solution of the above transformation is

$$\underset{\sim}{y}^{p} = \frac{2(\beta - \mu)}{1+\mu}\,\underset{\sim}{T}^{-1}\begin{bmatrix} \dfrac{1-\lambda_1^{k-1}}{1+\lambda_1^{k}}\,\dfrac{\lambda_1}{1-\lambda_1} & 0 \\ 0 & \dfrac{1-\lambda_2^{k-1}}{1+\lambda_2^{k}}\,\dfrac{\lambda_2}{1-\lambda_2} \end{bmatrix}\underset{\sim}{T}\begin{Bmatrix} 1 \\ 1 \end{Bmatrix}. \qquad (3.40)$$

The stability analysis of these outer branch periodic solutions is similar to the analysis for the undamped equations in (Section 3.2), except that the modulus of the eigenvalues of $\underset{\sim}{A}$ is less than unity (Eq. (3.37)). Therefore, Eq. (3.14) does not hold. Instead, the perturbations, $\varphi_n$, approach zero with n increasing, and thus the simple outer branch periodic solutions are asymptotically stable. Since all perturbations on the stability boundary given by Eq. (3.16) will map inside this region in one step, the stability domain for the undamped solutions will also be a stability domain for the damped solutions. However, the complete region of asymptotic stability for the damped solutions is larger, because the damped difference equations will map solutions lying outside the undamped stability region into this region. Thus, the backmapping of the boundary of the undamped stability region, Eq. (3.16), will define the stability region of the damped equations only as long as the backmapped perturbations do not map into $|y_n| < 1$.

### 3.6.3 The Bound on the Solutions

From the linear mapping transformations it can be shown that the Hamiltonian of the system decreases with each step in a half cycle.

Again, the Hamiltonian can only increase in mapping from one half cycle to the next, and the maximum Hamiltonian jump in mapping across the linear branch, $|y_n| < 1$, is given by

$$\Delta H_{max} = \frac{1}{2}\frac{(\gamma^2 - 1)}{1+\mu}\dot{y}_n^2 + \frac{(1+\gamma-2\mu)}{1+\mu}\dot{y}_n - 2\left(\frac{1-\mu}{1+\mu}\right) \qquad (3.41)$$

for $|y_n| = 1$ .

The quadratic term in the above equation is negative, and so for

$$|\dot{y}_n| > \left\{1 - 2\mu + \gamma + (4\mu^2 - 4\mu\gamma(1+\gamma) + 5\gamma^2 + 2\gamma - 3)^{\frac{1}{2}}\right\} \Big/ (1-\gamma^2), \quad (3.42)$$

The maximum Hamiltonian jump will always be negative, and Eq. (3.42) is thus a bound to the maximum possible solution growth.

# IV The Non-Autonomous Equations

## 4.1 The Transformations of the Difference Equations

In this chapter, the solutions to the non-autonomous difference equations which arise from a sinusoidal forcing function will be examined. The difference equations considered will be those which result from the time discretization of the following continuous, non-autonomous differential equation,

$$\left.\begin{aligned} &\ddot{x} + f(x) = F_0 \sin(\omega t + \phi') \\ &x(0) = x_0,\ \dot{x}(0) = \dot{x}_0 \ , \end{aligned}\right\} \quad (4.1)$$

where $\omega$ is the forcing frequency and $\phi'$ is the phase. The difference equations resulting from applying the trapezoidal rule to Eqs. (4.1) are

$$y_{n+1} - y_n = \dot{y}_{n+1} + \dot{y}_n \quad (4.2a)$$

$$\dot{y}_{n+1} - \dot{y}_n = -f_{n+1} - f_n + \eta \sin(n\theta_0 + \phi) \quad (4.2b)$$

where

$$\underset{\sim}{y_n} = \begin{Bmatrix} x_n \\ \alpha \dot{x}_n \end{Bmatrix}$$

$$f_n = \begin{cases} \mu y_n + (\beta - \mu)\,\mathrm{sgn}(y_n) & ;\ |y_n| \geq 1 \\ \beta y_n & ;\ |y_n| < 1 \ , \end{cases} \quad (4.3a)$$

$$\eta = 2\alpha^2 F_0 \cos(\theta_0/2) \ ,$$

$$\theta_0 = \omega\Delta t = 2\omega\alpha \tag{4.3b}$$

and $$\phi = \phi' + \theta_0/2 \ .$$

The difference between the form of the inhomogeneous and homogeneous equations (Eqs. (4.2) and (2.1), respectively) is only in the addition of the term $\eta \sin(n\theta_0 + \phi)$ to the homogeneous equations. Thus, the phase plane analysis for the autonomous equations of the two previous chapters can be used to examine the solutions of Eqs. (4.2). To simplify the problem and still retain the most important features of the solutions, particularly their boundedness and periodicity, we will consider only the outer branch solutions, $|y_n| \geq 1$.

As before, the separation of $f_n$ into its three linear regions divides the phase plane into nine regions. A linear transformation holds in each region. For the outer branch solutions, the transformations in the appropriate regions are as follows:

I: $y_n \geq 1, \ y_{n+1} \geq 1$

$$\left.\begin{aligned} \dot{y}_n &\geq \frac{1}{2}\{(\mu - 1)y_n - \eta \sin(n\theta_0 + \phi) + 1 + 2\beta - \mu\} \\ \underset{\sim}{y}_{n+1} &= \underset{\sim\sim}{A}\underset{\sim}{y}_n + \left[\eta \sin(n\theta_0 + \phi) - 2\,\frac{\beta - \mu}{1 + \mu}\right]\underset{\sim}{1} \end{aligned}\right\} \tag{4.4a}$$

III: $y_n \geq 1, \ y_{n+1} \leq -1$

$$\left.\begin{aligned} \dot{y}_n &\leq \frac{1}{2}\{(\mu - 1)y_n - 1 - \mu - \eta \sin(n\theta_0 + \phi)\} \\ \underset{\sim}{y}_{n+1} &= \underset{\sim\sim}{A}\underset{\sim}{y}_n + \eta \sin(n\theta_0 + \phi)\,\underset{\sim}{1} \end{aligned}\right\} \tag{4.4b}$$

$$\text{V:}\quad \begin{aligned} & y_n \le -1,\ y_{n+1} \le -1 \\ & \dot{y}_n \le \frac{1}{2}\{(\mu - 1)y_n - \eta \sin(n\theta_0 + \phi) - 1 - 2\beta + \mu\} \\ & \underset{\sim}{y}_{n+1} = \underset{\sim}{\underset{\sim}{A}}\underset{\sim}{y}_n + \left[\eta \sin(n\theta_0 + \phi) + 2\,\frac{\beta - \mu}{1 + \mu}\right]\underset{\sim}{1} \end{aligned} \qquad (4.4c)$$

$$\text{VII:}\quad \begin{aligned} & y_n \le -1,\ y_{n+1} \ge 1 \\ & \dot{y}_n \ge \frac{1}{2}\{(\mu - 1)y_n + 1 + \mu - \eta \sin(n\theta_0 + \phi)\} \\ & \underset{\sim}{y}_{n+1} = \underset{\sim}{\underset{\sim}{A}}\underset{\sim}{y}_n + \eta \sin(n\theta_0 + \phi)\,\underset{\sim}{1} \end{aligned} \qquad (4.4d)$$

where

$$\underset{\sim}{\underset{\sim}{A}}(\mu > 0) = \begin{bmatrix} \cos\theta & \dfrac{\sin\theta}{\sqrt{\mu}} \\ -\sqrt{\mu}\sin\theta & \cos\theta \end{bmatrix}$$

$$\underset{\sim}{\underset{\sim}{A}}(\mu = 0) = \begin{bmatrix} 1 & 2 \\ 0 & 1 \end{bmatrix}$$

$$\theta = \cos^{-1}\left(\frac{1 - \mu}{1 + \mu}\right) \quad \text{and} \quad \underset{\sim}{1} = \begin{Bmatrix} 1 \\ 1 \end{Bmatrix}.$$

Comparing these transformations with those for regions I, III, V, and VII of the homogeneous equations (Eqs. (2.6a, c, e, and g) and Eqs. (3.2a, c, e, and g)), it is seen that the inhomogeneity simply adds the translation term $\eta \sin(n\theta_0 + \phi)\underset{\sim}{1}$ to each of the transformations, independent of the mapping region. Since the transformations are slightly

different for $\mu = 0$ and $\mu > 0$, each case will be considered separately.

## 4.2 Analysis of Solutions for $\mu = 0$

Given the above mapping transformations for $\mu = 0$, then the transformation for a solution mapping $n$ times in region I is given by

$$\underset{\sim}{y}_n = \begin{bmatrix} 1 & 2n \\ 0 & 1 \end{bmatrix} \underset{\sim}{y}_0 - 2\beta \begin{Bmatrix} n^2 \\ n \end{Bmatrix} + \eta \cos \phi \sum_{k=1}^{n} \sin(n-k)\theta_0 \begin{bmatrix} 1 & 2(k-1) \\ 0 & 1 \end{bmatrix} \underset{\sim}{1}$$

$$+ \eta \sin \phi \sum_{k=1}^{n} \cos(n-k)\theta_0 \begin{bmatrix} 1 & 2(k-1) \\ 0 & 1 \end{bmatrix} \underset{\sim}{1} , \qquad (4.5)$$

which can be reduced to

$$\underset{\sim}{y}_n = \begin{bmatrix} 1 & 2n \\ 0 & 1 \end{bmatrix} \underset{\sim}{y}_0 - 2\beta \begin{Bmatrix} n^2 \\ n \end{Bmatrix} + \eta \underset{\sim}{g}^{\mu=0}(n, \theta_0, \phi) , \qquad (4.6)$$

where

$$\underset{\sim}{g}^{\mu=0} = \begin{Bmatrix} g_1(n, \theta_0, \phi) \\ g_2(n, \theta_0, \phi) \end{Bmatrix} = \cos \phi \begin{Bmatrix} 2\sin n\theta_0 I_s + 2\cos n\theta_0 I_c - F_s \\ F_s \end{Bmatrix}$$

$$+ \sin \phi \begin{Bmatrix} 2\cos n\theta_0 I_s - 2\sin n\theta_0 I_c - F_c \\ F_c \end{Bmatrix} \qquad (4.7)$$

$$F_s = \frac{\sin\theta_0 + \sin(n-1)\theta_0 - \sin n\theta_0}{2(1-\cos\theta_0)}$$

$$F_c = \frac{\cos\theta_0 + \cos(n-1)\theta_0 - \cos n\theta_0 - 1}{2(1-\cos\theta_0)}$$

$$I_s = \frac{\sin\frac{2n+1}{2}\theta_0 \sin\theta_0/2}{1-\cos\theta_0}\, n + \frac{\cos\theta_0 - \cos(n+1)\theta_0 - \sin n\theta_0 \sin\theta_0 - 1 + \cos n\theta_0}{2(1-\cos\theta_0)^2}$$

$$I_c = \frac{\cos\frac{2n+1}{2}\theta_0 \sin\theta_0/2}{1-\cos\theta_0}\, n + \frac{\sin(n+1)\theta_0 - \sin n\theta_0 - \sin\theta_0 - \sin\theta_0 \cos n\theta_0}{2(1-\cos\theta_0)^2} \,.$$

It is seen from the first term of both $I_s$ and $I_c$ that $\underset{\sim}{g}$ is an unbounded function of n and grows O(n) for all $\theta_0$ and $\phi$. $\underset{\sim}{g}$ is shown plotted versus n in Fig. 4.1. Although Eq. (4.6) holds for n mappings in

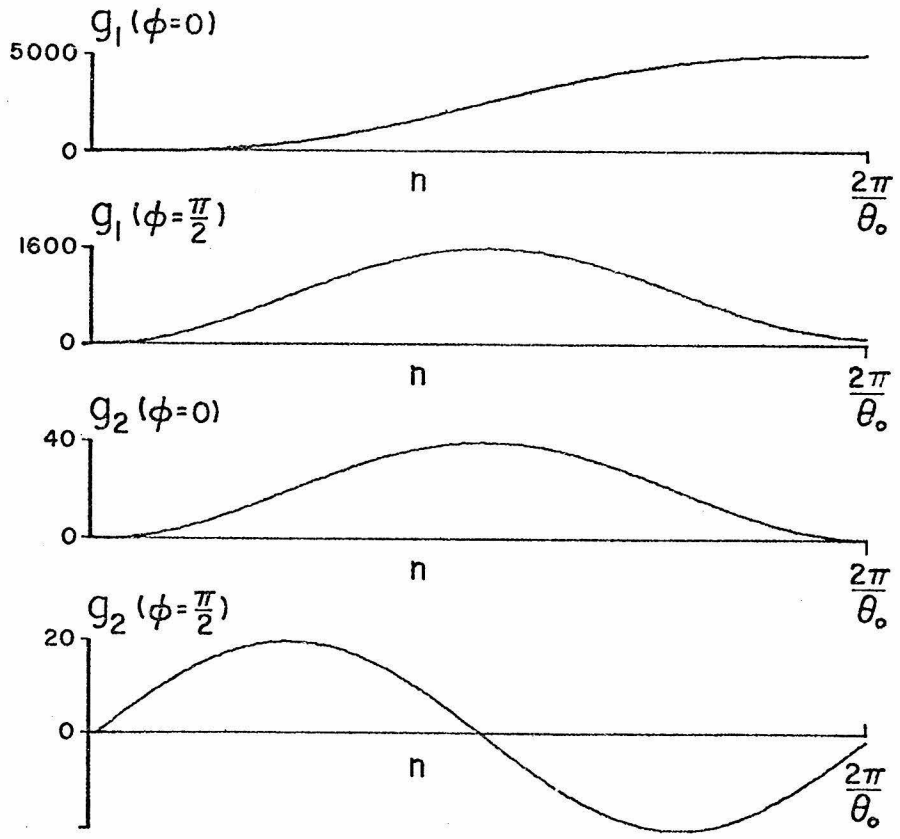


Figure 4.1 - Functions $g_1^{\mu=o}$ and $g_2^{\mu=o}$ for $\theta_0 = 0.05$

region I of the phase plane, it should be noted that the term $\underset{\sim}{g}^{\mu=o}(n, \theta_o, \phi)$ will retain the exact same form independently of the mapping behavior of $\underset{\sim}{y}_n$ in regions I, III, V, and VII. It is the form of the second term in Eq. (4.6), $-2\beta\{n^2\}$, that changes with each mapping from one half plane into the next.

Since the non-autonomous term in Eq. (4.2b) is of the form $\sin(n\theta_o + \phi)$, it is sufficient to consider only $0 < \theta_o < 2\pi$ for all possible solutions. With the difference equations being the discretized form of the continuous Eq. (4.1), this non-uniqueness of $\theta_o$ for a particular solution implies that for a given time step, high frequencies, $\omega$, in Eq. (4.1) will yield lower forcing frequencies, $\theta_o$, if the time step is not sufficiently small. This numerical phenomenon is called aliasing. Figure 4.2 shows the solutions dependence on the time step with all other parameters held constant. In order to uniquely represent the solution to a particular forcing frequency, $\omega$, the time step must be chosen such that

$$\Delta t < 2\pi/\omega \ ,$$

from Eq. (4.3b).

For a sufficiently small amplitude, $\eta$, the difference between the autonomous and non-autonomous solutions can be made arbitrarily small for any n. Thus the simple periodic solutions with a (k,k) mapping pattern which were found for the homogeneous equations in Chapter II can be shown to exist for the non-autonomous equations with $\eta$ small. Since n is an integer, the bounded terms of $\underset{\sim}{g}(n, \theta_o, \phi)$

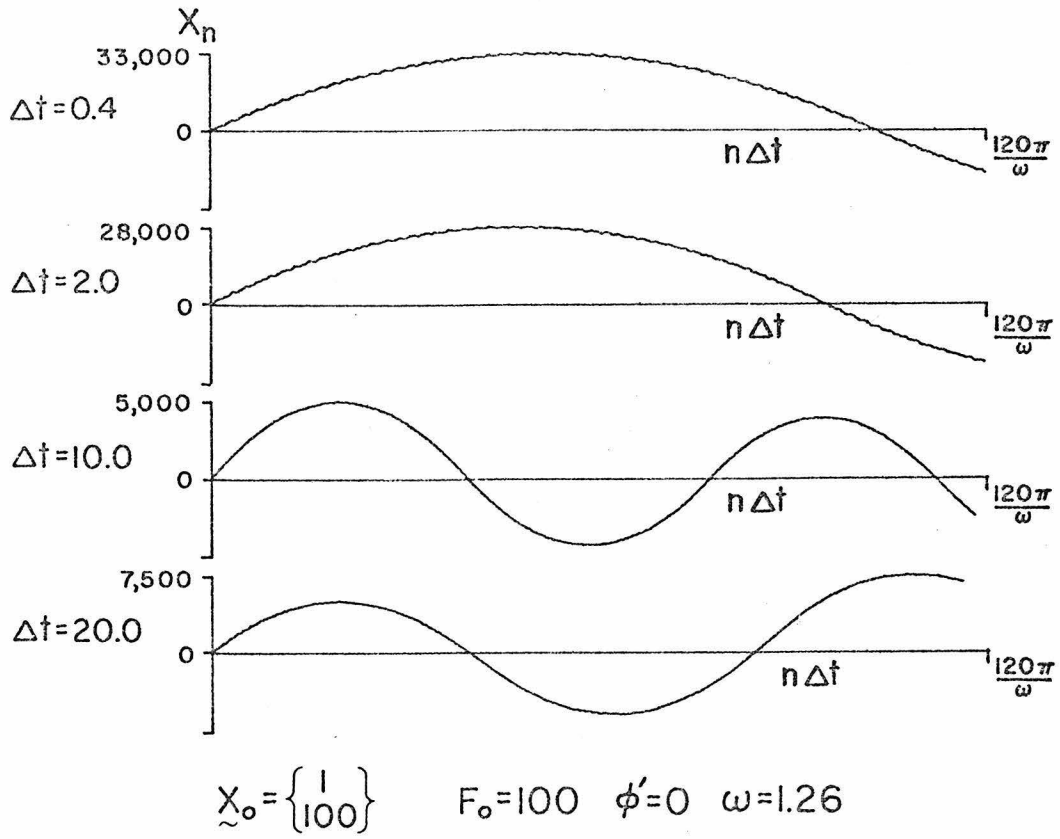


Figure 4.2 - Solutions of Equations (4.2) for $\Delta t = 0.4, 2.0, 10.0, 20.0$

in Eq. (4.7) are not periodic unless $\theta_0$ is a rational fraction of $\pi$. So if $\underset{\sim}{g}$ is not periodic, there exist no exactly periodic solutions to Eqs. (4.2). From the aspect of the difference equations representing some discretized differential equation, the proper choice of a time step, $\Delta t$, will make $\theta_0$ a rational fraction of $\pi$ via Eq. (4.3b). Assuming now that $\theta_0 = \ell\pi/m$ ($\ell$, m are integers), the (k, k) mapping transformation of the homogeneous solutions calculated from Eqs. (4.4a) to (4.4d) is

$$\underset{\sim}{y}_{2k} = \begin{bmatrix} 1 & 2k \\ 0 & 1 \end{bmatrix} \underset{\sim}{y}_0 + 4\beta \begin{Bmatrix} k - k^2 \\ 0 \end{Bmatrix} + \eta \underset{\sim}{g}^{\mu=o}(2k, \theta_0, \phi) \quad . \qquad (4.8)$$

For a periodic solution of this transformation to exist, it is found that

$$\dot{y}^p = \beta(k - 1) - \frac{\eta}{4k} g_1^{\mu=o}(2k, \theta_o, \phi) \quad , \tag{4.9}$$

$$\eta g_2^{\mu=o}(2k, \theta_o, \phi) = 0 \quad . \tag{4.10}$$

It can be seen from Eq. (4.7) that Eq. (4.10) is satisfied for $\eta \neq 0$ only if

$$\theta_o = \frac{m}{k}\pi \quad (m = 1,2,\ldots.) \quad , \tag{4.11}$$

which is our previously stated condition for the existence of any periodic solution. Applying Eq. (4.11) to Eq. (4.9) we then obtain

$$\dot{y}^p = \beta(k - 1) - \frac{\eta}{4}\left[\frac{\sin \theta_o}{1 - \cos \theta_o}\cos \phi + \sin \phi\right] \quad . \tag{4.12}$$

For a simple period solution to exist, $\underset{\sim}{y}^p$ must map into the k-step region on both half cycles. From Chapter II it is known that this must hold for $\eta = 0$. Since it is only necessary that the solution follow the (k,k) pattern in one cycle for a periodic solution to exist, then there must be an $\eta_{max}$ such that for $|\eta| \leq \eta_{max}$, the (k,k) inhomogeneous solution exists. Determining this $\eta_{max}$ is tedious in that it is necessary to follow the mappings step by step and calculate an $\eta_{max}$ for each. The stability of such periodic solutions is identical to the stability of the homogeneous solutions and thus they are all unstable to perturbations in $\dot{y}_n$.

One of the important effects on the solutions of the non-autonomous term is the change in the period with the amplitude. For the large amplitude, homogeneous solutions it was found that the period grew linearly with the amplitude (Section 2.1). Although the bounded terms of $\underset{\sim}{g}^{\mu=0}$ are periodic in $n = 2\pi/\theta_0$ steps, $\underset{\sim}{g}^{\mu=0}$ grows linearly with the number of steps, n, for large n. Thus, for the large amplitude, long period solutions the $y_n$ component of a half cycle transformation (from Eq. (4.6)) is

$$y_n = 2n\dot{y}_0 - 2n^2 + \eta\left[\cos\phi\,\frac{\sin\theta_0}{1-\cos\theta_0} + \sin\phi\right]n + O(1) \qquad (4.13)$$

for initial conditions $\underset{\sim}{y}_0$ that are O(1). The period of the half cycle mapping, $n_{hc}$, will then be such that $y_{n_{hc}} = O(1)$, and Eq. (4.13) yields

$$n_{hc} = \dot{y}_0 + \frac{\eta}{2}\left[\cos\phi\,\frac{\sin\theta_0}{1-\cos\theta_0} + \sin\phi\right] + O(1/n) \ . \qquad (4.14)$$

Therefore, for large amplitudes, the period of the solutions grows linearly with both $\dot{y}_0$ and $\eta$. Equation (4.14) also points out the dependence of the period on the phase, $\phi$, particularly for $\theta_0 \ll 1$, since

$$\frac{\sin\theta_0}{1-\cos\theta_0} = \frac{2}{\theta_0} + O(\theta_0) \ . \qquad (4.15)$$

Figure (4.3) shows some of these long period solutions and their dependence on the phase.

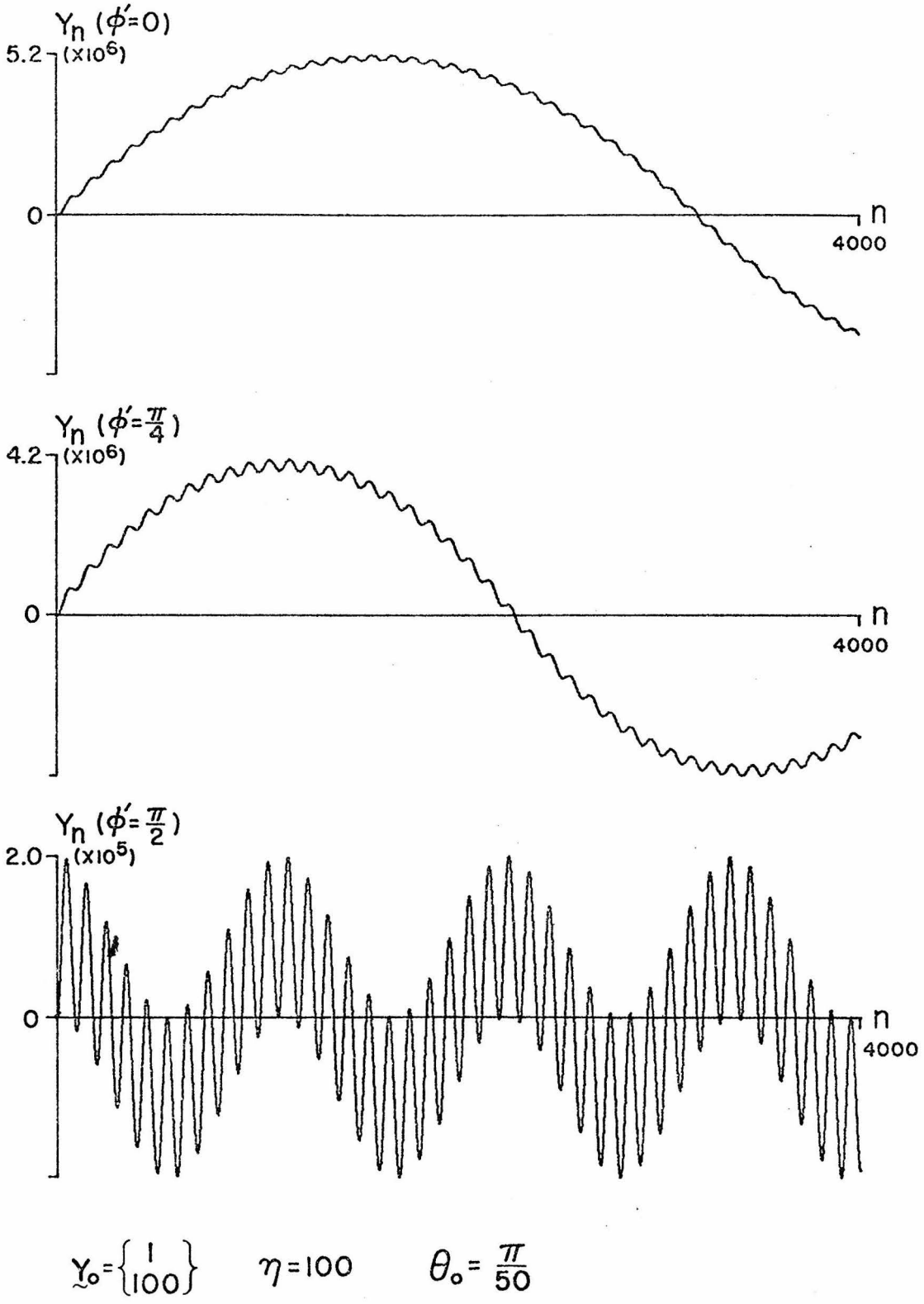


Figure 4.3 - Variation of the Solution with the Phase

If the unbounded solutions to the non-autonomous equations exist they can not grow with the same mapping structure as the autonomous solutions in Section 2.4. This is because the period of $\underset{\sim}{g}^{\mu=0}$, $2\pi/\theta_0$, is not changing to match the period of the homogeneous part of the solution, which grows linearly with the amplitude. Numerical calculations of this type of unbounded solution were tried for small $\eta$, and the solutions grew in amplitude following the homogeneous mappings until the contribution of the inhomogeneity carried the solutions away from the growing homogeneous solutions and changed their mapping behavior. No other possibly unbounded solutions were found for the numerical computations performed.

To find a bound on the growth rate of the solutions, the change in the Hamiltonian for each step is calculated from Eqs. (2.8) and (4.4), and it is

$$H\Big|_{n}^{n+1} \leq \left|\eta \sin(n\theta_0 + \phi)(\dot{y} + \eta/2 \sin(n\theta_0 + \phi) - \beta)\right| \quad . \tag{4.16}$$

Thus, for $\dot{y}$ large

$$\Delta H_{max} \leq \left|\eta\dot{y}\right| + O(1) \quad . \tag{4.17}$$

For the next time step the Hamiltonian is

$$H_{n+1} = \frac{1}{2}\dot{y}_{n+1}^2 + \beta\left|y_{n+1}\right| \leq H + \Delta H_{max} = \frac{1}{2}\dot{y}^2 + \left|\eta\dot{y}\right| + \beta\left|y\right| \quad , \tag{4.18}$$

and considering a growth in $\dot{y}$

$$\dot{y}_{n+1} \leq |\dot{y}_n|(1 + |\eta/\dot{y}_n|)^{\frac{1}{2}} + O(1/\dot{y}_n)$$

or

$$\Delta\dot{y} = \dot{y}_{n+1} - \dot{y}_n \leq |\eta/2| + O(1/y) \quad .$$

Thus for n large

$$\dot{y}_n \leq |\eta/2|n + O(1) \quad , \tag{4.19}$$

and from Eq. (2.8)

$$H_n \leq \frac{1}{8}\eta^2 n^2 + O(n) \quad . \tag{4.20}$$

The maximum Hamiltonian growth is $O(n^2)$ compared to $O(n)$ for the autonomous equations in Chapter II. This is due to the fact that, although the period is still unbounded, the Hamiltonian can increase with each mapping instead of only with each half cycle, as in the homogeneous equations.

## 4.3 Analysis of Solutions for $\mu > 0$

Following the same idea as in the previous section the transformation for the $n^{th}$ step in a half cycle mapping is calculated from the repeated linear transformations of region I. This outer branch solution is

$$\underset{\sim}{y}_n = \underset{\sim}{A}^n \underset{\sim}{y}_0 - 2\,\frac{(\beta-\mu)}{1+\mu} \sum_{k=0}^{n=1} \underset{\sim}{A}^k \underset{\sim}{1} + \eta \sum_{\ell=1}^{n} \sin((n-\ell)\theta_0 + \phi)\underset{\sim}{A}^{\ell-1}\underset{\sim}{1} \quad , \qquad (4.21)$$

$$\underset{\sim}{A} = \begin{bmatrix} \cos\theta & \dfrac{\sin\theta}{\sqrt{\mu}} \\ -\sqrt{\mu}\sin\theta & \cos\theta \end{bmatrix} .$$

The summations in the above equation can be reduced and we obtain

$$\underset{\sim}{y}_n = \underset{\sim}{A}^n \underset{\sim}{y}_0 - 2\,\frac{\beta-\mu}{1+\mu} \begin{Bmatrix} a_n(\theta) + 1 + \dfrac{b_n(\theta)}{\sqrt{\mu}} \\ a_n(\theta) + 1 - \sqrt{\mu}\, b_n(\theta) \end{Bmatrix}$$

$$+ \eta \underset{\sim}{g}^{\mu>0}(n, \theta, \theta_0, \phi) \quad , \qquad (4.22)$$

where

$$\underset{\sim}{g}^{\mu>0} = \begin{Bmatrix} g_1 \\ g_2 \end{Bmatrix} = \frac{1}{2} \begin{Bmatrix} (-\gamma_c + \dfrac{1}{\sqrt{\mu}}\gamma_s)\cos\phi + \\ (\gamma_c + \sqrt{\mu}\,\gamma_s)\cos\phi + \end{Bmatrix}$$

$$\begin{Bmatrix} (-\delta_c + \dfrac{1}{\sqrt{\mu}}\delta_s)\sin\phi \\ (\delta_c + \sqrt{\mu}\,\delta_s)\sin\phi \end{Bmatrix} \qquad (4.23)$$

and

$$\gamma_c = \sin n\theta_0[a_n(\theta - \theta_0) + a_n(\theta + \theta_0)] + \cos n\theta_0[b_n(\theta - \theta_0) - b_n(\theta + \theta_0)]$$

$$\gamma_s = \sin n\theta_0[\, b_n(\theta - \theta_0) + b_n(\theta + \theta_0)] - \cos n\theta_0[a_n(\theta - \theta_0) - a_n(\theta + \theta_0)]$$

$$\delta_c = 2\cos n\theta + \cos n\theta_0[a_n(\theta + \theta_0) + a_n(\theta - \theta_0)] + \sin n\theta_0[b_n(\theta + \theta_0) - b_n(\theta - \theta_0)]$$

$$\delta_s = 2\sin n\theta + \sin n\theta[a_n(\theta - \theta_0) - a_n(\theta + \theta_0)] + \cos n\theta[\, b_n(\theta - \theta_0) + b_n(\theta + \theta_0)]$$

$$a_n(\theta) = \frac{\cos\theta + \cos(n-1)\theta - \cos n\theta - 1}{2(1 - \cos\theta)}\ ,\quad a_n(0) = n - 1$$

$$b_n(\theta) = \frac{\sin\theta + \sin(n-1)\theta - \sin n\theta}{2(1 - \cos\theta)}\ ,\quad b_n(0) = 0\ .$$

We will start by examining the existence of the periodic solutions of Eqs. (4.2), which depends on the behavior of the non-autonomous term, $\underset{\sim}{g}$. Equation (4.23) shows that $\underset{\sim}{g}$ is bounded for all n except at $\theta = 0$ and $\theta_0 = \pm\theta$, and for these cases it grows with O(n). Figure 4.4 shows the typical behavior of $\underset{\sim}{g}(n, \theta_0, \phi)$. Since $\underset{\sim}{g}$ is composed of trigonometric functions of $\theta - \theta_0$, $\theta + \theta_0$, and $\theta$, it will be periodic independently of $\phi$ only if $\theta - \theta_0$, $\theta + \theta_0$, and $\theta$ are rational fractions of $\pi$. This implies that

$$\theta_0 = r\theta\ ,\quad r = \ell/m\ \ (\ell, m \text{ integers})\ .$$

Therefore, for periodic solutions of the non-autonomous equations to exist, we must satisfy

$$\theta_0 = r\theta = r'\pi \tag{4.24}$$

where r and r′ are rational fractions.

If the above conditions for a periodic solution are satisfied, then

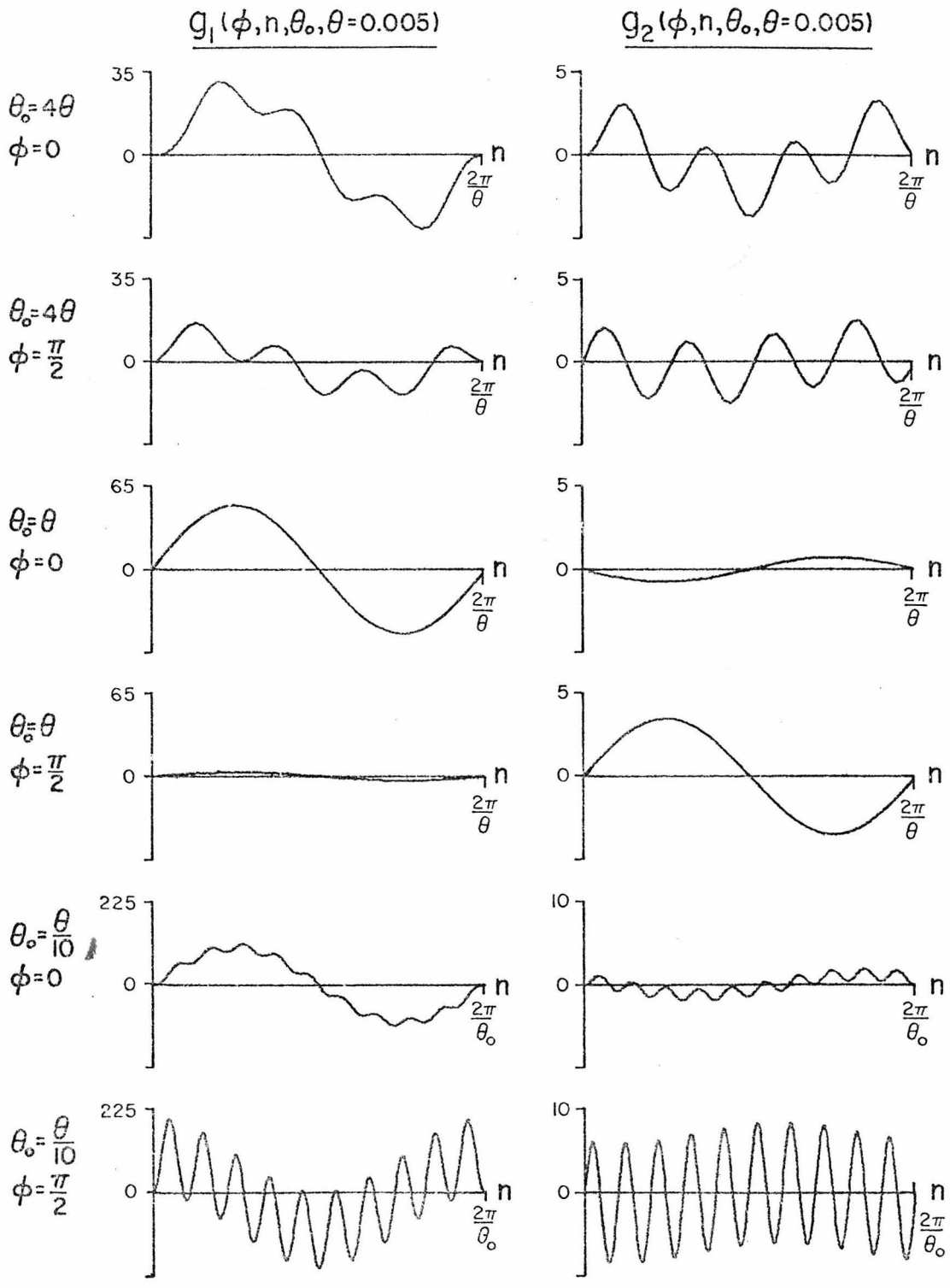


Figure 4.4 - Functions $g_1$ and $g_2$ for $\theta = 0.005$; $\theta_o = 4\theta$, $\theta$, and $\theta/10$; and $\phi = 0$, $\pi/2$

for $\eta$ sufficiently small, the (k,k) simple periodic solutions for the non-autonomous equations will exist for some value of $\theta_0$. In particular, as long as $\underset{\sim}{y}_n$ maps within the stability regions of the autonomous periodic solutions for each step, then the non-autonomous (k,k) periodic solution will exist for a proper range of $\eta$. This periodic solution is the fixed point of the (k,k) transformation which is

$$\underset{\sim}{y}^{p}_{2k} = \frac{\beta - \mu}{1+\mu} \frac{\cos\theta + \cos(k-1)\theta - \cos k\theta - 1}{(1-\cos\theta)(1+\cos k\theta)} \begin{Bmatrix} 1 \\ 1 \end{Bmatrix}$$

$$+ \frac{\eta}{2(1-\cos 2k\theta)} \begin{Bmatrix} (1 - \cos 2k\theta + \sin 2k\theta/\sqrt{\mu})g_1(2k, \theta, \theta_0, \phi) \\ (1 - \cos 2k\theta - \sqrt{\mu}\sin 2k\theta)g_2(2k, \theta, \theta_0, \phi) \end{Bmatrix} . \quad (4.25)$$

If Eq. (4.25) is a periodic solution, the non-autonomous term in Eq. (4.2b) must be periodic in 2k mappings. Otherwise the phase will change with each cycle and thus we are restricted to

$$\theta_0 = \frac{m\pi}{k} \quad m = 1, 2, 3, \ldots \ .$$

The first term in Eq. (4.25) is the homogeneous (k,k) periodic solution, and an $\eta_{max}$ guaranteeing the existence of the non-autonomous periodic solutions is found such that $\underset{\sim}{y}_n$ always maps into the stability regions of the homogeneous periodic solution. For $\theta_0 \neq \theta$ $\underset{\sim}{g}$ is bounded by

$$|\underset{\sim}{g}| \leq \begin{cases} |\cos \phi| \dfrac{\sqrt{\mu}+1}{\sqrt{\mu}} \dfrac{\sqrt{2}}{1-\cos\theta} + \\ \\ |\cos \phi|(1+\sqrt{\mu}) \dfrac{\sqrt{2}}{1-\cos\theta} + \end{cases}$$

$$\begin{cases} |\sin \phi| \dfrac{\sqrt{\mu}+1}{\sqrt{\mu}} \dfrac{\sqrt{2}+1-\cos\theta}{1-\cos\theta} \\ \\ |\sin \phi|(1+\sqrt{\mu}) \dfrac{\sqrt{2}+1-\cos\theta}{1-\cos\theta} \end{cases} . \qquad (4.26)$$

The condition that the difference between the autonomous and non-autonomous solutions lie in the stability region for each step is given by Eq. (3.16) and it is

$$\eta^2(g_2^2+\mu g_1^2) \leq \mu(y_{2k}^p - 1)^2 \ ,$$

where $y_{2k}^p$ is the autonomous periodic solution in Eq. (3.10). Thus the maximum $\eta$ for the existence of a (k,k) periodic solution, using the bound on $\underset{\sim}{g}$ in Eq. (4.26), is

$$\eta_{max} = \frac{(y_{2k}^{np} - 1)(1-\cos\theta)}{\sqrt{2}|\cos\phi| + (\sqrt{2}+1-\cos\theta)|\sin\phi|} \sqrt{\frac{\mu}{1+\mu+\sqrt{\mu}}} \ . \qquad (4.27)$$

As previously mentioned, $\underset{\sim}{g}^{\mu>o}$ grows linearly with n, the number of mappings, when $\theta_0 = \theta$. For the linear equations, $\beta = \mu$, all of the solutions to Eqs. (4.2) are unbounded. When f(x) is piecewise linear, however, the boundedness of the second term in Eq. (4.22) can not be determined a priori without knowledge of the number of mappings

the solution makes in each half cycle. Thus the piecewise linearity of f(x) can possibly bound solutions which would resonate in the linear case. Figure 4.5 shows several of the growing solutions of Eqs. (4.2) for $\theta_0 = \theta$.

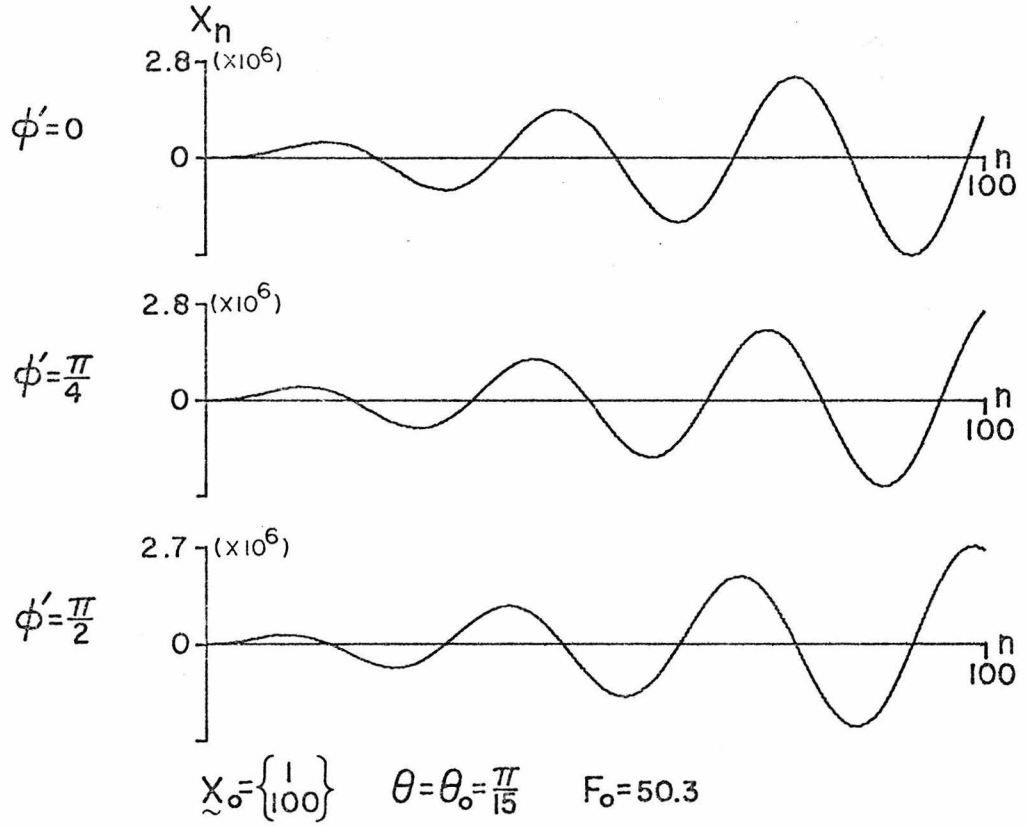


Figure 4.5 - Unbounded Non-Autonomous Solutions for $\theta = \theta_0 = \pi/15$

It can be shown that there exist such resonating solutions for $\theta = \ell\pi/m$ ($\ell$ and m integers), because the solutions starting in the $k_{max}$ step region of $I_a$ (Fig. 3.2) will always map with $k_{max}$ steps per half cycle for the proper values of $\eta$ and $\phi$ and for $k_{max} = \pi/\theta$. This can be seen from the transformation of the solution in one cycle with $k_{max}$ steps per half cycle,

$$\underset{\sim}{y}_{2k} = \underset{\sim}{y}_0 + 2\,\frac{(\beta - \mu)}{(1+\mu)} \begin{Bmatrix} 1/\mu \\ \\ -\ 1 \end{Bmatrix} + \eta \underset{\sim}{g}(2k, \theta, \theta_0, \phi) \qquad (4.28)$$

and $k = k_{max} = \pi/\theta$ .

The above equation represents a translation of the solution with each cycle. If $\underset{\sim}{y}_n$ continually maps into the $k_{max}$ -step region, this translation will map the solution up to a larger amplitude with each cycle. The restriction that $\underset{\sim}{y}_n$ must map into the $k_{max}$ step region limits the values of $\eta$ and $\phi$ for this resonating solution to exist. With $\underset{\sim}{y}_0$ lying in the $k_{max}$ - step region, $\underset{\sim}{y}_{2k}$ will map back into the $k_{max}$ -step region if the slope of the translation vector is both positive and greater than $-\sqrt{\mu}\cos(k_{max} - 1)\theta / \sin(k_{max} - 1)\theta$ (from Eq. (3.4b)). This condition can be written as

$$\frac{\eta g_2(2k_{max}, \theta, \theta_0, \phi) - \left(\frac{\beta - \mu}{1+\mu}\right)}{\eta g_1(2k_{max}, \theta, \theta_0, \phi) + \frac{1}{\mu}\left(\frac{\beta - \mu}{1+\mu}\right)} > \sqrt{\mu}\,\mathrm{ctn}\ \theta \ , \qquad (4.29)$$

which for a given $\eta$ (or $\phi$) specifies $\phi$ (or $\eta$) such that all solutions $\underset{\sim}{y}_0$ in the $k_{max}$ -step region grow unboundedly.

All that was required for this resonance was that Eq. (4.28) mapped $\underset{\sim}{y}_0$ into the $k_{max}$ region and that $\underset{\sim}{g}(2k_{max}, \theta, \theta_0, \phi)$ be periodic. Thus, a resonating solution would exist for solutions with $\theta_0 = m\pi/k_{max}$ , $m = 2, 3, \ldots$ satisfying Eq. (4.29), these solutions being the subharmonic forcing functions. However, Eq. (4.23) yields

$$\underset{\sim}{g}^{\mu>0}(2k_{max}, \theta, \theta_0, \phi) = 0 \qquad \theta_0 = \frac{m\pi}{k_{max}} \ , \quad m = 2,3,\ldots$$

and so Eq. (4.29) is not satisfied.

The growing solutions discussed above have a half cycle period of $k_{max} = \pi/\theta$, which is the maximum period for the homogeneous solutions. Generally, however, the non-autonomous equations admit solutions of larger periods depending on $\eta$ and $\theta_0$. This effect of the inhomogeneity on the period can be examined from the equation for the $y_n$ component of a solution for a half cycle mapping, Eq. (4.22),

$$y_n = \cos n\theta\, y_0 + \frac{\sin n\theta}{\sqrt{\mu}}\,\dot{y}_0 - 2\left(\frac{\beta-\mu}{1+\mu}\right)\left(a_n(\theta) + \frac{b_n(\theta)}{\sqrt{\mu}} + 1\right)$$

$$+ \eta g_1^{\mu>0}(n, \theta, \theta_0, \phi) \ , \qquad (4.30)$$

which is bounded by

$$y_n \le \cos n\theta y_0 + \frac{\sin n\theta}{\sqrt{\mu}}\dot{y}_0 + b' + |\eta| g_1' \qquad (4.31)$$

$$b' = \left(\frac{\beta-\mu}{1+\mu}\right)\frac{3 + 2\sqrt{\mu}(3 - \cos\theta)}{\sqrt{\mu}(1-\cos\theta)}$$

$$g_1' = \left(\frac{1+\sqrt{\mu}}{\sqrt{\mu}}\right)\frac{1}{4(1 - \cos\theta\cos\theta_0)}\Big[14(1 - \cos\theta\cos\theta_0)\cos\phi$$

$$+ (16(1 - \cos\theta\cos\theta_0) + \cos\theta + \cos\theta_0)\sin\phi\Big] \ .$$

For $(b' + |\eta| g_1')$ small, the period of the half cycle mapping is thus bounded by $n$ such that $y_n \le 0$ in Eq. (4.31). If the right hand side

of Eq. (4.31) has no zero, i.e. for $|\eta|$ large, then the term $\eta \underset{\sim}{g}^{\mu>0}$ dominates the solution in Eq. (4.22) and $y_n$ is bounded by the period of $g_1^{\mu>0}$ which is $\max(\pi/\theta, \pi/\theta_0)$.

A bound on the growth of any of the solutions of Eq. (4.2) can be found from the Hamiltonian of the equations, which is no longer conserved for the mappings in regions I and V. From Eqs. (3.23), (4.4a), and (4.4b), the change in the Hamiltonian for each mapping in regions I or V is given by

$$H\Big|_n^{n+1} = \eta \sin(n\theta_0 + \phi) \left\{ -\mu y_n + \dot{y}_n + \frac{1+\mu}{2} \left( \eta \sin(n\theta_0 + \phi) - 2\,\frac{\beta - \mu}{1+\mu} \right) \right\} , \qquad (4.32)$$

and for solutions, $y_n$, in regions III and VII it is

$$H\Big|_n^{n+1} = \left\{ \eta \sin(n\theta_0 + \phi) + 2\left(\frac{\beta - \mu}{1+\mu}\right) \right\} \left( -\mu y_n + \dot{y}_n + \left(\frac{1+\mu}{2}\right) \eta \sin(n\theta_0 + \phi) \right) . \qquad (4.33)$$

Thus, the maximum jump in the Hamiltonian for any outer branch solution is

$$\Delta H_{max} = \xi(\mu|y_n| + |\dot{y}_n| + \gamma) \tag{4.34}$$

$$\xi = |\eta| + 2\frac{\beta - \mu}{1+\mu}$$

$$\gamma = \left(|\eta| + 2\frac{\beta - \mu}{1+\mu}\right)(1+\mu) \ .$$

The Hamiltonian of the solution for the next time step is, then,

$$H_{n+1} = \frac{1}{2}\dot{y}_{n+1}^2 + \frac{1}{2}\mu y_{n+1}^2 + (\beta - \mu)|y_{n+1}| \le H_n + \Delta H_{max} \ .$$

for $|\underset{\sim}{y}_n| >> 1$

$$\dot{y}_{n+1} \le (\dot{y}_n^2 + 2\xi|\dot{y}_n|)^{\frac{1}{2}} + O(1)$$

$$y_{n+1} \le (y_n^2 + 2\xi|y_n|)^{\frac{1}{2}} + O(1),$$

and the jump in $\underset{\sim}{y}_n$ becomes

$$\Delta\dot{y}_n = \dot{y}_{n+1} - \dot{y}_n \le \xi + O(1/\dot{y}_n)$$

$$\Delta y_n = y_{n+1} - y_n \le \xi + O(1/y_n) \ .$$

So, for n large

$$\dot{y}_n = \xi n + O(1) \ , \quad y_n = \xi n + O(1) \ . \tag{4.35}$$

The Hamiltonian is therefore bounded by

$$H_n \le \frac{1}{2}(1+\mu)\,\xi^2 n^2 + O(n) \ . \tag{4.36}$$

The non-autonomous solutions are bounded by a linear growth in n and

a growth in the Hamiltonian of $O(n^2)$, as in the autonomous case. However, the coefficient of this bound, $\xi$, has increased by $|\eta|$ from the autonomous case.

# V The Solutions of the Trapezoidal and Energy Conserving Difference Equations as Approximations to the Differential Equation Solutions

## 5.1 The Dependence of the Solutions on the Time Step

In this chapter we examine the characteristics of the difference equation solutions from the aspect that they are the approximate solutions of the differential Eq. (1.1a) via the trapezoidal rule. When f(x) is a linear function, the trapezoidal rule is a useful differencing scheme for solving differential equations. This is because the solutions to the associated linear difference equation conserve the Hamiltonian and are $O(\Delta t^2)$ accurate. However, the results of the analysis in Chapters II and III show that these desirable properties of the solutions are not generally present when f(x) is non linear. It was seen that only particular initial conditions yield solutions of Eqs. (2.5) that conserve the energy for each step, and for $\mu = 0$ there exists unbounded solutions. Since energy conservation is an important property of the differential equation for dynamical systems, this feature should be retained by the numerical solutions of the equations, [8, 9].

The difference Eqs. (2.5) can be modified to conserve the energy by satisfying the energy conservation equation for each step,

$$E_{n+1} = \frac{1}{2}\dot{x}^2_{n+1} + \int_{x_0}^{x_{n+1}} f(\eta)d\eta = E_n = \text{constant} \quad , \tag{5.1}$$

instead of the equation of motion. The resulting difference equations are

$$x_{n+1} - x_n = \frac{\Delta t}{2}(\dot{x}_{n+1} + \dot{x}_n)$$

$$\dot{x}_{n+1} - \dot{x}_n = \Delta t \, \frac{F(x_{n+1}) - F(x_n)}{x_{n+1} - x_n} \qquad (5.2)$$

$$F(x_n) = \int_{x_0}^{x_n} f(\eta) d\eta \quad .$$

The solutions of these implicit difference equations will conserve the energy for all $\Delta t$.

In the numerical analysis of differential equations, the stability and accuracy of the approximate solutions are functions of the increment in the discretized independent variable (in this case the time step). It is simplest to examine first the dependence of the solutions on $\alpha$, the time step variable, through the $\underset{\sim}{y}$ phase plane solutions and then use the transformation Eq. (2.3) to go back to the solutions of Eqs. (2.1), $\underset{\sim}{x}_n$. Unlike the linear equations, the solutions of the nonlinear difference Eqs. (2.5) are strongly dependent on the time step chosen. The existence of both unbounded and periodic solutions for $\mu = 0$ proves that for fixed initial conditions, $\underset{\sim}{x}_0$, solutions for various values of $\alpha$ can be quite different in behavior. On the other hand, the existence of stability regions around the periodic solutions for $\mu > 0$ proves that for sufficiently small changes in the time step a solution will still map in the stability region of a periodic solution. Thus there is a continuous range of time steps which admits solutions with similar behavior.

A more explicit example of the influence of the time step choice on the solutions' characteristics can be seen in the dependence of $\dot{x}^u_{min}$

on $\alpha$. $\dot{x}^u_{min}$ is the minimum $\dot{x}$ necessary for unbounded solutions of the difference equations when $\mu = 0$, and is calculated from Eq. (2.27) with $k = k^u_{min}$. It can be shown that, for the unbounded solution mapping pattern $(mk, k+1)$, the set of solutions for $m = 1$ contain the lowest values of $\dot{y}^u$. $k^u_{min}$ is calculated from Eq. (2.28) with the requirement that $y^u(k^u_{min}) > 0$, and is

$$k^u_{min}(m=1) \geq 2\,\frac{\beta+1}{\beta}\ , \qquad \beta = \alpha^2 a\ . \tag{5.3}$$

$k^u_{min}$ must also satisfy the conditions on the minimum number of steps for an outer branch mapping given by Eq. (2.16). $\dot{x}^u_{min}$ as a function of $\alpha$ is shown in Fig. 5.1. From this figure we see that the minimum velocity for the unbounded solutions can be made as large as necessary by the proper choice of $\alpha$.

Although the phase plane is dominated by the inner and outer branch type of mappings, the solutions for $\underset{\sim}{x}_0$ fixed will not exactly follow these mapping structures for a sufficiently small time step. Instead, the solutions will successively map several times into the linear region on each half cycle before mapping into an outer branch region $|y_n| \geq 1$. In terms of the mapping regions of Figs. 2.1 and 3.1, this corresponds to the solutions that map from region II (or VI) several times into region IX and then map into region IV (or VIII). This mapping behavior is characteristic of solutions in region $I_a$ with $|\dot{y}| < 1$ and $y >> \dot{y}$.

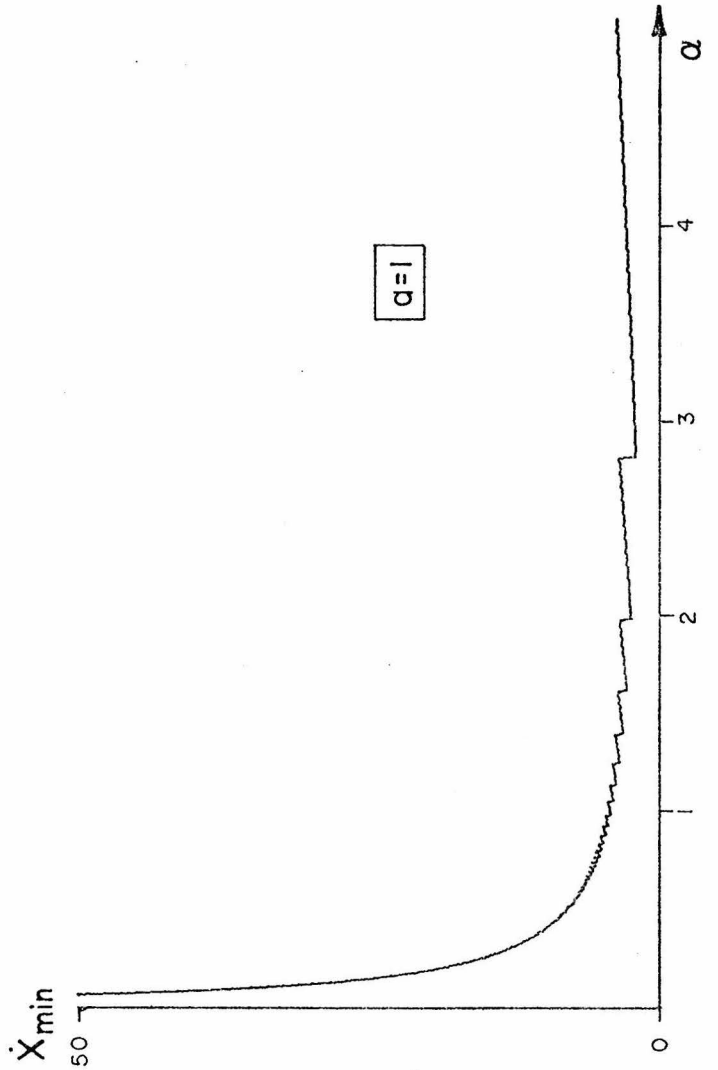


Figure 5.1 - Minimum $\dot{x}$ for Unbounded Solutions as a Function of $\alpha$ ($\Delta t = 2\alpha$)

The perturbation equation for such half cycle transformations is different from those of the outer branch solutions for $\mu = 0$, Eq. (2.19). To determine the stability of such solutions the mapping pattern is assumed to consist of k steps in $|y_n| \geq 1$ and $m - 1$ steps in $|y_n| \leq 1$. The condition for the perturbation equation to have complex conjugate eigenvalues (i. e. stable solutions) is

$$\left|\{3\beta - 1 + 2\beta k(1 - \beta)\}\cos m\theta + \right.$$

$$\left.\{3\sqrt{\beta} - 2\beta\sqrt{\beta} + k\sqrt{\beta}(1 - \beta)(2 - \beta)\} \sin m\theta\right| < 1 \quad , \qquad (5.4)$$

and $\theta$ is given in Eq. (3.2j). Although Eq. (5.4) can be satisfied for non-zero $\Delta t$, it is not satisfied for $\Delta t = 0$, and therefore there are no stable outer branch solutions for $\Delta t = 0$. This is to be expected since the solutions of the differential equation are not stable but are orbitally stable. The existence of stable periodic solutions is a peculiarity of the nonlinear difference equations (Eqs. (1.2) and (1.3)).

The accuracy of finite difference solutions in approximating the differential equation solutions is generally difficult to assess quantitavely for nonlinear equations. The bounds on the difference solutions due to damping or periodicity serves,at best, only to put a bound on the approximation error of the difference equation solutions. A consequence of this error is the existence of an error in approximating the period of the differential equation solutions. This period error is an important characteristic of numerical solutions of dynamic equations. Although all of the solutions of the differential equation, Eq. (1.1), are periodic

in one cycle, only the simple periodic solutions of the difference equations possess this behavior. We will examine the period error of these simple periodic solutions.

For $\mu = 0$ the periods of the differential and difference equation solutions, denoted $T_e$ and $T$ respectively, are

$$T_e = \frac{4\dot{x}}{a} + 2\sqrt{a}\tan^{-1}\left(\frac{\sqrt{a}}{\dot{x}}\right)$$
$$T = \frac{4}{a}(\dot{x}^2 + 2a + \alpha^2 a^2)^{\frac{1}{2}} \quad , \tag{5.5}$$

with the initial conditions $x_0 = 1$ and $\dot{x}_0 = \dot{x}$. $T$ is the period of the simple periodic solutions, and due to the phase plane mappings, the outer branch periodic solutions are restricted to $\alpha > \frac{1}{\dot{x}}$. Figure 5.2 shows the relative period error, $(T_e - T)/T$, plotted versus $\ln \alpha$ for several values of $a$ and $\dot{x}$. As shown in this figure, the period of the finite difference solutions, $T$, over or underestimates the exact period, $T_e$, depending on the values of $a$ and $\alpha$. This is unlike the linear equations for which $T > T_e$.

## 5.2 Comparisons of the Energy Conserving and Trapezoidal Algorithms

Although the solutions of both the energy conserving and trapezoidal algorithms converge to the exact solution for $\Delta t$ approaching zero, practical applications require the choice of a time step which yields reasonably accurate solutions and yet is not too small that the equations are economically unfeasible to solve. As seen from Chapters II and III, the boundedness of the trapezoidal difference solutions for

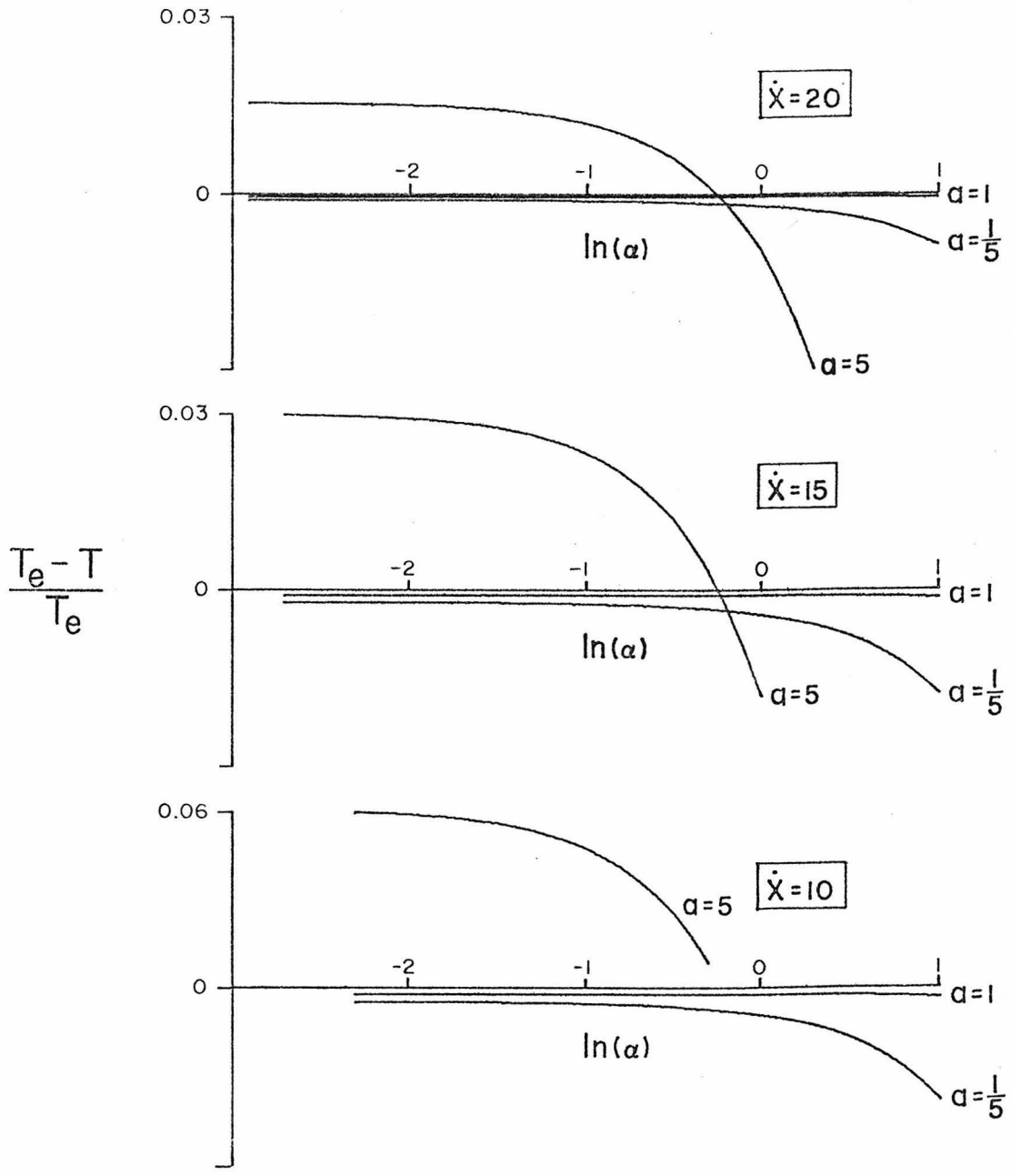


Figure 5.2 - Period Error of the Simple Periodic Difference Solutions

arbitrary initial conditions can not be guaranteed for any nonzero $\Delta t$. Therefore, the trapezoidal quadrature does not seem suitable as a general differencing scheme for nonlinear problems. The inherent nature of the energy conserving difference equations to conserve the energy of the system for each time step surpasses the trapezoidal algorithm since the boundedness of the energy conserving solutions is insured for all time steps. An assessment of the approximation accuracy of the energy conserving solutions can be made since these solutions must lie on the closed phase plane trajectory of the exact solution with the same initial conditions. This approximation error can therefore be thought of as a phase shift between the exact and energy conserving solutions which is a function of the number of steps. The error is a maximum for a phase shift of $\pi$ and equal to twice the maximum value of the exact solution.

Figures (5. 3a), (5. 3b), and (5. 3c) show the exact, trapezoidal, and energy conserving solutions for various initial conditions, values of s, and time steps. These examples show the energy growth and decay of the trapezoidal difference solutions and the phase shift of the energy conserving solutions. Although there seems to be no way to quantitatively assess the approximation error of the energy conserving solutions, it appears, from these examples, that the accuracy of the solutions tends to improve with the time step decreasing. The choice of a time step for an energy conserving solution to be an accurate approximation of the exact solution depends on the initial conditions, and the time length of the solution used.

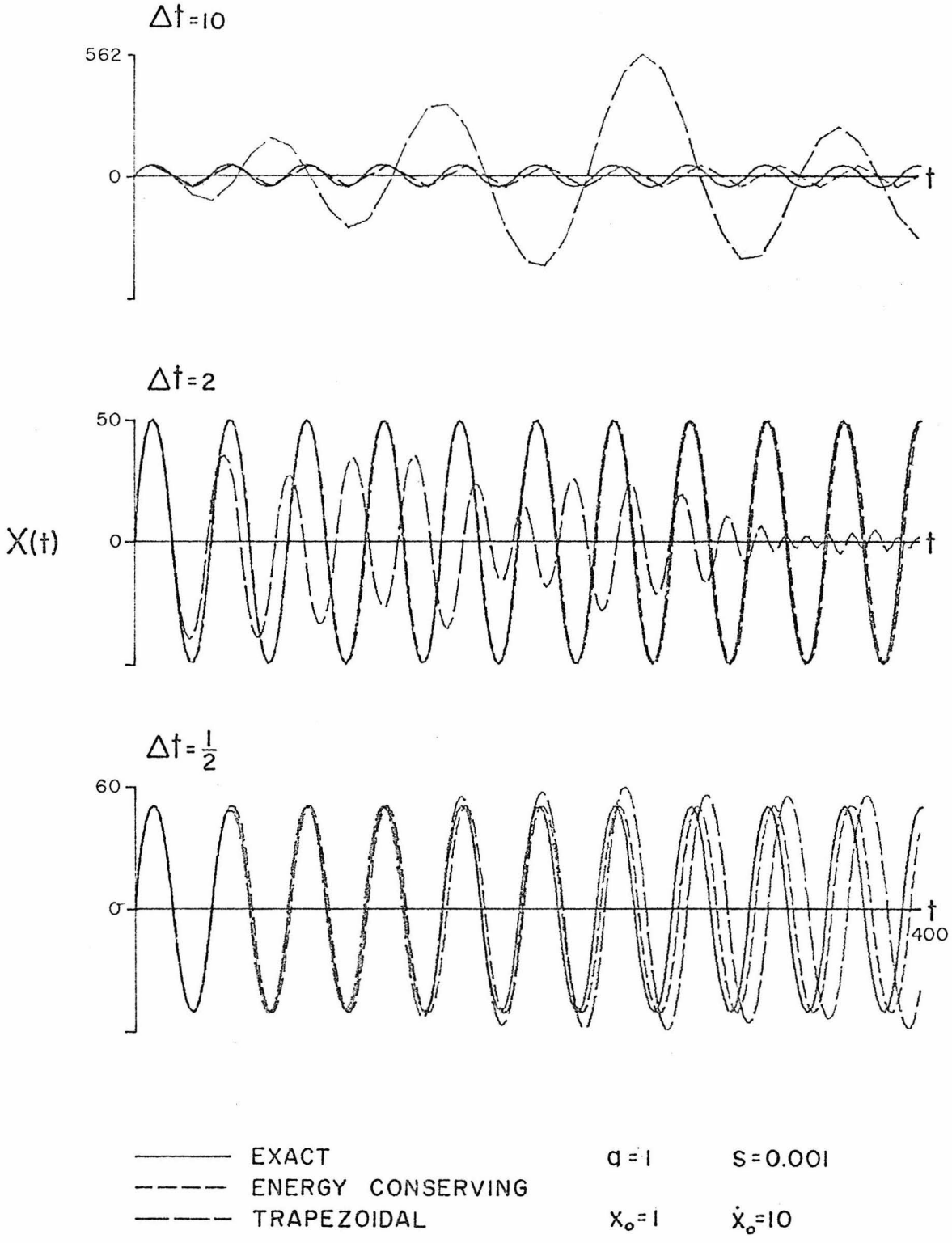


Figure 5.3a - Exact, Trapezoidal, and Energy Conserving Solutions for Various Time Steps

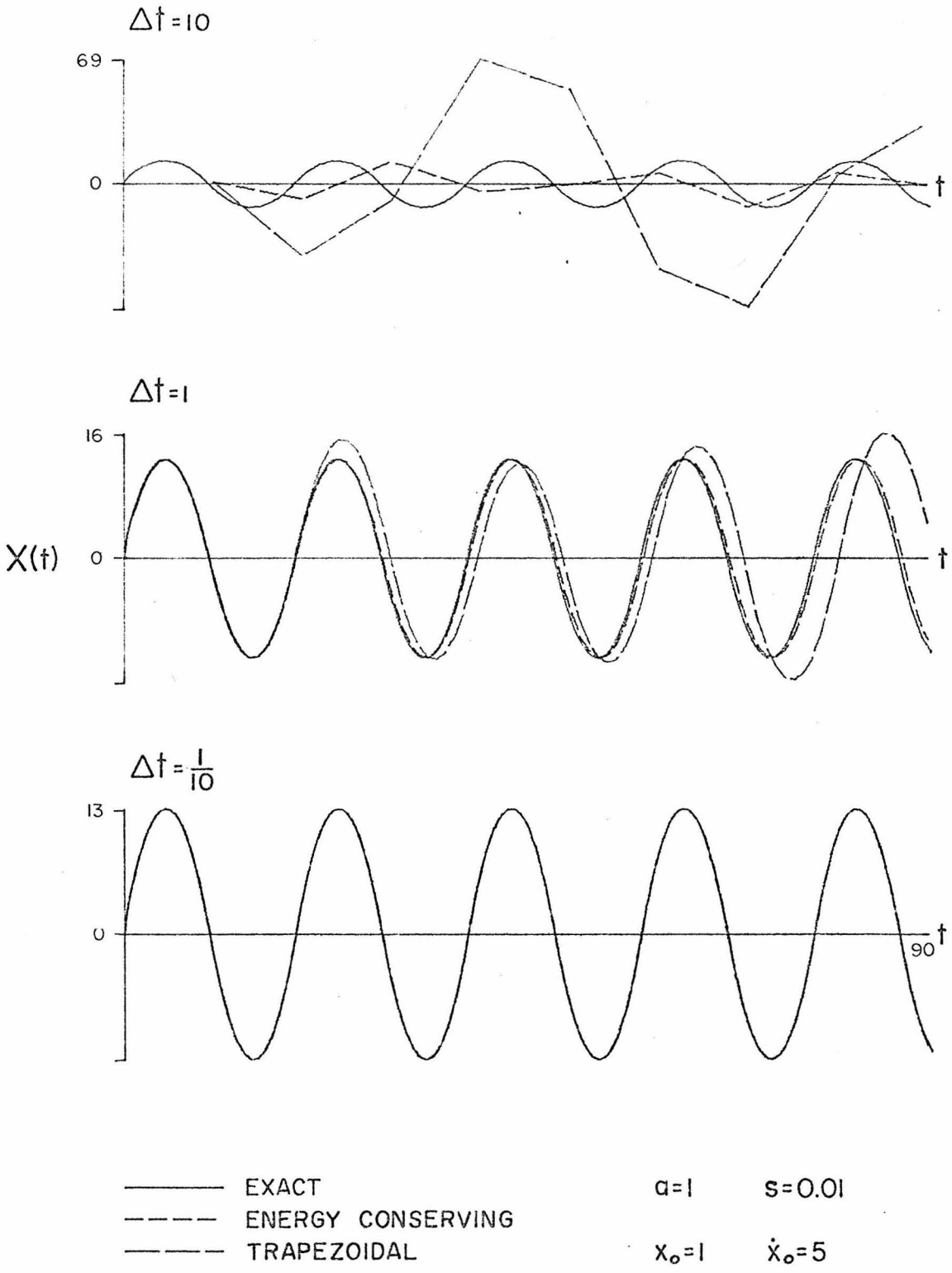


Figure 5.3b - Exact, Trapezoidal, and Energy Conserving Solutions for Various Time Steps

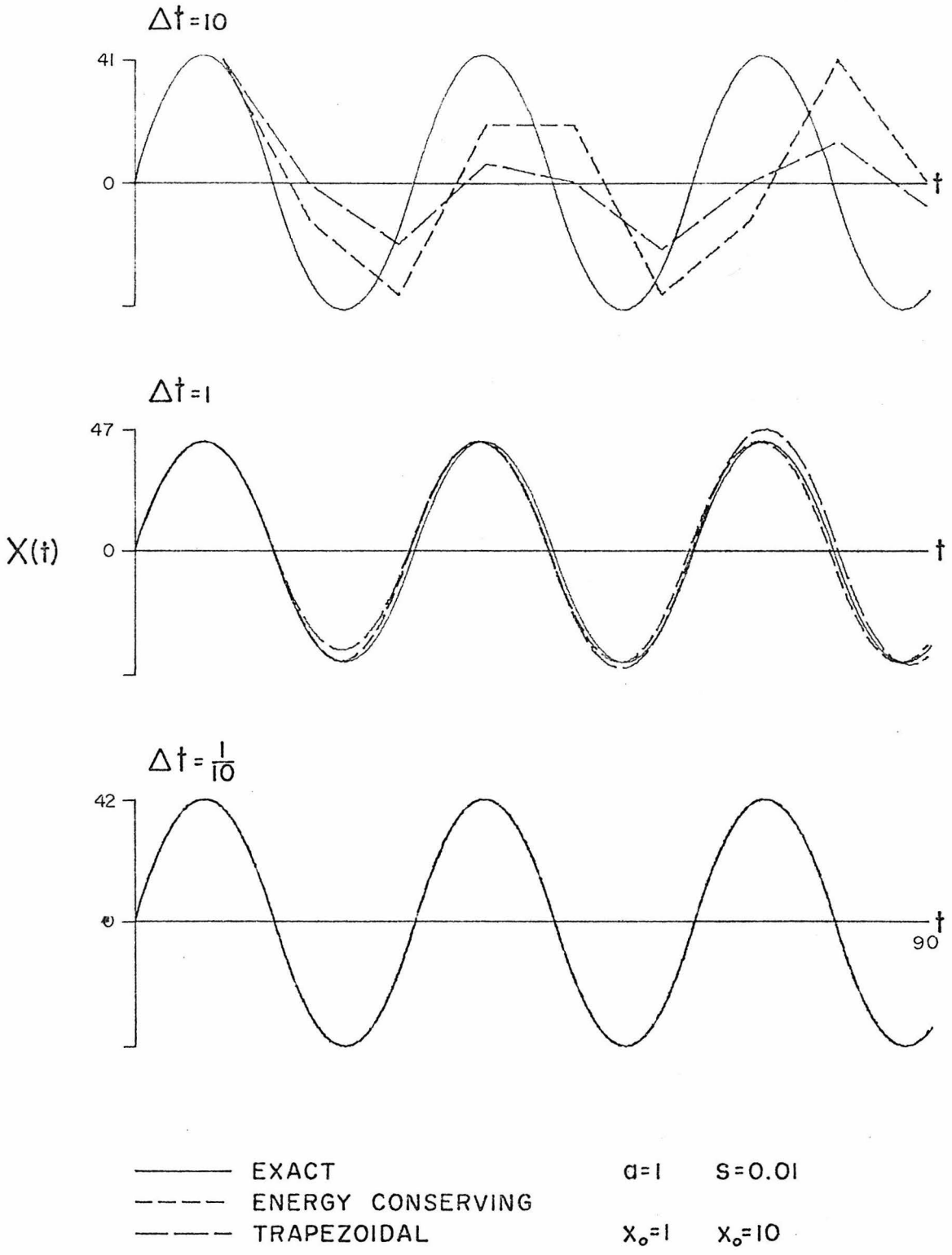


Figure 5.3c - Exact, Trapezoidal, and Energy Conserving Solutions for Various Time Steps

## VI Summary and Conclusions

A transformation oriented method was used in this dissertation to find the periodic and unbounded solutions of certain difference equations. The half cycle transformations of the solutions were examined and used as a basis for determining both the simple periodic solutions (i. e. solutions with a (k,k) mapping pattern) and the more complicated multiple-cycle periodic solutions. These solutions were calculated from transformation equation associated with the particular mapping. Although the half cycle transformations allow one to estimate the possible behavior of all of the solutions, the large number of mappings of some solutions makes any quantitative analysis concerning their structure forbidding without the aid of a computer. Only the fundamental solutions were examined in detail in this study, and the characteristics of the half cycle mappings were used to compose more highly structured, possibly periodic, and unbounded solutions.

In Chapter II the solutions for $s = 0$ were examined and the basic one cycle outer branch mapping patterns of the form $(k,k-1)$, $(k,k)$, or $(k,k+1)$ were found. Utilizing this mapping behavior, an infinite set of simple periodic solutions were shown to exist. Due to the form of the perturbation matrix, all of the outer branch periodic solutions are unstable. A more complicated set of periodic solutions of the form $(mk, k+1, m(k+2), k+1)$ was also found, and these mapping patterns were then used to construct a set of the unbounded, growing solutions which continually map into larger step regions. The maximum possible Hamiltonian growth of the solutions was calculated, assuming that the

solutions map into regions such that the Hamiltonian jump is a maximum for each half cycle. This bound on the rate of Hamiltonian growth is shown to be $H_n \leq 2\beta^2 n + O(1)$ using the fact that the period of the solutions must grow with the amplitude.

A similar analysis in Chapter III also showed a $(k,k-1)$, $(k,k)$, or $(k,k+1)$ outer branch mapping of the solutions was present for $s>0$. A finite set of simple periodic solutions was found from the $(k,k)$ mapping transformations, the finiteness of the set due to the bound on the maximum number of steps per half cycle. The perturbation matrix of the outer branch periodic solutions has conjugate eigenvalues with a modulus of one, and thus the periodic solutions are stable. An infinite set of periodic solutions with the mapping pattern $(m k_{max}, k_{max}-1)$ exist when $\theta$ is a rational fraction of $\pi$, and these solutions grow linearly in amplitude with $m$. A bound on the maximum Hamiltonian growth is shown to be $O(n^2)$ although no solutions were noticed which grew unboundedly. The question of the boundedness of the solutions for $s>0$ still remains open but the fact that there do exist solutions which grow and decay in energy by large amounts is sufficient to demonstrate the inaccuracy involved in using such solutions to approximate differential equations solutions. For $s \ll 1$ the difference equation solutions with sufficiently small initial conditions behave in a manner similar to the solutions for $s = 0$. That is, for $k < k_{max}/2$, there exist solutions which grow in amplitude with the $(mk, k+1, m(k+2), \ldots)$ mapping pattern found for the $s = 0$ solutions. The mapping structure changes at $k = k_{max}/2$, and thus these types of solutions are bounded by

$\dot{y} = \frac{\pi}{4}\frac{a}{\sqrt{s}} + O(1)$ (for $\dot{y}$ lying in region $I_a$ of the phase plane). The addition of damping to the equations puts bounds on the growth of the solutions, and for small enough damping the simple periodic solutions exist and are asymptotically stable.

In Chapter IV the solutions of the non-autonomous equations with a sinusoidal forcing term are examined. The outer branch solutions are found from the transformations, and from these solutions the dependence of the period on the phase of the forcing term is shown. Growing solutions exist for $s>0$ which are similar to resonating solutions for linear systems in that the period of the inhomogeneous term must match the maximum period of the homogeneous solutions, $k_{max}$. The existence of these resonating solutions and their rate of growth also depends on the phase and initial conditions.

The choice of the time step, $\Delta t$, clearly dictates the behavior of the solutions as seen from the analysis. The solutions are expressed in terms of the $y$, $\dot{y}$ variables and are then transformed back into the $x$, $\dot{x}$ variables via Eq. (2.3). Thus, a change in $\Delta t$ will change the initial conditions of the solution in the $y$, $\dot{y}$ phase plane. The stability regions of the periodic solutions for $s>0$ insure that for only small changes in the time step will a solution remain in a particular stability region. Therefore, the boundedness of a solution is definite for only a quantized range of time steps. This phenomenon is not characteristic of linear differential equations. Due to the difference solutions' wide range of growth and decay in number of mappings per half cycle, the period of a solution varies greatly with the initial conditions. However,

the period of the simple periodic solutions when compared to the period of the differential equation solutions shows that the difference solution's period can over or underestimate the exact period. These characteristics are discussed in Chapter V along with a comparison of several solutions of the trapezoidal and energy conserving difference equations to the exact solutions for various time steps.

The existence of unbounded solutions proves that the trapezoidal algorithm does not retain its unconditional stability and energy conserving properties for nonlinear dynamic equations. It can be seen from the exact periodic and unbounded solutions that the stability of the difference solutions is dependent on both the time step and the initial conditions. For practical purposes there seems to exist a balance between the disadvantages of the energy conserving and trapezoidal algorithms. For the trapezoidal algorithm the time step necessary to insure stable solutions for a wide range of initial conditions may be too small to allow economical solutions for large systems, while the unconditionally stable energy conserving algorithm is generally more difficult to implement than the trapezoidal scheme.

# REFERENCES


1. Artstein, Z., "On the Limiting Equations and Invariance of Time Dependent Difference Equations", Stability of Dynamical Systems, Lecture Notes in Pure and Applied Math., Edited by J. Graef, vol. 28, pp. 3-9.

2. Chaundy, T. W. and Phillips, E., "The Convergence of Sequences Defined by Quadratic Recurrence Formulas", Quarterly J. of Math., (Oxford Series), vol. 7, 1936, pp. 74-80.

3. Dunford, N. and Schwartz, J. T., Linear Operators, New York, N. Y.: Interscience Publishers, Inc., 1964, pp. 468-470.

4. Edwards, D. B., "Time Domain Analysis of Switching Regulators", Doctoral thesis, Calif. Instit. of Tech., March 1977.

5. Hahn, W., "Theory and Application of Liapunov's Direct Method", Prentice-Hall, Englewood Cliffs, New Jersey, 1963, Section 39.

6. Hsu, C. S., Yee, H. C., and Cheng, W. H., "Determination of Global Regions of Asymptotic Stability for Difference Dynamical Systems", J. Appl. Mech., vol. 44, Trans. ASME (March 1977) pp. 147-153.

7. Hsu, C. S., and Yee, H. C., "Behavior of Dynamical Systems Governed by a Simple Nonlinear Difference Equation", J. Appl. Mech., vol. 42, Trans. ASME (December 1975) pp. 870-876.

8. Hughes, T. J. R., "Stability, Convergence, and Growth and Decay of Energy of the Average Acceleration Method in Nonlinear Structural Dynamics", Computers and Structures, vol. 6 (1976) pp. 313-324.

9. Hughes, T. J. R., Caughey, T. K., and Liu, W. K., "Finite Element Methods for Nonlinear Elastodynamics which Conserve Energy", J. Appl. Mech., to appear.

10. Hurt, J., "Some Stability Theorems for Ordinary Difference Equations", Siam J. of Numerical Analysis, 4, 1967, pp. 582-596.

11. Kalman, R. E., and Bertram, J. E., "Control System Analysis and Design via the Second Method of Liapunov, II. Discrete Systems", J. Basic Engrng., vol. 82, Trans. ASME Ser. D, 1960, pp. 394-400.

12. LaSalle, J. P., "Difference Equations. Discrete Semidynamical Systems", The Stability of Dynamical Systems, Regional Conference Series in Applied Math., SIAM, vol. 25, pp. 1-25, 45-50.

13. Lorenz, E. N., "The Problem of Deducing the Climate from the Governing Equations", Tellus, vol. 16, 1964, pp. 1-11.

14. May, R. M., "Biological Populations with Non-overlapping Generations: Stable Points, Stable Cycles, and Chaos", Science, vol. 186, 15 November 1974, pp. 645-647.